Role of brain-muscle circadian clock communication in skeletal muscle homeostasis and aging

Mireia Vaca Dempere

TESI DOCTORAL UPF / 2022

DIRECTORS DE LA TESI: Dra. Pura Muñoz Cànoves
Dr. Antonio Luis Serrano Sánchez

Departament de Medicina i Ciències de la Vida

Universitat Pompeu Fabra Barcelona

Als meus pares,

i a la meva germaneta.

`Curiouser and curiouser!' cried Alice;

`now I'm opening out like the largest telescope that ever was!

Good-bye, feet!'

Lewis Carroll, *Alice's Adventures in Wonderland*

ACKNOWLEDGMENTS

És curiós que la secció d'agraïments siga la primera en aparèixer en una tesi, ja que és (o sol ser) l'última en escriure's. És el postre. La part dolça. I jo sóc de dolç més que de salat, així que en el meu cas, és deixar-me el millor per al final. Ser conscient de tot el que m'ha donat aquesta etapa, i tot el que m'heu donat vosaltres és sense dubte el millor. No sóc la mateixa persona que fa 5 anys, ja que he après unes cuantes coses, sobre ciencia i sobre la vida. I me les heu ensenyat vosaltres, alguns a les bones i altres a les males. Però us dec moltíssim.

Així que comencem pel principi. Els primers als que he de donar gràcies és, sense dubte, als meus pares. M'ho doneu tot. M'ensenyeu tot el que sabeu. I el més important, m'ensenyeu a tindre fe en mi mateixa; creieu tan incondicionalment en mi, que em fau creure que puc fer tot allò que em propose; i al final ho faig. I sense dubte, és gràcies a vosaltres. A vosaltres, i a tu, germaneta. Tot i que eres més jove, els consells que m'has anat donant quan ho veía tot negre, no tenen preu. La meva filòsofa sàbia. Gràcies, familia meva. Per estar al meu costat i ajudar-me sempre. Per ser el meu motor i fer-me feliç. Per ser tan excepcionals. Vos estime moltíssim.

La segona persona a qui agraïr aquesta tesi és a Isabel Fariñas. Aquella profe de la carrera que em va saber transmetre la passió per la investigació, i que em va ajudar quan més ho necessitava. Sense ella, no hagués conegut aquest laboratori. Gràcies.

Gràcies als meus directors, Antonio i Pura. Antonio, gracias por ayudarme con mi primer *lab meeting* y con la última parte de esta tesis. Pura, gràcies per haber-me permès fer la tesi al teu laboratori. Tot i que no ha sigut gens fácil, tot el que he viscut ací, el bo i el dolent, m'ha fet més forta…

…I m'ha permès conéixer a gent excepcional. La primera d'questes persones és Vicky, la meva companya de viatge. Vicky, no tienes comparación. Trabajadora, lista, fuerte, y resiliente como nadie. Todas las dudas que tenia al principio fueron contestadas por ti. Así que gracias a ti pude dar mis primeros pasos. Me gusta pensar que las dos hemos influido mucho la una en la otra, y que nos hemos hecho crecer. Contaremos siempre la una con la otra, no me cabe duda. Muchas gracias por todo, Vicks.

Mi otro compi de viaje, Antonio, ya acabó hace algún tiempo… y ahora no hay quien le pare. Gracias por tus enseñanzas, por mantenerme alerta, y por compartir conmigo música y bailes. Por tu apoyo y tus abrazos. Y por seguir ahí, por tener siempre un huequecito para mi. Gracias.

Unos se fueron, y otros vinieron. Valentina vino. Esta post-doc se unió al loco mundo de los ritmos circadianos. Creo que ni tu ni yo sabíamos muy bien dónde nos metíamos al empezar nuestros proyectos... Pero fue una suerte que mi poyata y mi escritorio acabaran al lado de los tuyos. He podido discutir experimentos contigo, trabajar mano a mano contigo, y reír contigo, reir mucho. Ah, y comer buena comida italiana y beber buen café. He aprendido mucho de ti, de la ciencia y de la vida. Nunca olvidaré todo lo que me has ayudado tanto profesionalmente como personalmente. Eres, sin lugar a duda, fuente de inspiración para mi. Una gran científica y aun mejor persona, que ha enriquecido mucho mi tesis. Gracias, amiga mia. Aquí estaré siempre.

Another good friend I encountered on this long journey has been Jacob. How long are you here in the lab? 4-5 months? Honestly, it feels like I know you for a pretty more time… Thanks for helping me so much in everything, for giving me good advice, for discussing science with me, for making my project a better one, and for wanting me to work with you. It means a lot. Oh, and of course, for reading many times this thesis! We will keep helping each other in one way or another, I am sure of that. With the clicks and with the clocks. Thanks, Jacob.

Moltes gràcies també a tu, Àlex, per la teua alegría contagiosa, per tot el que m'has ajudat en aquest camí i per ser un magnífic company de bailoteos i de *beer sessions*! Tenim una ravalada pendent, no se m'oblida. I a Andrés, que encara que et definisques com a "home de poques paraules", sempre que parles em dones molt bons consells. Molta sort amb la vostra última etapa, la tindreu segur. Vosaltres ho valeu.

Aquest labo no seria el que és sense aquest grup de dones extraordinàries i treballadores com ningú. Vera, Eva, Laura, Jess, Aida i Mercé. Sou realment increíbles. Verita, menos mal que tus risas han llenado el laboratorio en todo momento, das vida allá donde ries. Las noches de matanzas fueron mucho más fáciles riendo contigo. No dejes de reír jamás. Evi, gràcies per estar amb mi fins i tot quan tocava fer coses una mica xungues als ratolins. Sent els malsons que t'haja produït, i gràcies per ajudar-me tant! Lauri, gràcies per genotipar, fer comandes, cuidar dels cultius... i mil coses més. Gràcies per ser una *superwoman*! Et dec una bona ració infinita de croquetes, que sé que t'agraden. Jessica, he pogut comptar amb tu sempre que t'ho he demanat. Sobretot per a fer mil i una aurores al principi de la tesi… Quanta paciència vas tindre! Moltíssimes gràcies. Aida Navarro (o New York para los amigos), gracias por ser nuestro apoyo siempre. Para hacer inmunos, cortes, para ser conductora, jugadora de volley aunque te pillen exámenes… Gracias por tu eficiencia en todo. Mercé, quina pena em va donar quan et vas jubilar! La història d'aquest laboratori és la que és gràcies al teu suport incondicional. Tots et devem molt, fins i tot aquells qui no han arribat a conéixer-te. Moltes gràcies per tot el teu treball, que ens ha ajudat molt a tothom que hem passat pel laboratori de Biologia Cel·lular. Gràcies a totes, sou excepcionals.

Oleg, thanks a lot for all your help. Without it, this entire project would not have been possible. I lo mismo te digo, Jesús. Muchas gracias por todo durante el tiempo que estuviste por aquí. Te echamos mucho de menos.

Gràcies a Aida, Aina, Claudia, Guillem, per ser l'aire fresc del lab. Us he trobat ja a l'última part del camí, però sense vosaltres s'haguera fet molt més dura.

A Alejandra i a Alejandro, dos estudiants intrèpids que ara estan fent la tesi pel món. Joves científics que m'alegre d'haver conegut, i que també serán amics meus sempre. Somieu en gran, que vosaltres ho valeu. Gràcies per creuar-vos en el meu camí.

A Eusebio y Maria, por vuestra importante aportación al proyecto.

Thanks to all the people that have collaborated on this project, and have helped to make it evolve into what it is now. Salva, Valentina, Guiomar, Paloma, Carmelo, Tom, Patrick, Paolo, Kevin, Carolina. Amazing collaborators that have taught me everything about the wonderful field of circadian rhythms. Gracias también a ti, David. Sin ti muchos experimentos que están en esta tesis no podrían haberse llevado a cabo.

Gracias a todos los que se fueron del lab: Javi, Joana, William, Marta, Sonia, Ana, Kostya. Y a todo el equipo de Madrid: Nacho, Xiaotong, Silvia, Joan, Ángela, Merche, Jose, Laura y compañía. También a Mònica. Somos una familia enorme y de todos he aprendido cosas.

També gràcies a tota la gent del departament que ha fet més fácil la meua estancia. Gràcies al Pedro, al Marc, a l'Eva, a la Maria, a les fantàstiques dones de la cuina, i a Regina. Moltes gràcies per tot.

Però hi ha un munt de gent que també ha enriquit aquest treball, donant-me moments de felicitat i aprenentatge de moltes coses diferents, que al final han impactat també en la qualitat d'aquest treball. Gent que senzillament em fa feliç i em dona forces.

Per això, gràcies a tota la gent del meu poble, Vila-real. Gràcies a les amigues i amics de tota la vida, en especial a Sandra, que m'ha acompanyat molt durant els últims anys. Encara que estiga lluny, sempre seré una orgullosa vila-realenca.

Gràcies a la gent de l'orquestra, del swing, del francés, del 11F. He aprés molt més que de ciència aquests anys gràcies a vosaltres.

Gràcies a totes les meues amigues i tots els meus amics de la carrera. Bioquímiques i bioquímics que ara hem pres camins professionals diferents, pero bioquímics al cap i a la fi. La carrera va ser (junt amb la tesi) l'etapa de la vida que més m'ha definit. Sense dubte, una de les més felices. Quin honor tindre-vos encara com amics. Ho sereu sempre.

Gràcies a totes i tots els meus companys i amics del màster, als que es quedaren en Barcelona i als que no. De totes maneres tots us heu quedat tots a dintre del meu cor. Quina sort haver-vos trobat, i haver compartit junts aquesta importantíssima etapa de la vida, i omplir-la de moments preciosos: findes de cases rurals que donen enveja als anuncis d'Estrella Damm, sopars gratis a Shoko, festes en Plataforma, fer-nos disfresses a última hora (i que siguen xulíssims), correbars, Eurovisions (fins el nostre propi)… i eixa actitud que tenim quan estem junts per celebrar qualsevol cosa que se'ns acudiscai: des de San Kiwi fins defenses de tesi. No hi ha en el món una nova generació de científics tan esplèndida. Senzillament, *et al.*

Gracias a mis queridas Marta, Maria y Nuria. Por haber sido mi pequeña familia en Barcelona. Tan diferentes las cuatro y queriéndonos tanto. Habéis sido un apoyo incondicional cuando más lo necesitaba. E hicisteis de la quarentena un período que, a pesar de haber sido duro, fue fructífero en muchos aspectos. Recuerdo muchos momentos con vosotras que me dieron mucha fuerza. Y se que vendrán muchos más, porque nos tendremos siempre. Os quiero.

Finalment, l'últim mosset d'aquest dolç postre. Gràcies a Guille, per ser un company de pis, de lindy, d'orquestra, i de vida tan meravellós. Per encendre la llum quan estava rodejada de foscor i dubtes i per buscar solucions amb mi. Per escoltar totes les meues històries diàries sobre els experiments que sortien bé. I els que sortien malament. Per fer-me riure sempre. Per ajuntar el teu món amb el meu i enriquir-lo. Gràcies per formar un equip tan fantàstic amb mi.

Gràcies a totes i tots per tot.

ABSTRACT

Tissue physiological functions require daily time-keeping for efficient organ function and systemic metabolic homeostasis, processes that are integral to life and that decline with aging. To ensure the correct functional coordination among different tissues the suprachiasmatic nucleus (SCN) is considered the main synchronizer of all the peripheral clocks, although each tissue has its own level of autonomy governed by the presence of local clocks. To date, it is unclear which tissue functions are driven by tissue-autonomous clocks and which rely on the communication with other clocks, such as the SCN. It is also unknown how these dependencies and clock network interactions change during aging. To examine this, we generated a mouse model devoid of the essential core clock protein BMAL1 in all tissues, with the exception of brain and skeletal muscle. Unexpectedly, we found that the intrinsic muscle clock acts as a gatekeeper for brain-derived signals to prevent *de novo* rhythmic oscillations in the muscle, and that this basic brain–muscle communication network is sufficient to drive key components of the functional daily program of muscle and to prevent the appearance of aging traits. We also identified key brain–controlled inputs to the muscle clock, including adrenal signals and feeding rhythms that support central–peripheral communication. Finally, we examined the role of imposed feeding rhythms in old mice, as a trainer to circumvent tissue clock misalignments that occur during aging.

Keywords: skeletal muscle, aging, circadian clocks, inter-organ communication, time-restricted feeding

Les funcions fisiològiques dels teixits requereixen ser realitzades en moments específics del dia per assolir l'eficiència funcional dels diferents òrgans i l'homeòstasi metabòlica de l'organisme, processos que són integrals a la vida i que decauen amb l'envelliment. Per garantir la correcta coordinació funcional entre els diferents teixits, el nucli supraquiasmàtic (NSQ) es considera el principal sincronitzador de tots els rellotges dels teixits perifèrics, encara que cada teixit té el seu propi nivell d'autonomia regit per la presència de rellotges locals. Fins ara, es desconeixen quines funcions dels teixits estan impulsades pels rellotges autònoms i quines depenen de la comunicació amb altres rellotges, com el del NSQ. També es desconeixien com aquestes interaccions entre els diferents rellotges canvien durant l'envelliment. Per examinar-ho, hem generat un model de ratolí desproveït de BMAL1 (proteïna essencial de la maquinària bàsica del rellotge molecular) en tots els teixits, a excepció del cervell i del múscul esquelètic. De manera inesperada, vam trobar que el rellotge muscular intrínsec actua com a guardià, filtrant els senyals derivats del cervell per prevenir oscil·lacions rítmiques *de novo* en el múscul, i que aquesta xarxa de comunicació bàsica entre el cervell i el múscul és suficient per a impulsar funcions bàsiques diàries dels músculs i per prevenir l'aparició de trets d'envelliment en aquest teixit. També vam identificar els senyals clau que utilitza el cervell per dirigir el rellotge muscular, que inclouen hormones suprarenals i els ritmes en l'alimentació, els quals donen suport a la comunicació central-perifèrica. Finalment, vam examinar com l'alimentació restringida per temps en ratolins vells es pot usar per a evitar les desalineacions que es produeixen durant l'envelliment entre els rellotges dels diferents teixits.

Paraules clau: múscul esquelètic, envelliment, rellotges circadians, comunicació entre òrgans, alimentació restringida per temps

PREFACE

The work presented in this Doctoral Thesis was done in the Cell Biology Group at the Department of Medicine and Life Sciences.

This thesis provides new knowledge on the importance of maintaining circadian rhythms in mammalian physiology. Our work describes the role of circadian clock in skeletal muscle, with a special focus on how its function decays with aging. This knowledge may help to develop new therapies to prevent muscle aging through the modulation of the circadian system. Parts of this Thesis have been submitted for publication.

TABLE OF CONTENTS

INTRODUCTION

Skeletal muscle

Skeletal muscle is the most abundant tissue in the organism. In humans, it accounts for 40% of body weight and comprises more than 600 different muscles. Besides sustaining locomotion and providing postural support [1], it has a crucial role in maintaining daily energy homeostasis, continuously sensing the nutritional status of the body and adapting its metabolism to nutrient availability [2]. During the postprandial state, blood insulin levels increase, after which muscle fibers take up a major proportion of the blood glucose [3]. During starvation, muscle is the predominant tissue in which fatty acid oxidation occurs. This dynamic metabolic profile is key to maintaining body homeostasis, and altering the normal function of skeletal muscle can lead to dyslipidemia, hyperglycemia, obesity, and an increase in the risk of cardiovascular diseases and type 2 diabetes, disorders associated with aging [4–9]

Skeletal muscle structure and composition

To perform its basic function of contracting to produce force and movement, the components of skeletal muscle are highly organized (Figure 1). Each muscle of our body is composed of thousands of long postmitotic and multinucleated cells, called myofibers. Each myofiber is composed of basic units assembled in parallel called myofibrils. Myofibers are covered by a thin sheath of connective tissue, named endomysium. A bundle of myofibers surrounded by a thick layer of connective tissue (known as perimysium) is termed fascicle. Finally, every muscle is composed of several fasciculi, and it is surrounded by the epimysium. This epimysium or fascia establishes the connection of muscle to the tendons [8].

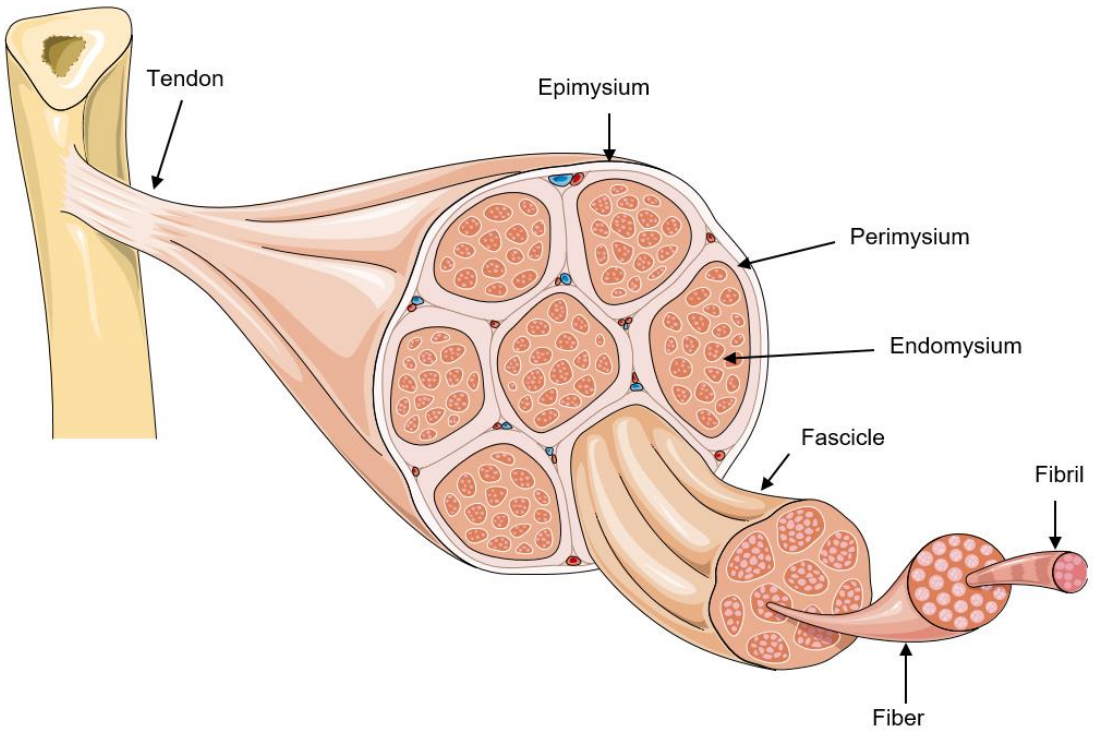

Figure 1. Major components of skeletal muscle. Fibrils are the basic units of fibers. Myofibers, covered by the endomysium, are grouped in fascicles. A fascicle is covered by the perimysium. Muscle is formed by bundles of fascicles that are surrounded by the epimysium, which at the muscle forms the tendon (Image source: https://smart.servier.com/).

Myofibrils (the basic unit of myofibers) comprise thick filaments that are myosin rich, and thin filaments containing mainly actin, along with tropomyosin and troponin. Filaments are arranged in a tightly ordered pattern, forming the sarcomeres, which are the basic contractile units of skeletal muscle. In addition to these proteins, the cytoplasm of the myofiber (sarcoplasm) includes a highly dynamic mitochondrial network. This network is essential for producing the energy required for the pulling motion of actin filaments during contraction [10]. Transverse tubular system (T-tubules) are formed by invaginations of the sarcolemma (the cell membrane of a muscle cell), with an important role in the conduction of the nerve action potential to the inner part of the cell (Figure 2). The sarcoplasmic reticulum is essential to maintain calcium homeostasis, as it contains the sarco/endoplasmic reticulum Ca^{2+}-ATPase (SERCA) and calsequestrin proteins. SERCA is responsible for the calcium uptake after muscle activation and calsequestrin binds calcium loosely within the sarcoplasmic reticulum [11]. T-tubules contact with two terminal cisternae from the sarcoplasmic reticulum in a structure called a triad. This structure allows translation of action potential from the sarcoplasm to the sarcoplasmic reticulum, allowing calcium flow into the cytoplasm to initiate muscle contraction [12].

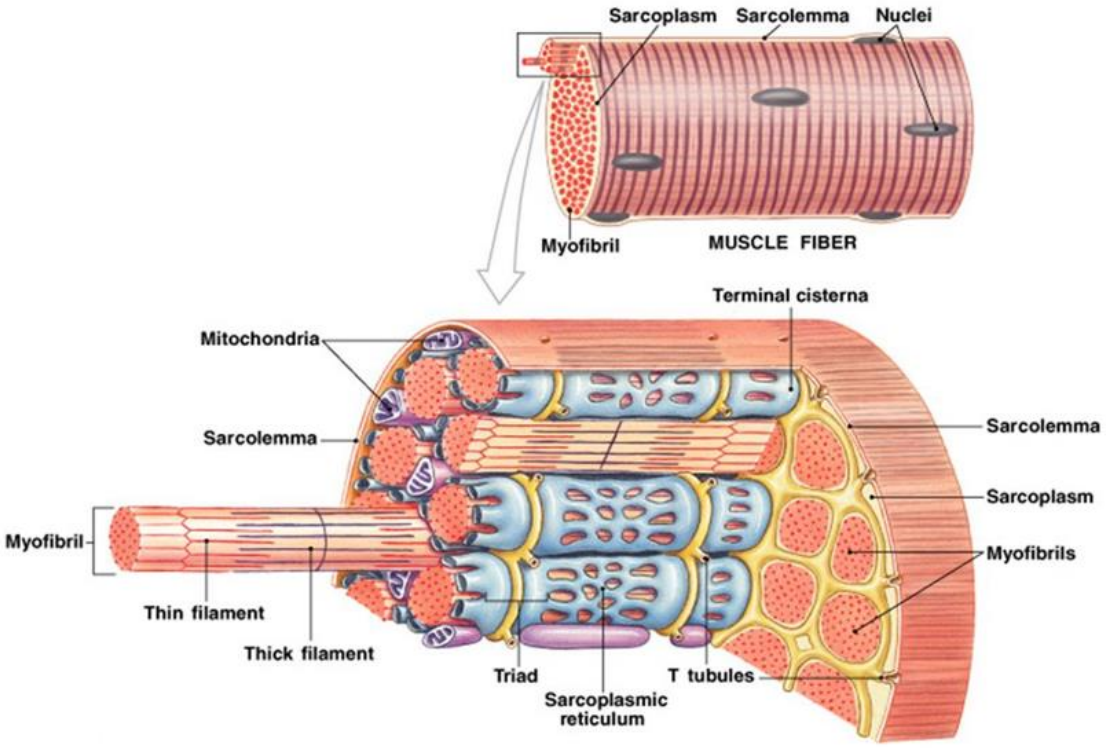

Figure 2. Components of a muscle fiber. The myofiber (surrounded by the sarcolemma), is composed mainly of fibrils which are groups of thin (actin-rich) and thick (myosin-rich) filaments. Other important components of myofibers are the mitochondria (which are the fiber energy supplier) and the sarcoplasmic reticulum (which stores calcium) (Image source: Pearson Education).

Contraction of myofibers starts when an action potential arrives at the plasma membrane. It travels into the T-tubules, which get depolarized and induce calcium exit from the sarcoplasmic reticulum. Calcium then attaches to troponin C, which causes a conformational change that induces the displacement of tropomyosin from the myosin-binding sites, allowing the actin filament to slide onto myosin filaments [13].

Actin and myosin comprise approximately 70–80% of the total protein content of fibers. Depending on the type of myosin they express, fibers are classified as type I (slower contractions, higher mitochondrial content, oxidative metabolism, fatigue-resistant and contributing to endurance performance), IIA (fast contractions, oxidative, intermediate metabolic properties), and IIx or IIb (fastest contractions, glycolytic metabolism, fatigable; contributing to intense activities as sprinting). Fiber-type composition is not static but rather it changes through a lifespan in response to exercise and in pathological situations [14].

In addition to myofibers, muscle also contains many other cell types, such as immune cells, satellite cells, fibro/adipogenic progenitors (FAPs), endothelial cells, and glial cells [15] (Figure 3). These cells are also crucial to maintaining the homeostasis of the muscle and repairing it after injury: immune cells promote inflammation [16]; satellite cells are the stem cell precursors to regenerated new fibers [17]; FAPs are mesenchymal stromal cells that play a supportive role during the formation of new myofibers [18]; endothelial cells secrete anti-apoptotic and myogenic factors [19]; and glial cells have an important role after nerve injury and are implicated in extracellular matrix remodeling in the neuromuscular junction [20]. Altogether, these mononuclear cells communicate with myofibers to influence homeostasis, immunity, and metabolism in skeletal muscle.

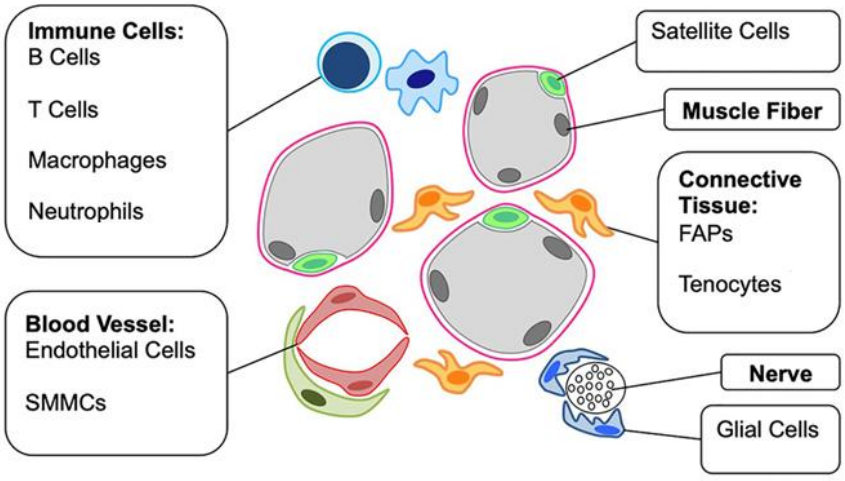

Figure 3. Basic cell composition of skeletal muscle. Different cell types are found in skeletal muscle, influencing its homeostasis. SMMCs: smooth muscle-mesenchymal cells. FAPs: fibro-adipogenic progenitors. Image source: Giordani *et al.* 2019 [21].

Skeletal muscle aging

During later stages of life, the structure and composition of the muscle tissue is altered, leading to significant effects on muscle performance. One of the most studied age-dependent changes is the loss of muscle quantity, attributed to a decrease in fiber size (i.e. atrophy) and to a selective decrease in the number (i.e. hypoplasia) of type II fibers. [22,23]. Although there are several factors contributing to this atrophy, this loss of fibers has been strongly associated with the denervation that occurs at the later stages of life: fibers that are de-innervated will disappear if they are not re-innervated by a pre-existing motoneuron [24]. Moreover, during aging, there is also a decrease in the number of satellite cells, the cellular precursors for myofibers that are activated upon damage to proliferate and fuse to the existing myofibers. The depletion of satellite cells directly affects the

formation of new fibers after damage and the preservation of muscle architecture [25,26]. This dysfunctional remodeling is coupled with a switch of the muscle stem cells from a myogenic to a fibrogenic [27] or adipogenic linage [28]. The first one is translated into an increase in collagen depositions, leading to increased stiffness of the connective tissue, which contributes to defective muscle performance [29]. The second one leads to fat accumulation between muscle bundles, which can lead to insulin resistance because of the release of pro-inflammatory cytokines such as tumor necrosis factor-α (TNF-α) which inhibits insulin signaling [30,31]. Moreover, there is a deregulation of autophagy, which induces the accumulation of toxic cellular waste in myofibers and satellite cells; this deregulation is associated with impaired muscle function and regeneration [32,33].

In aging, the energy production in muscle is also altered, based on a change in the redox status of the cell due to an increase in ROS and blunted antioxidant defenses. This results in mutations of mitochondrial DNA, leading to the production of dysfunctional electron transport chain components, and defective oxidative phosphorylation, thereby causing a further rise in ROS [34]. Mitochondrial morphology is also affected during aging, which interferes with energy production and increases mitochondrial-mediated apoptosis [35,36]. Moreover, muscle aging is characterized by its impaired mitophagy, leading to accumulation of damaged mitochondria, which is detrimental to muscle homeostasis [37,38]. There is a correlation between the release of damaged mitochondrial components into the extracellular matrix and the accumulation of pro-inflammatory cytokines in the plasma of elderly humans, contributing to the chronic inflammation termed 'inflamm-aging' [39].

All these events participate in the wasting of muscle during aging, in a process called sarcopenia. Sarcopenia is a major contributor to frailty and morbidity in the elderly. It has been shown that people aged ~75 years lose their muscle mass at a rate of 0.64–0.7% per year in women, and 0.8–0.98% per year in men, and that their muscle function is also lost at a rate of 3–4% per year in men and 2.5–3% in women [40]. There is an urgent need to find treatments and/or therapies that can prevent the development of sarcopenia or reduce the speed of its progression, as the progressive loss of skeletal muscle impacts several physiological parameters in a negative manner, such as breathing, vision, thermoregulation, movement, and metabolic body homeostasis [41].

Skeletal muscle in body metabolism

Apart from providing physical movement and support, skeletal muscle also plays a role in systemic energy balance. Muscle absorbs the majority of circulating glucose in the fed state, which can then be stored in form of glycogen for local energy production [42]. Approximately 40% of circulating glucose goes to muscle, 25–30% to liver, 15–20% to brain, and 10% to kidney. Apart from muscle, only liver, kidney, and astrocytes can form reserves of glucose in the form of glycogen [43,44], which can be utilized when there is no available glucose from the diet, such as during fasting or exercise. Apart from glucose, muscle can also use circulating lactate as a source for the tricarboxylic acid (TCA) cycle to produce energy [45]. Glycogen breakdown in muscle liberates glucose for local energy production, and the glucose liberated by glycogen breakdown from the liver supports circulating glucose levels to supply other tissues. After an extended period of fasting, glucose is produced by gluconeogenesis in the liver (and, to a lesser extent, in kidneys) and then is distributed to other tissues. Ultimately, when the need for gluconeogenesis is greatest after prolonged fasting or under severe metabolic stress, muscle protein can be depleted by catabolism, as certain gluconeogenic amino acids can be used as a substrate for glucose production [43]. For example, alanine and glutamine can be metabolized as substrates for gluconeogenesis in the liver, which in turn sends the resulting glucose into the bloodstream to supply other tissues. Although it is believed that skeletal muscle is the main source of amino acids, it has been recently observed that in the fasted state kidneys and liver also secrete essential amino acids (which cannot be synthesized by mammals and are only produced by protein breakdown) to the bloodstream and that the muscle incorporates these essential amino acids [46]. As part of the glucose-alanine cycle, alanine from skeletal muscle travels to the liver via the circulation, where it serves as a substrate of gluconeogenesis, and the glucose liberated is then taken up by the muscle [47]. In addition, in the Cori cycle, muscle-derived lactate is taken up by the liver and converted to pyruvate for use in gluconeogenesis [48]. Adipose tissue is also an important regulator of systemic energy homeostasis, as it stores glycerol and fatty acids in excess nutrient conditions. In nutrient deficit conditions, it supplies nutrients to other tissues through lipolysis [49]. To note, it has been recently observed from experiments in pigs, that muscle tissue may also act as a source of fatty acids in the bloodstream [46]. Each of these metabolic tissues plays a key role in supporting energy balance in the body (Figure 4). Temporal coordination of these tissue-specific metabolic outputs is a crucial component of systemic homeostasis and physiological functions maintenance.

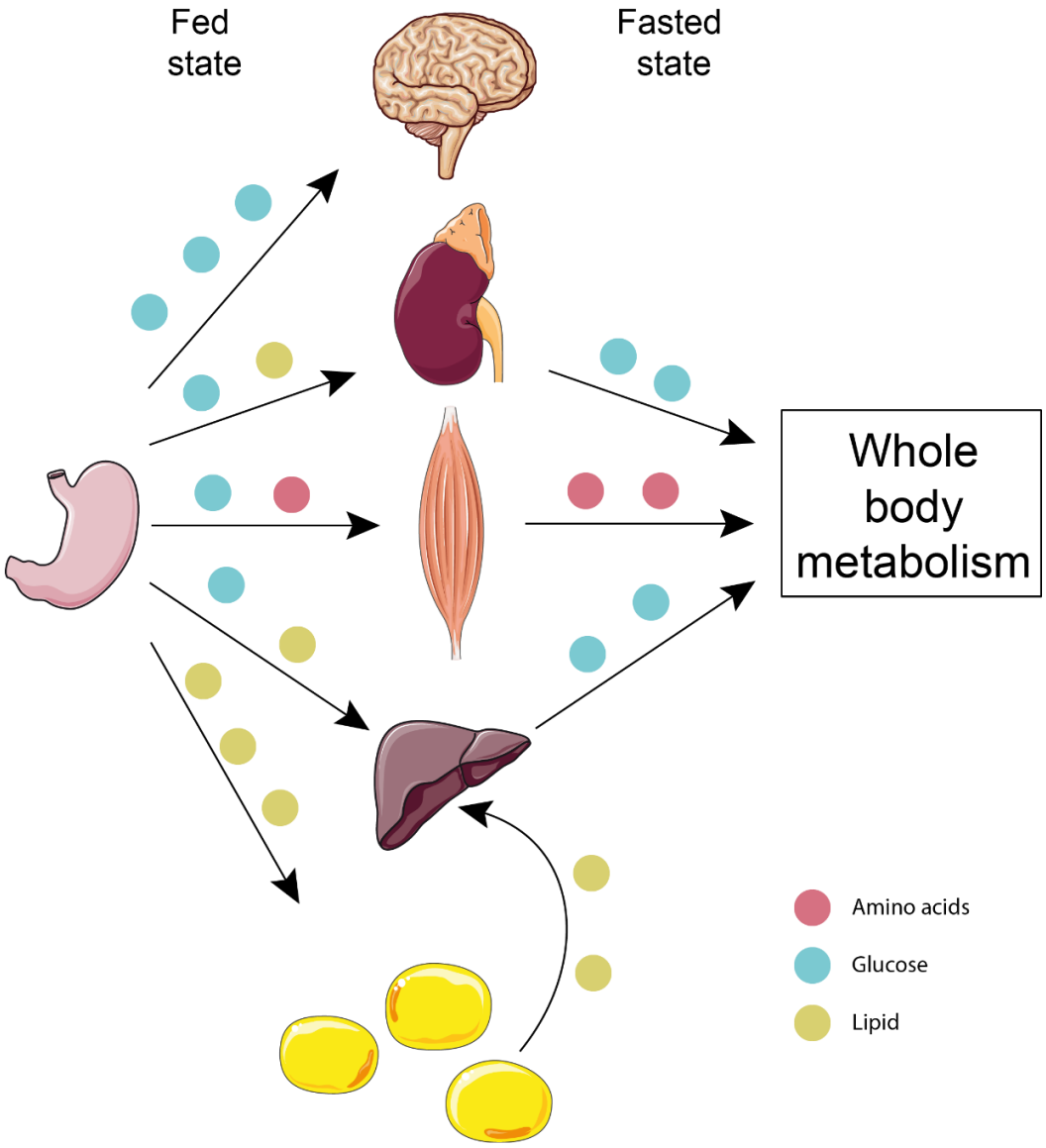

Figure 4. Scheme of nutrient metabolism. In the fed state, glucose, lipid, and amino acids are used or stored in the different organs. In the fasted state, these stored nutrients are used for the metabolic needs of the body. Image source: Argilés J. M. *et al.* 2016 [43] and (https://smart.servier.com/).

Circadian rhythms

Earth's daily rotation period creates a cycle of light and dark that lasts 24 hours. Consequently, the behavior and physiology of photosensitive beings are shaped to adapt to this circadian rhythm (stemming from the Latin '*circa diem*', "about a day"). The temporal organization of the internal processes provides an evolutionary rationale to explain why organisms should adapt to these day and night cycles. If an organism can anticipate environmental cues, it can use energy in a more efficient manner depending on the requirements of a specific moment of the day, and it can be prepared to avoid

radiation damage in advance. As such, evolution has endowed almost every organism with a circadian clock system, that allows them to sustain this rhythmicity robustly, even if light and dark cycles are absent. The first experiment that demonstrates this internal timekeeping is from 1,729 when Jean Jacques d'Ortous de Mairan realized that *Mimosa pudica,* which opens its leaves during the day and closes them during the night, was able to perform the same behavior even in constant darkness. Apart from light, other environmental cues (which are called *Zeitgebers*), such as time of feeding or time of exercise, can entrain specific components of the clock system within mammals [50,51]. Circadian alignment between cells and tissues is associated with health, whereas it is becoming increasingly clear that its misalignment is associated with increased incidences of diseases such as obesity, cancer, and cardiovascular disorders [52,53].

Organization of the circadian network in mammals

A small hypothalamic region called the suprachiasmatic nucleus (SCN), comprising 10,000 neurons and associated cell types in mice, is the central clock of our body [54]. It receives photic information directly from a specific cell type in the retina, called intrinsically photosensitive retinal ganglion cells (ipRGCs). ipRGCs are the only cells that communicate light information via the retinohypothalamic tract (RHT) to non-image-forming centers in the brain, such as the SCN [55–57]. When light signaling input arrives at the SCN, it triggers a transcriptional program that is coupled in all the neurons in this region of the brain [58,59]. These neurons, which are characterized by their enriched expression of vasoactive intestinal peptide (VIP) and arginine vasopressin (AVP), use GABAergic synapses to communicate [60]. In this way, the time of the SCN is aligned to the environmental time. Then, the SCN synchronizes the timing of all other tissues outside the brain via (i) sympathetic neuronal connections, (ii) the release of neuropeptides, and (iii) the release of hormones, through endocrine glands [61,62]. Although peripheral tissues respond to these hormonal signals, the SCN is not affected by them, thereby preserving its ability to respond solely to light-dark information [63].

VIP-expressing neurons of the SCN innervate the hypothalamic paraventricular/dorsomedial (PVN/DMH) nuclei which in turn signals to the pituitary and subsequently controls the secretion of corticosterone from the adrenal cortex [64–66]. Consequently, SCN lesions abolish these secretion rhythms [65]. This neuroendocrine control is not only limited to the hypothalamus-pituitary-adrenal (HPA) axis, as the SCN also coordinates the hypothalamic-pituitary-thyroid (HPT) axis. The thyroid-stimulating hormone (TSH), which stimulates the production of thyroid hormones from the thyroid

gland, is secreted rhythmically in humans and rats, and this rhythmicity is abolished after the ablation of the SCN [67–69]. Influencing these axes, the SCN has a role in controlling the homeostasis of metabolic functions within the body and regulating stress responses [69,70].

Apart from this neuroendocrine control, SCN-generated behavioral rhythms are important mechanisms by which the tissues of the body maintain their physiological functions aligned and coordinated with each other. SCN generates feeding/fasting, rest/activity cycles, and circadian modulation of body temperature [71]. Without a functional central clock, animals became arrhythmic in their activity and consume similar proportions of food during light and dark phases, impacting their metabolism [72]. By contrast, animals bearing SCN lesions can restore their circadian rhythms by implantation of fetal SCN tissue [73]. Similar to the mammalian suprachiasmatic nucleus, in plants, shoot apexes play a dominant role within the plant circadian system, which confirms that this ability of a central clock to sustain peripheral clocks is present in different eukaryotic kingdoms [74].

Until the 1980s, the SCN was considered to be the only pacemaker in mammals. However, the clock genes were then discovered and found to be expressed in virtually all the tissues of the body adding another layer of complexity to the circadian program, [75–78]. Already in the 1990s, it was discovered that the SCN was not the only tissue impacting the circadian rhythms of the entire body, but that every tissue has its own circadian oscillator governed by the clock genes, which in peripheral tissues are named peripheral clocks [79,80]. Today, it is accepted that each peripheral clock has its own level of autonomy from the SCN to drive some rhythmic function of the tissue (Figure 5). However, this level of autonomy has been only demonstrated *in vivo* in liver and skin as a result of mouse models in which only these specific peripheral clocks are present [81,82].

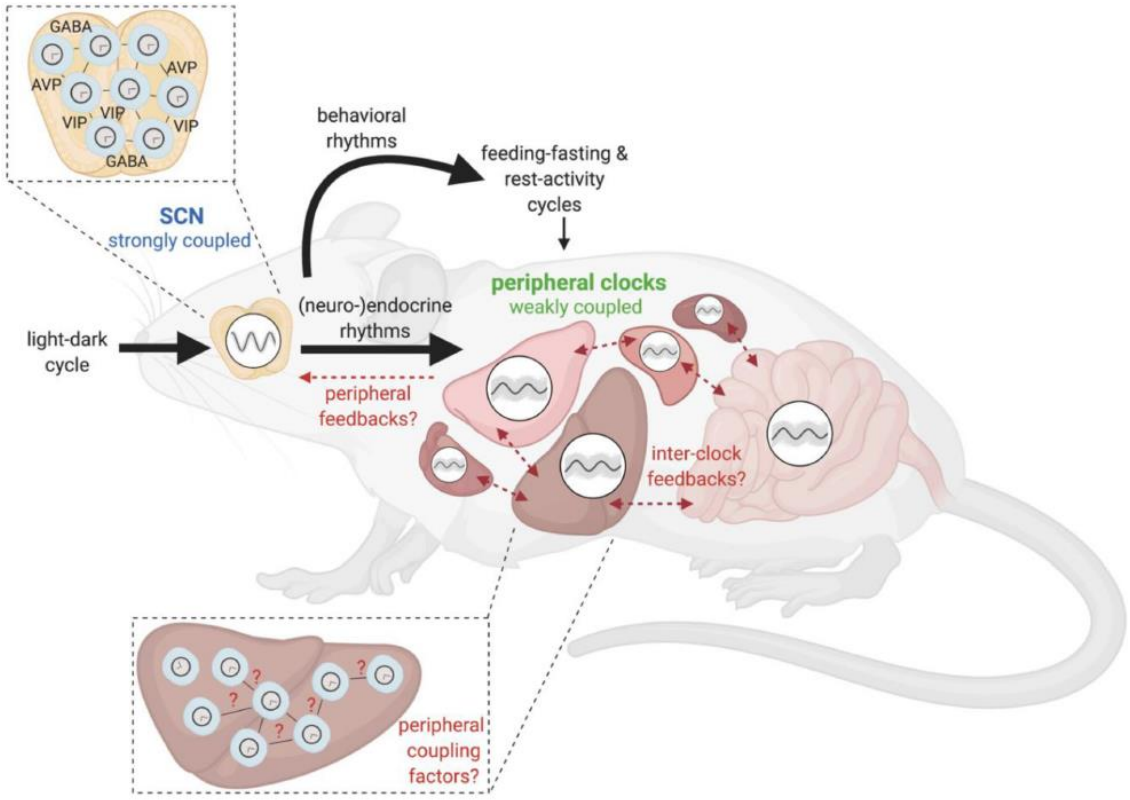

Figure 5. The central clock has the main role of coupling the peripheral clocks. The SCN in the hypothalamus constitutes a robust oscillator network that receives information about the light/dark cycle. It then produces behavioral and neuroendocrine rhythms that synchronize the peripheral clocks. These, in turn, have their autonomous oscillators. Image source: Finger, A.-M. & Kramer, A. 2021 [83].

Cell-autonomous clock molecular program

To maintain its circadian synchrony systems-wide, each tissue of the body requires that all of its cells (e.g., within that tissue) are functionally aligned with each other. To that end, there is a cell-autonomous clock molecular oscillator in virtually every cell of the body. The molecules implicated in this program have been extensively studied, and in 2017, Michael W. Young, Michael Rosbash, and Jeffrey C. Hall were awarded the Nobel Prize for their early studies on the molecular clock [75–78].

The cell-autonomous molecular oscillator is composed of a transcriptional-translational feedback loop (TTFL), in which the positive regulators are the transcription factors CLOCK (Circadian Locomotor Output Cycles Kaput) and its interacting protein BMAL1 (Brain and Muscle ARNT-Like 1). They form heterodimers and bind to the E-box motif of clock-controlled genes (CCG) which are tissue-specific, regulating their transcription (Figure 6). BMAL1 has been described as an essential, non-redundant component of the

circadian clock program in mammals, as its loss results in a complete loss of circadian rhythmicity in mice [84]. Among other core clock genes that need to have a circadian expression to accomplish cell rhythmic functions, *Per* (*Period, 1–3*) and *Cry* (*Cryptochrome, 1–2*) are targets of CLOCK/BMAL1 complex, and their transcription is directly regulated by them. When PER and CRY proteins located in the cytoplasm are translocated into the nucleus, the transcriptional activity of BMAL1/CLOCK is blocked, thereby serving as the negative regulators of the TTFL and inhibiting their own transcription [77,85]. Three kinases (kinase 1ϵ, CK1δ; mitogen-activated protein kinase [MAPK], and glycogen synthase kinase-3 beta) are involved in the phosphorylation of the clock components and trigger their subsequent degradation by 26S proteasome [86–90] (Figure 6).

The defined TTFL is the main component of the cell-autonomous program and lasts 24 hours. There are additional regulators involved in providing robustness to the core clock, such as REV-ERBα (also called NR1D1), REV-ERBβ (NR1D2), and ROR (RAR-related orphan receptor), that compete and bind to the DNA-binding elements (ROREs) in the *Bmal1* promoter, suppressing (REV-ERB elements) or activating (ROR) its transcription [91] (Figure 6).

In addition, the TTFL is further regulated by several post-translational modifications and interactions with other proteins, adding another layer of complexity to the cell circadian program. For example, CLOCK and BMAL1 interact with histone acetyltransferases (HATs) p300 and CREB-binding protein (CBP) respectively allowing histone acetylation and the promoting chromatin accessibility [92–94]. It is also known that the NAD^+-dependent histone deacetylase (HDAC) sirtuin 1 (SIRT1) associates with CLOCK, BMAL1 and PER2 [95,96]. *Nampt*, which is a target gene of BMAL1/CLOCK, produces rhythmic levels of NAD+ that in turn leads to a circadian SIRT1 activity, which inhibits the BMAL1/CLOCK complex [97].

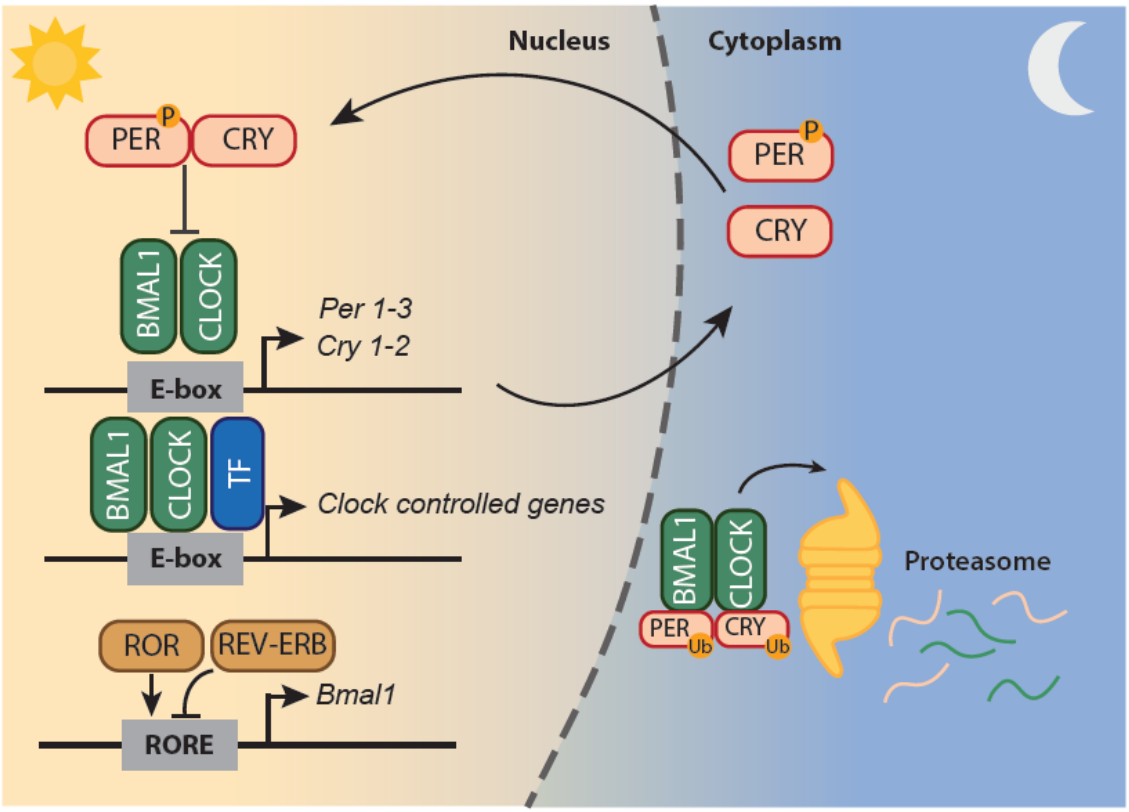

Figure 6. Circadian clock molecular program. Molecular clocks comprise the transcription factors (TFs) CLOCK/BMAL1, which bind to E-boxes as a heterodimer and drive the expression of their inhibitory proteins PER/CRY. A PER/CRY protein complex enters the nucleus, where it inhibits the CLOCK/BMAL1 transcriptional activity, in an autoregulatory transcriptional-translational feedback loop. Phosphorylation of these protein complexes by several kinases promotes their polyubiquitination and subsequent degradation by the 26S proteasome complex. The regulators REV-ERB and ROR can repress or activates, respectively, *Bmal1* transcription. Image source: Vaca-Dempere. *et al.* 2022 [98].

The proteins that form part of the TTFL also have other functions outside the described loop. For example, the CRY and REV-ERB proteins interact with glucocorticoid receptor (GR), thereby inhibiting its transcriptional activity [99,100]. CRY also imposes a timing for glucagon effect on gluconeogenesis [101] by inhibiting signaling downstream of the glucagon receptor. Altogether, the molecular clock interacts cooperatively with different TFs to further drive a large number of cell type-specific, rhythmic molecular programs that will specify the rhythmic functional output of each cell type [102].

Circadian rhythms in skeletal muscle

Although all cells share the same circadian transcriptional program, the output in each cell type is different, depending on their metabolic requirements. The circadian

transcriptome of skeletal muscle was described for the first time in 2007 [103]. In this first study, microarray analyses were used to determine the rhythmicity of the transcripts. A total of 215 circadian genes were identified, which have roles in transcription, lipid metabolism, protein degradation, ion transport, and vesicular trafficking. Moreover, muscle genes, such as *MyoD, Ucp3, Atrogin1,* and *Myh1*, demonstrate a rhythmic pattern of expression.

Role of the clock in muscle function and maintenance

Bmal1 total knockout (KO) mice show a premature muscle aging phenotype, which includes progressive myofiber atrophy, reduced muscle force, decreased activity level, and a shortened lifespan [104]. The muscle of these animals develops less specific tension (a measure of muscle function), which may be a result of the disrupted arrangement of the thin and thick filaments in their myofibers as well as of the decreased mitochondrial volume [105]. *Bmal1* KO mitochondria exhibited a pathological morphology with disruption of cristae, which had a direct effect on their function. Impaired muscle oxidative capacity was also detected, together with a decreased cross-sectional area (CSA), an accumulation of fibers with central nuclei, an increase in fibrosis, and a decrease of satellite cells in muscles from these KO animals [106]. However, additional circadian clock mutants also present muscle alterations. *Clock* mutant mice (*Clock*$^{\Delta 19/\Delta 19}$) present a clear myofilament structure disarrangement and alterations in the mitochondrial content of skeletal muscle [107]. In addition, although the muscle of *Clock*$^{\Delta 19/\Delta 19}$ female mice can uptake glucose to the same levels as their wild-type littermates, it presents significantly reduced fatty acids uptake [108]. *Rev-erbα* KO mice exhibit reduced mitochondria content and oxidative function in skeletal muscle, resulting in a compromised exercise capacity [109]. *Rev-erbα* deficiency deactivates the STK11–AMPK–SIRT1–PPARGC1-α signaling pathway whereas autophagy is upregulated, resulting in impaired mitochondrial biogenesis and increased clearance [109]. Lastly, mice with disrupted *Per2* present a loss in circadian locomotor activity in constant darkness [110,111]. Altogether, these studies highlight the effects of molecular clock disruption on the whole organism and shed light also on the importance of circadian clock integrity in skeletal muscle structure and performance.

Apart from these whole-body mutants, several groups have generated models to specifically silence core clock genes in the skeletal muscle tissue, which can give a better idea of the role of the autonomous clock in muscle. In this regard, muscle-specific *Bmal1-KO* (mKO) has been the model most extensively studied. These mKO mice have a

regular lifespan and growth curve, and their muscles present an increased weight, which is not present in their other tissues, such as epididymal fat [112]. Muscle ultrastructure and histology are also apparently normal. Although these mice do not show any prominent signs of muscle aging, they do have a slight decrease in muscle force [112]. As expected, oscillation of core clock genes is largely abolished in their skeletal muscle. At a transcriptional level, there is deregulation in the insulin signaling pathway in mKO muscles, which is accompanied by a decrease in muscle deoxyglucose uptake. This impaired glucose uptake by muscle is not dependent on the developmental stage in which *Bmal1* is silenced, as this insulin insensitivity was also detected with an inducible muscle *Bmal1*-KO model (imKO) [112]. Additionally, although this imKO model showed normal force after 5 months of *Bmal1* depletion, it was reduced after 14 months [106,112]. Finally, imKO mice show an increase in the fibrosis content of muscles. These studies using both constitutive and inducible models of skeletal muscle *Bmal1* KO strongly suggest that *Bmal1* has a critical role in muscle function.

Although it is subject of some controversy, there is also a possible role of the molecular clock in the control of myofiber formation. There are studies suggesting that *Myod1* (myogenic determination factor 1), a master regulator of myogenesis, shows circadian oscillation under the control of the molecular clock and that its rhythmicity is abolished in *Bmal1*$^{-/-}$ and *CLOCK*$^{\Delta 19}$ mice [107,113]. Moreover, MYOD has been proposed to control *Bmal1* expression and amplitude through a feedforward regulatory loop, as it binds at the enhancer of its promoter [114]. However, this is still subject to debate [115]. Other important muscle genes (such as these encoding myosin heavy chain, troponin, and calcium regulatory proteins), and pathways important for muscle maintenance (such as Wnt, MAPK, AMPK, and mTOR), have been suggested to be under the control of the muscle clock, [103,116–118]. Nonetheless, more studies are needed to properly define the role of the clock in fiber formation and skeletal muscle structure development.

Clock functions in muscle metabolism

Skeletal muscle is critical in the daily control of whole-body energy, metabolism, and glucose homeostasis. The first pieces of evidence came from studies showing that, in mouse muscle, glycogen content peaks at 8 AM and falls at 8 PM, and that it is dependent on feeding and fasting conditions, as well as modulated by endurance exercise [119,120]. These results emphasize that skeletal muscle continuously senses and responds to relevant inputs, including the nutritional status of the body. Correct synchronization with the nutritional status of the organism is crucial for muscle since

rhythmic anabolism and catabolism can define muscle structure. Moreover, soleus and *tibialis anterior* (TA), which are predominantly formed of slow and fast fibers respectively, have remarkable differences in their circadian transcriptome, which highlight the cell-type specificity of clock action, influencing muscle metabolism [121].

When the muscle circadian transcriptome was described for the first time, it was evidenced that metabolism is temporally tightly organized in this tissue already at the level of gene expression. Of the rhythmic genes detected, 21% of them were involved in metabolism. More specifically, 12% of genes had a role in protein metabolism, highlighting the importance of enduring proper temporal degradation and synthesis of proteins in this tissue [103]. In addition, in the same study, it was found that *Clock* mutants were having a phase shift in the expression of pyruvate dehydrogenase kinase 4 (*Pdk4*), which codifies for a kinase that regulates the activity of pyruvate dehydrogenase (PDH) which, in turn, catalyzes the conversion of pyruvate to acetyl-CoA during glucose oxidation. This was already suggesting that glucose metabolism was highly dependent on the muscle clock [103], which has been supported by later studies. For example, it is known that during the rest/fasting phase, there is reduced contractile activity and decreased glucose uptake, whereas fatty β-oxidation is promoted, the moment in which PDK4 is activated and PDH inhibited. During the active/feeding state, there is a rise in blood glucose together with an increase in locomotor activity, which promotes the activation of pyruvate dehydrogenase phosphatase catalytic subunit 1 (PDP1), which is dependent on the increase of intracellular calcium that occurs during contraction stimulation [122]. This results in the activation of PDH complex. Muscles from both *Bmal1* mKO and imKO animals presented a significantly decreased PDH activity, via reduced expression of glucose transporter 4 (GLUT4) and TBC1D1 (a Rab-GTPase involved in GLUT4 translocation to the plasma membrane), and an altered expression of *Pdk4* and *Pdp1*. This deregulation results in a loss in metabolic flexibility in skeletal muscle, and a glucose metabolism channeled to alternative pathways including the polyol, pentose phosphate, and glucuronic acid pathways. This propitiates the muscle insulin resistance observed in these animal models [112]. However, whole-body levels of glucose remain unmodified in animals with an incompetent muscle clock.

Glucose is the main fuel of muscle during the active state, but fatty acids are used by this tissue in the resting phase. Thus, the muscle should perfectly coordinate these two events. In 2015, the muscle circadian transcriptome was analyzed to investigate whether the genes involved in these functions were rhythmic and interdependent. As previously suggested [102], this study identified that during the mid-inactive period, genes involved in

fatty-acid breakdown were peaking, pointing to lipids as the main source of energy during this time [123]. During the early active period, this pattern changes, and genes that regulate glycolysis and glycolytic flux reach their maximum expression, suggesting a shift of fuel utilization from lipids to carbohydrates. Finally, genes involved in glucose and lipid storage peaked toward the end of the active phase, where excess energy is stored for usage during the post-absorptive phase [123] (Figure 7). Muscles from imKO animals had disrupted expression of genes involved in lipid and carbohydrate metabolism [123]. This shows that the muscle-autonomous clock regulates such fuel utilization not only by controlling the timing of glucose metabolism but also by coordinating it with lipid metabolism. Muscles from mKO animals present impaired lipid storage; in wild-type animals, intramuscular triglyceride content varies from day to night, yet these rhythms are abolished in mKO [124], which could be a result of deregulated expression of important genes involved in lipid mobilization and storage (e.g., *Atgl, Pnpla2* and *Plin5*).

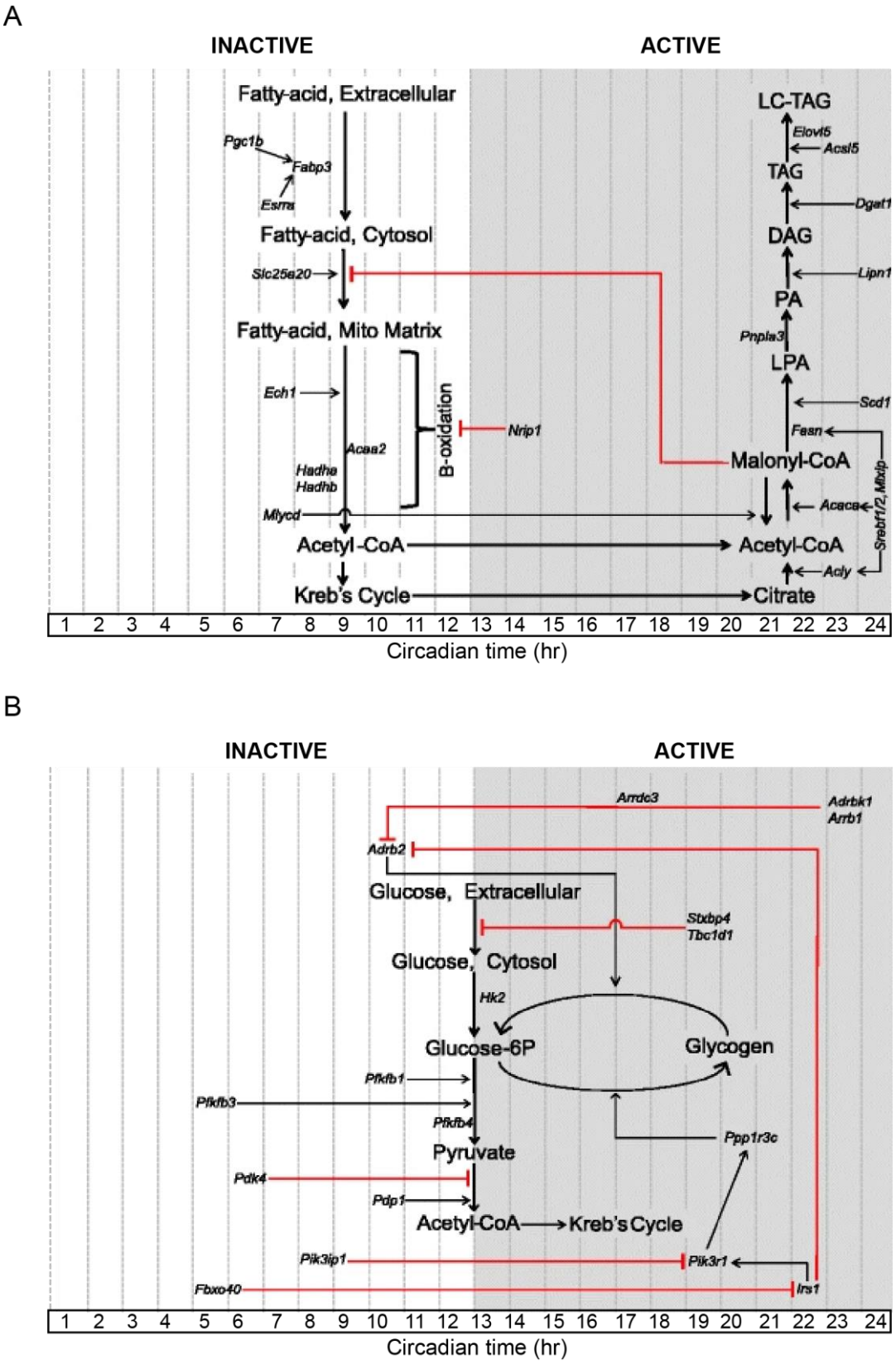

Figure 7. Diagram of muscle circadian genes involved in lipid and glucose metabolism. Circadian genes are involved in A) lipid and B) glucose metabolism. The genes shown in italics have their peak of expression in the corresponding circadian time shown on the x-axis. Image source: Hodge, B. A. *et al.,* 2015. [123]

In addition to lipid and carbohydrate metabolism, muscle also needs to regulate amino acid metabolism. When glucose availability is low in the body, muscle uses lipids as a source of energy, and at the same time increases protein degradation for the production and release of amino acids destined for gluconeogenesis [125]. Previous work suggested that REV-ERBα is involved in the mobilization and metabolism of lipids and amino acids, together with BMAL1 in skeletal muscle [124]. In addition, REV-ERBα cooperates with GR to regulate important genes for protein turnover, such as *Trim63, Fbxo32,* and *Ubc.* Rescuing REV-ERBα in mKO via electric-pulse mediated gene transfer led to 20%-50% reduced expression of genes involved in the ubiquitin-proteasome system (*MuRF-1*, *Atrogin-1*, *polyubiquitin-C*, and genes codifying for proteasome subunits) which directly affects protein metabolism by inhibition of the ubiquitin-proteasome system [124]. Moreover, in muscles from mKO there is a huge increase in glucogenic amino acids. In particular, the alanine content is increased also in serum of mKO mice, which indicates an energy deficit and an increase in proteolysis in these muscles, or a muscle defect in energy sensing related to loss of BMAL1 in muscle that can impact systemic energy homeostasis [124].

Finally, metabolism of carbohydrates, lipid, and amino acids are intimately linked to mitochondria function. Mitochondria are the ATP suppliers of the cell, and in skeletal muscle, their role is crucial to sustaining a normal muscle function. Several rate-limiting mitochondrial enzymes accumulate in a diurnal manner and are dependent on the clock proteins [126]. In addition, its fission/fusion rate is also rhythmic, which in turn regulates mitochondrial metabolism [127]. In humans, the oxidative capacity of skeletal muscle mitochondria displays day/night oscillations [128]. Notably, the clock has also a role in the maintenance of the integrity of mitochondria, as whole-body clock mutants present a 40% reduction of mitochondrial mass, with aberrant morphology and uncoupling of respiration, which is suggested to be driven by the altered expression of *Pgc* genes present in these mice [107].

Muscle clock regulation by food intake

Although the main trainer of our circadian clock is light, other *zeitgebers* can shape the phase of our body clock. Our bodies respond to stimuli differently, depending on the time when the stimulus is applied as well as on the intensity of the signal. The timing of eating is a powerful *zeitgeber*. Although in normal conditions the brain generates feeding/fasting rhythms [129,130], forcing eating during the inactive time of animals can produce an uncoupling from the central pacemaker to peripheral tissues. This happens because the

SCN clock is not affected by the changes in the feeding time, whereas peripheral tissues completely shift their autonomous clock to be aligned to the time of food availability. Interestingly, the kinetics of synchronization to the feeding paradigm depends on the tissue, being faster in the liver and slower in the kidney, heart, or pancreas [131]. Notably, under adrenalectomy conditions, this shift in peripheral tissues is even faster. This suggests that the SCN activity patterns, which are driven by light, use the adrenal gland to force the peripheral tissues to remain in the same phase. However, when the adrenal glands are removed, peripheral tissues are "free" from the central clock to align their phase faster to the new feeding paradigm [132].

Eating mainly during the active time of the day helps to temporally organize biochemical pathways that are not compatible. For instance, in humans, mistimed eating can promote the development of metabolic diseases [50]. Moreover, control of feeding time through time-restricted feeding (TRF) can prevent obesity and hyperinsulinemia in mice subjected to a high-fat diet (HFD) regimen [124]. Specifically, when food is only available for 8 hours during their active time (which is the dark phase, during which mice normally consume 80% of their calories), animals under TRF and HFD do not present the metabolic problems of their *ad libitum* counterparts, although the amount of ingested calories were the same [133].

In addition to preventing metabolic diseases in normal animals, feeding rhythms are powerful enough to restore rhythmic patterns and circadian gene expression in several clock-deficient mouse models. For example, in *Cry*-deficient animals (*Cry1*;*Cry2* KO), metabolic parameters such as respiration exchange ratio (RER), do not oscillate under *ad libitum* conditions; however, under TRF, RER gains oscillation in these mutants [134]. In addition, the disrupted liver circadian transcriptome of this model can be partially restored by rhythmic food intake [135] and it is suggested that the circadian clock and feeding time also dictates the levels of lipids in the liver, regulating its metabolism [136]. Apart from this clock mutant model, liver-specific *Bmal1* KO*,* and *Rev-erbα/β* KO transgenic lines, have also been used to assess the effects of TRF. Using metabolic cages (which allow measuring RER, physical activity, and food/water intake), it was evident that these transgenic mice have absent rhythms in terms of fuel utilization. These defects were remarkably recovered by applying TRF, even in the absence of a circadian clock [134]. Recent studies have shown that there is an interdependent role of feeding time and the cell-autonomous clock for rhythmic gene expression in the liver [137].

In addition to metabolic regulation, TRF has also a powerful effect on preventing the aging phenotype of clock mutants, as shown in flies in which cardiac aging is reduced via TRF through the circadian clock, the TRiC chaperonin, and mitochondrial electron transport chain (ETC) components [138]. It has also been demonstrated that intermittent TRF (iTRF, with flies fasting for 20 h every other day, starting at mid-morning, with a day of *ad libitum* feeding between fasting days) extends the fly lifespan through a mechanism involving circadian rhythms and autophagy, and delayed the onset of aging markers in the muscles and gut [139].

Although the majority of the studies that focus on the effect of feeding rhythms in clock have focused on the whole body physiology or liver-only functions, some have shed light on the specific impact of feeding rhythms on skeletal muscle. For instance, mice forced to eat only during the daylight phase (which is their inactive time) showed alterations in their skeletal muscle clock. The expression phase of *Bmal1, Per1,* and *Per2* shift for almost 12 hours under this feeding paradigm; this impressive effect on muscle was not achieved with other interventions that are known to cause changes in muscle functional properties (such as denervation), which proves the importance of the coordination between feeding rhythms and muscle clock [121]. The effect of TRF in preventing the detrimental effects of obesity on the muscle of flies showed that 12 hours of TRF attenuated myofibrillar and mitochondrial abnormalities in muscle fibers of these flies by suppressing AKT activation levels, fat deposits, and insulin resistance [140]. In mice, mitochondrial respiration rhythms of soleus can be abolished in light phase–fed conditions, which is accompanied by an altered expression of genes involved in mitochondrial biogenesis and the fission/fusion machinery [141]. In humans, recent studies have started to investigate the beneficial effect of TRF on muscle tissue. In young adults, there is an increase in glucose and branched-chain amino acids uptake in muscle after two weeks of TRF [142]. In overweight persons, TRF regulates the rhythmicity of genes controlling amino acid transport and affects the rhythmicity of serum and muscle metabolites [143]. However, the effect on the skeletal muscle of older persons is still under examination [144].

HYPOTHESIS AND OBJECTIVES

Each tissue has a molecular circadian clock, but this has limited capabilities to drive autonomously the tissue's required daily physiological functions. Indeed, tissues rely on a network of molecular clocks that are essential for whole organism health, which can be disrupted by aging and lifestyle changes. However, several key issues remain largely unknown, including the identity of the key signaling nodes of this complex network, the manner in which clock communication is supported, and how can it be sustained during aging. There is evidence showing that the brain sends continuous cues in form of hormonal signals, feeding/fasting, and activity/resting cycles, which are integrated by the skeletal muscle to perform its metabolic and locomotor functions at the appropriate time of the day. We hypothesize that the simultaneous activation and communication of the central and peripheral muscle clocks (but not of either one alone) could sustain a large proportion of daily muscle physiological functions. Moreover, as muscle largely relies on HPA axis to regulate its daily internal pathways, we hypothesize that the adrenal gland can have a role in this communication. In addition, as feeding/fasting cycles have a powerful effect on muscle function, we propose that it is a dominant output of the central brain to drive the muscle clock. Finally, during aging, there is a dampening of muscle function, which affects the homeostasis of the whole body. To prevent this performance loss, we propose that scheduled feeding cycles can restore muscle circadian functions in physiological or prematurely aged mice, which in turn will improve healthspan.

The main objectives of this thesis were to determine the role of the central and peripheral clock on muscle physiology, how they communicate, and to define the importance of this node in muscle aging. The specific objectives were:

1. To understand the importance of central and peripheral muscle clocks in muscle homeostasis in a context in which these two clocks can be activated selectively in an otherwise clock-less animal.
2. To determine the mechanism of communication between brain and muscle clocks
    a. Characterize in-depth the role of the adrenal gland in this communication.
    b. Study the effect of feeding/fasting rhythms on the muscle-autonomous clock.
3. To study the effect of time-restricted feeding in muscle as a possible strategy to delay physiological aging.

MATERIALS AND METHODS

Animals

Mice were bred and maintained at the animal facilities of the Barcelona Biomedical Research Park in strict accordance with the Spanish and European Union regulations. All experimental protocols were approved by the Catalan Government, following applicable legislation and the guidelines of the Institutional Animal Care and Use Committee (IACUC) of the Barcelona Science Park.

To study the role of several clocks in muscle circadian regulation, *Bmal1-stop*FL mice were generated as described in Welz *et al*. [81]. Using a gene trap approach, a stop cassette was flanked by loxP sites and introduced after the first translated exon (exon 5) of the *Bmal1* gene. This cassette contains a splice acceptor (SA), a mCherry reporter gene, a poly-A tail, and a neomycin resistance cassette flanked by FRT sites. The neomycin resistance cassette flanked by FRT sites was used for clonal selection and removed by FLP-mediated recombination after successful germline transmission. The presence of this cassette prevented the translation of BMAL1 protein. Upon Cre recombinase expression in the tissue of interest, the stop cassette is removed and *Bmal1* expression is rescued specifically in that tissue under its own promoter. The genetic approach is outlined in Figure 8.

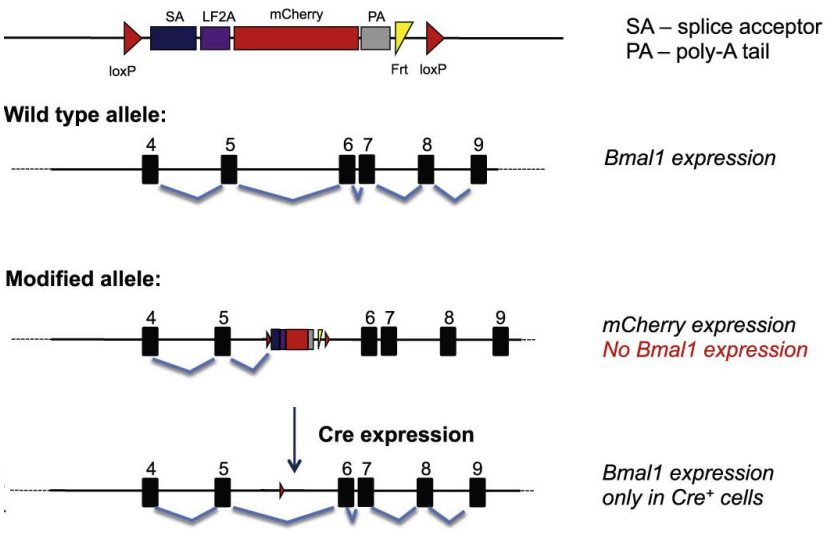

Figure 8. *Bmal1-stop*FL genomic targeting scheme. *Bmal1* is expressed only in the tissue of interest following the excision of the stop cassette upon Cre recombinase expression. Image source: Welz, P. S. *et al.*, 2019. [81]

Due to the sterility of homozygous mice for *Bmal-st-fl* allele, heterozygous mice for that locus were crossed with mice expressing the Cre recombinase under the regulation of

Acta1 (Hsa) promoter (Hsa-Cre), and the synaptotagmin10 (*Syt10*) promoter (*Syt10*-Cre) to obtain the following experimental mice: (1) WT (*Bmal1-stop*FL$^{wt/wt}$), (2) muscle-RE (*Bmal1-stop*FL$^{f/f}$ Hsa-Cre$^{tg/wt}$), (3) KO (*Bmal1-stop*FL$^{f/f}$ *Hsa*-Cre$^{wt/wt}$ *Syt10*-Cre$^{wt/wt}$), (2) brain-RE (*Bmal1-stop*FL$^{f/f}$ Hsa-Cre$^{wt/wt}$ *Syt10*-Cre$^{tg/wt}$), and (5) RE/RE (*Bmal1-stop*FL$^{f/f}$ *Hsa*-Cre$^{tg/wt}$ *Syt10*-Cre$^{tg/wt}$). Figure 9 outlines the breeding strategy. The mice genotypes were confirmed by PCR.

Figure 9. Breeding strategy to obtain experimental animals. Overall, 6.25% of the progeny obtained are KO, muscle-RE, brain-RE, or RE/RE.

Animals were maintained in standard 12 h:12 h light/dark photoperiods and fed *ad libitum* unless otherwise specified. All mice were used at an average age of 10 weeks (range 9–12) and 26 weeks (range 25–28), except physiologically aged mice, which were used at 85–116 weeks of age. All animals were generated in a C57BL/6 background.

Male and female littermates were used for lifespan, metabolic cages analysis, and RNA-seq experiments (whereby 2 males and 2 females were used per timepoint unless otherwise specified). For histological analysis and adrenalectomy experiments, female mice were used; for all other experiments (body weight, food consumption, *extensor digitorum longus* [EDL] *ex vivo* force measurements, and oral glucose tolerance test), males were used.

Genotyping

To confirm the genotypes of the mice, an earsnip was digested to obtain genomic DNA. Three different polymerase chain reactions (PCR) are performed to determine the haplotype of the mice: 1) *Hsa*-Cre; 2) *Syt10*-Cre and 3) *Bmal-stop*FL. The primers used are listed in Table 1. The PCR programs used are described in Figure 10.

Table 1. Primers were used to determine the genotypes of the experimental animals. Fw: forward; Rv: reverse

HSA-Cre	
HSA-Cre Fw	CCCGCAGAACCTGAAGATGT
HSA-Cre Rv	CAGCGTTTTCGTTCTGCCAA
SYT10-Cre	
SYT10-Cre Fw	AGACCTGGCAGCAGCGTCCGTTGG
SYT10-Cre Rv	AAGATAAGCTCCAGCCAGGAAGTC
SYT10-Cre common	GGCGAGGCAGGCCAGATCTCCTGTG
***Bmal1-st* FL-Cre**	
Bmal1 -stFL-Cre Fw	CCCCCTACTCCTCTTCACCT
Bmal1 -stFL-Cre Rv	TCAGCCAGAGTAGCCAGACA
Bmal1 -stFL-Cre common	GCCTGTCCCTCTCACCTTCT

HSA-Cre		
Temperature (ºC)	Time (minutes)	Cycles
94	1	1
94	0,5	30
62	0,5	
72	0,75	
72	7	1
4	∞	

SYT10-Cre		
Temperature (ºC)	Time (minutes)	Cycles
95	3	1
95	0,5	38
63	1	
72	1	
72	5	1
4	∞	

***Bmal1-st* FL-Cre**		
Temperature (ºC)	Time (minutes)	Cycles
95	3	1
95	0,5	38
63	1	
72	1	
72	5	1
4	∞	

Figure 10. PCR programs to determine the genotype of the experimental animals.

Using a 1.5% agarose gel, the bands detected were:

1. *Hsa*-Cre: a 400 basepair (bp) band for *Hsa*-Cre^{tg} allele; no band for *Hsa*-Cre^{wt} allele;
2. *Syt10*-Cre: a 350 bp band for *Syt10*-Cre^{wt} allele and a 500 bp band for *Syt10*-Cre^{tg} allele;
3. *Bmal1-st*FL: a 294 bp band for *Bmal1*-stopFL^{wt} allele and a 444 bp band for *Bmal1*-stopFL^{tg} allele.

Time-restricted feeding

Mice under a time-restricted feeding (TRF) regime had free access to food for 9 to 10 hours during their active phase (e.g., the dark phase) from zeitgeber time (ZT) 13/14 to ZT22/23 (with lights on at ZT0) from Monday to Friday, and for 7 to 8 hours, from ZT12 to ZT19/20, on weekends. Mice were put on TRF starting at 10 weeks of age until 24 to 27 weeks of age. For physiologically aged animals, TRF started at 63–76 weeks of age and finished at 85–107 weeks of age (5–7 months).

Indirect calorimetry and locomotor activity

The exchange of carbon dioxide for oxygen was measured by indirect calorimetry. In this method, the ratio between oxygen and carbon dioxide changes depending on the fuel of energy the animal uses (carbohydrate, fat, protein or a mixture of the three). Oxygen consumption (VO_2) and CO_2 production (VCO_2), are used to determine energy expenditure (EE), respiration exchange ratio (RER), and glucose and lipid oxidation of the animals [145–147].

Measurements of indirect calorimetry and ambulation were performed using an indirect calorimetry system (Oxymax, Columbus Instruments). Mice were acclimatized into the metabolic cages for 1 to 2 days, and then data were recorded for 3 consecutive days. To assess indirect calorimetry measurements, 3 to 7 mice per condition were used.

Western blot

Total homogenates from gastrocnemius muscles were obtained in RIPA lysis buffer (50 mM Tris-HCl pH 8, 150 mM NaCl, 5 mM EDTA, 15 mM $MgCl_2$, and 1% NP-40), supplemented with protease and phosphatase inhibitors (Sigma Aldrich, Complete Mini; Sigma Aldrich, Phosphatase Inhibitor Cocktail 1 and Phosphatase Inhibitor Cocktail 2).

Samples were lysed for 30 min on ice and centrifuged at 13,000 rpm for 15 min at 4ºC, and the supernatant was collected. Protein concentrations were measured using the Bradford method (Protein Assay, Bio-Rad). About 30 to 60 µg protein from each sample was resolved on 4%–12% gels (BioRad) and transferred to nitrocellulose membranes, which were blocked with 5% instant non-fat milk in TBS-T (0.1% Tween-20, TBS) for 2 hours at room temperature. The following primary antibodies were used (diluted in 5% milk TBS-T) and incubated overnight (O/N) at 4 ºC: anti-phosphorylated BMAL1 (Ser42) (Cell Signalling #13936), anti-BMAL1 (Abcam #93806), and monoclonal anti-α-tubulin antibody (Sigma-Aldrich, #T-6199). Following HRP-conjugated secondary antibody incubation (Jackson ImmunoResearch Donkey anti-rabbit IgG #711-001-003; Agilent Dako Rabbit anti-mouse immunoglobulins/HRP, #P0260) for 1 hour at room temperature, blots were visualized with ChemiDoc MP (BioRad, ChemiDoc™ MP Imaging System #12003154). The α-tubulin signal was used as the loading control.

The antibodies used are listed in Table 2.

Table 2. Antibodies used for Western blot. pBMAL1: phosphoBMAL1; HRP: HorseRadish Peroxidase; TBS-T: Tris-buffered saline Tween-20.

Antibody	Dilution	Blocking	Description	Reference number
pBMAL1 (Ser42)	1:1000	5% milk in TBS-T	Rabbit polyclonal	Cell Signalling #13936
BMAL1	1:1000	5% milk in TBS-T	Rabbit polyclonal	Abcam #93806
α-tubulin	1:1000	5% milk in TBS-T	Mouse monoclonal	Sigma-Aldrich, #T-6199
HRP-conjugated	1:10000	5% milk in TBS-T	Donkey anti-rabbit IgG	Jackson ImmunoResearch #711-001-003
HRP-conjugated	1:4000	5% milk in TBS-T	Rabbit anti-mouse immunoglobulins	Agilent Dako #P0260

Muscle force measurements

Ex vivo force measurements of EDL muscle were assessed as previously described [148,149]. Briefly, mice were sacrificed, and muscles were taken and placed into Krebs–Ringer bicarbonate buffer solution, with 10 mM glucose, continuously oxygenated. The ankle end of the EDL muscle was linked to a fixed clamp, whereas the knee end was connected to the lever arm of an Aurora Scientific Instruments 300B actuator/transducer system. To maintain the EDL muscle in this position, a nylon thread was used to tie the tendons of the muscle to the machine. A stimulation frequency ranging from 1 to 200 Hz was used to determine the maximum isometric-specific tetanic force, taking this value from the plateau of the curve. Then, the force was normalized per muscle area (obtained by dividing the muscle mass by the product of longitude and the density of muscle [1.06 mg/mm^3]) to calculate the specific force (mN/mm^2).

Muscle electroporation and MitoTimer visualization

For MitoTimer gene transfection in muscle, MitoTimer plasmid (Addgene #52659) was purified using an Endrofree plasmid kit (Qiagen #12362) and dissolved in PBS at a final concentration of 2.5μg/mL. 30 μL of this solution were injected directly into *tibialis anterior* (TA) muscle of anesthetized animals. After injection, an electroporator (BTX™ ECM™ 830 Electroporation Generator, Fisher Scientific #450052) was used to apply 10 pulses of 20 ms per muscle (175 V/cm, 1 Hz). The application of an electrical field to the muscle increases the permeability of the cell membrane, allowing the efficient delivery of plasmid DNA *in vivo*.

To observe MitoTimer labeling in muscle, 10-μm thick cryosections were cut longitudinally for visualization.

Oral glucose tolerance test

To measure glucose tolerance, mice were fasted from ZT0 to ZT6. A fragment of 1-2 mm of the tail tip was cut to collect drop blood from the animal. Initial blood glucose was measured with a glucometer (Safe-Accu, SinoCare). Then, an oral gavage was used to introduce a solution of 1.5 grams of glucose/kilogram of body weight. Blood glucose was measured with the glucometer after 15, 30, 60, and 120 minutes. To analyze the curve of each animal, the initial blood glucose level was subtracted from the rest of the time points.

Bilateral adrenalectomy

To remove adrenal glands, animals were anesthetized with isofluorane. A midline incision was done in the abdominal cavity. The fat attached to the adrenal gland was pulled out of the cavity. After dissection of the adrenal gland, the fat was returned to the cavity and the skin was sewn. After two days, the contralateral adrenal gland was removed. 0.9% of saline supplemented with 1% glucose to compensate for the loss of aldosterone [150,151]. A sham-operated group was used as a control.

Animals were allowed to recover for a minimum of 2 weeks after bilateral adrenalectomy and anesthesia effects, and then muscle samples were collected for subsequent analysis.

Corticosterone detection

Blood corticosterone was detected using an enzyme-linked immunosorbent assay (ELISA). This is a plate-based technique where a specific antibody is pre-coated and blocked. After the addition of a solution with the antigen, an enzymatic reaction is used to visualize the amount of target present in the added solution.

Blood was extracted from the tip tail of the mice and was collected using tubes that prevented blood coagulation (Sarstedt microvette, CB 300). Samples were centrifuged at 3000 g for 10 minutes and the supernatant was collected. Corticosterone detection was performed according to manufacturer's instructions (Abcam, #ab108821).

Dexamethasone and adrenaline intraperitoneal injection

For dexamethasone treatment, 5 mg/kg of dexamethasone 21-phosphate disodium salt (Sigma-Aldrich, #D1159) was injected intraperitoneally (IP) [152,153].

For adrenaline treatment, an IP injection of adrenaline·HCl (0.5 mg/kg; Sigma-Aldrich, #E4642) [154] was performed as described previously [155]

Both drugs were solved in 0,9% filtered saline and administrated for 10 consecutive days at ZT12 (moment in which endogenous corticosterone or adrenaline are secreted).

Immunohistochemistry and immunofluorescence

Muscle samples were embedded in OCT solution (TissueTek #4583), frozen in isopentane cooled with liquid nitrogen, and stored at −80 °C until analysis. Muscle cryosections (10-µm thick) were collected and used for the following staining:

- Hematoxylin & eosin (H&E, Sigma-Aldrich, #HHS80 and #45235). Briefly, slides were immersed in hematoxylin solution and then washed with tap water. They were rapidly submerged in acid ethanol 2 times, and then in eosin. After that, the slides were dehydrated with ethanol. Slides were then put into xylol and mounted. This staining was used to visualize the morphology of the myofibers and the position of their nuclei.

- Sirius red (Sigma-Aldrich #365548). Briefly, sections were covered with Bouin solution overnight and then washed first with tap water for 5 minutes and then with a picric acid solution (90 mL of saturated picric acid + 10 mL of 1% direct red80 diluted in water). After that, the slides were washed rapidly in 2% acetic acid and dehydrated with ethanol. Finally, they were cleared with xylol and mounted. This staining method allows the extracellular matrix in muscle to be visualized.

- Oil Red O (Sigma-Aldrich #O0625) staining. Sections were fixed in 3.7% formaldehyde for 1 hour at room temperature (RT), rinsed with deionized water and then stained with Oil red O solution for 30 minutes. The excess of the solution was removed with tap water, and sections were mounted with 10% glycerol. This staining method allows the lipid depositions in muscle to be visualized.

- Succinate dehydrogenase (SDH) staining. Sections were incubated for 1 hour at 37ºC in a solution containing 10 mL of 0.2 M phosphate buffer with 270 mg of sodium succinate and 10 mg of nitro blue tetrazolium (NBT) and then washed with deionized water. The unbound NBT was then removed with three exchanges of 30, 60, and 90% acetone, with an increasing-to-decreasing concentration. Finally, the slides were mounted with an aqueous medium. This staining demonstrates the activity of the SDH enzyme, which is an indirect measurement of the oxidative capacity of the myofiber.

- Fiber-type staining. Sections were treated with 3% of H_2O_2 for 30 minutes to inactivate endogenous peroxidase, washed with PBS, and then blocked with MOM blocking solution (Vector #MKB-2213) for 1 hour at room temperature. Slides were then covered with the primary antibodies for specific fiber types. The primary monoclonal antibodies used were anti-myosin heavy chain type I (A4.840), anti-myosin heavy chain IIA (A4.74), and anti-myosin heavy chain IIB (BF-F3) (Developmental Studies Hybridoma Bank). Slides were then washed with PBS, covered with a biotinylated secondary antibody solution for 30 minutes at RT, embedded in a solution of avidin-biotin complex (Vector, #PK-6100) for 30 minutes at RT, and then incubated with diaminobenzidine solution until optimal reaction. Finally, slides were dehydrated with increasing concentrations of ethanol and mounted in DPX. This staining method allows the visualization of the different fiber types.

- Immunostaining for $CD11b^+$ cells. Slides were fixed for 15 minutes with 4% PFA, washed with PBS, and then blocked with 10% goat serum and 3% bovine serum albumin (BSA) for 1 hour at RT. Slides were then incubated with primary antibodies against CD11b and laminin overnight. After washing with PBS, slides were incubated with secondary antibodies for 1 hour at room temperature and DAPI. Finally, they were mounted in aqueous mounting media. This staining method allows the visualization of myeloid cells.

A list of all antibodies used and their dilution factor is shown in Table 3.

Table 3. List of antibodies used for immunochemistry and immunofluorescence.

Antibody	Dilution	Blocking	Description	Reference number
Myosin I			Mouse monoclonal	A4.840
Myosin IIA			Mouse monoclonal	A4.74
myosin IIB			Mouse monoclonal	BF-F3
CD11b	1:100	10%Goat 3%BSA	Rat monoclonal	eBioscience, #14-0112-85
Laminin	1:200	10%Goat 3%BSA	Rabbit polyclonal	Sigma-Aldrich, #L9393
anti-rabbit AF568	1:500	10%Goat 3%BSA	Goat anti-rabbit IgG	Invitrogen, #A11036
anti-mouse AF488	1:500	10%Goat 3%BSA	Goat anti-mouse IgG	Invitrogen, #A21121
anti-rat AF488	1:500	10%Goat 3%BSA	Goat anti-rat IgG	Invitrogen, #AA11006

Microscopy and image analysis

Digital images were acquired using the Leica DMR600B microscope equipped with a DFC300FX camera for histochemical color pictures and a confocal TCS SP8 MP microscope (Leica Microsystems) for fluorescence pictures; Fiber type distribution, CSA, percentage of muscle area positive for Sirius red, and Oil red staining were quantified using Image J software. Images from MitoTimer-positive fibers were analyzed by quantifying the red: green ratio with Image J software.

Statistics

For mouse experiments, no specific blinding method was used, but mice in each sample group were selected randomly. The sample size (n) of each experimental group is represented in each figure. GraphPad Prism software was used for all statistical analyses. Quantitative data displayed as histograms are expressed as means ± standard error of the mean (represented as error bars), and results from each group were averaged and used to calculate descriptive statistics. For each experiment, statistical tests and significance thresholds are provided in each figure legend.

RNA extraction

Total RNA was extracted from TA muscle. Briefly, after homogenization with Qiazol reagent (Qiagen #1023537), RNA, DNA, and protein were separated with chloroform. RNA was separated and then precipitated and cleaned with miRNeasy Mini Kit (Qiagen #1038703); samples were digested with DNase (Qiagen #1010395) according to manufacturer instructions.

RNA sequencing

RNA quality was checked using Nanodrop and RNA 6000 Nano Assay on a Bioanalyzer 2100 (Agilent). RNA-seq libraries were sequenced in paired-end mode with a read length of 150 base pairs with an average of 2 × 25 million reads for each sample. Four biological replicates (2 males and 2 females) at each ZT point were used to collect RNA samples (except in adrenalectomy experiments, where 4 females were used at each ZT). A total of 360 mouse RNA samples (24 mouse samples × 15 conditions) were sequenced to generate the total circadian RNA transcriptome.

RNA-seq data processing

Sequencing reads were pre-processed using the nf-core/RNAseq pipeline [156], and read quality was assessed by FastQC. TrimGalore was used to trim sequencing reads, eliminate Illumina adaptor remains, and discard short reads. The resulting reads were mapped onto the mouse genome using HiSAT2 [157] and quantified using featureCounts [158]. Overall, 9 samples were removed due to quality issues: WT_10W_ALF_3.ZT0, WT_26W_ALF_12.ZT8, WT_26W_ALF_21.ZT20, brain-RE_10W_ALF_11.ZT8, brain-RE_26W_ALF_6.ZT4, brain-RE_26W_ALF_21.ZT20, KO_26W_TRF_7.ZT4, KO_26W_TRF_20.ZT16 and WT_ADX_ZT0_1. Variance-stabilizing transformation of raw count data was applied using Bioconductor package DEseq2 [159] to visualize the sample-to-sample distances in principal component analysis (PCA). Trimmed mean of M-values (TMM)-normalized fragments per kilobase per million mapped reads (FPKM) values were calculated using Bioconductor package edgeR [160] and log2-transformed with a pseudo count of 0.01. In each analysis performed, the expression data were adjusted for biological (sex) and technical (batch) effects using the Bioconductor package limma [161]. Overall, 14,413 genes with average non-transformed FPKM expression > 0.5 in at least one-time point of at least one experimental condition were considered for further analysis.

Identification of rhythmic transcripts

The detection of rhythmic transcripts was performed by non-parametric Jonckheere-Terpstra-Kendall (JTK_CYCLE) algorithm [162], which detects cosine waveform and provides amplitude and phase output of rhythmic genes over 20 to 24 hours. Genes were considered rhythmic over the circadian cycle if their permutation-based, the adjusted $P < 0.05$. GraphPad Prism software was used to plot the abundance of most representative rhythmic genes. Heatmaps of the expression of the rhythmic transcript were plotted by R package pheatmap. Amplitude density plots and phase histograms were generated using R package ggplot2. Circular plots showing peak phase distribution of core clock genes were made with R package circlize medn [163]. Visualization of the intersections of rhythmic genes was generated using BioVenn [164], R package UpSetR [165] and GraphPad Prism software.

Functional profiling of rhythmic transcriptome

For functional characterization of the global rhythmic transcriptome in each condition, the Phase Set Enrichment Analysis (PSEA) was performed with the following parameters: domain from 0 to 24 hours, minimum of 10 genes per gene set, and maximum 10,000 simulations. Files containing the list of cycling genes and their peak phases of expression were used as input. Tests were run separately for Molecular Signatures Database (MSigDB) Gene Ontology biological processes (GOBP) and canonical pathways (KEGG and Reactome) gene sets [166]. The enrichment was tested against a uniform background distribution to summarize any overall synchronization of peak phases within gene sets. Kuiper Q value < 0.05 was used as a significance threshold. R package circlize [163] was used to plot rhythmic functions on a temporal scale. A semi-automated approach was applied to aggregate individual gene sets into broad muscle tissue-oriented functional categories based on semantic similarity, positions in hierarchical trees of corresponding databases, and the analysis of gene set descriptions. This allowed us to get distributions of peak phases (vector-average values) within the main rhythmic functions, to visualize their span and temporal synchronization across the diurnal cycle. In addition, plots for selections of individual rhythmic pathways were done with GraphPad Prism software.

To study the difference in rhythmic mitochondrial pathways between experimental conditions, Reactome [167] pathway enrichment analysis was used for a subset of cycling genes annotated in MitoCarta [168]. Over-representation analysis was performed using R

package gProfiler2 [169] with correction method “FDR” and “custom_annotated” full reference genome as a statistical domain. R package pheatmap was used to plot negative log10-transformed FDR values of selected pathways. For functional characterization of rhythmic gene intersections, over-representation analyses of gene sets from GOBP [170] and KEGG [171] were performed using gProfiler web server [169], with the correction method “FDR”, and “custom_annotated” full reference genome was used as a statistical domain. GraphPad Prism software was used to plot negative log10-transformed FDR values of selected pathways.

Differential gene expression analysis

Differential analysis of gene expression between experimental conditions was carried out by limma-trend with empirical Bayes approach [161]. The same samples that were included in the circadian transcriptome analysis, irrespective of the time point, were used as replicates (except for adrenalectomy experimental samples). *Zeitgeber* time was decomposed into sine and cosine of a 24-hour period to account for possible rhythmicity. Genes with adjusted $P < 0.01$ were considered as differentially expressed.

Functional profiling of differentially expressed genes

Different enrichment methods were used: 1) Gene set enrichment analysis (GSEA) webserver using the Molecular Signatures Database (MSigDB) [166] canonical pathways and hallmarks gene sets; and 2) KEGG pathway [171] enrichment analyses of the genes differentially expressed between WT_10W and other experimental conditions were conducted using R package gprofiler2 [169] with the following parameters: correction method “FDR”, “custom_annotated” full reference genome as a statistical domain. Over-represented pathways passing FDR < 0.05 threshold were considered significantly coherent. A set of KEGG pathways common between the physiological and premature aging was defined as the ones perturbed under ad libitum feeding (ALF) in old WT mice (old_96W_ALF) and 26-week-old muscle BMAL1 knock-out mice (brain-RE_26W_ALF and KO_26W_ALF), but not affected in normal phenotypes (muscle-RE_10W_nF, RE/RE_26W_nF, WT_26W_ALF). R package pheatmap was used to plot negative log10-transformed FDR values to represent selected pathways.

RESULTS

1. Restoration of the brain:muscle clock maintains homeostasis and prevents premature aging in otherwise circadian clock-deficient mice

1.1 Characterization of the mouse models

When *Bmal1* is not expressed in their body, mice are not able to maintain their circadian functions. Moreover, the constitutive deficiency of this gene produces premature sarcopenia [104]. When *Bmal1* is lacking specifically in skeletal muscle, it causes impairment of glucose metabolism in this tissue [112]. However, none of these models can describe the level of autonomy of muscle clock, nor its dependency on other tissue clocks (such as the central clock). To address this issue, we used a mouse model that prevents *Bmal1* expression (*Bmal1-stop*FL mice) but in which *Bmal1* expression can be reconstituted uniquely in the tissue of interest through Cre-mediated recombination [81,82] (Figure 8). We mated these *Bmal1-stop*FL mice (knockout [KO] mice) with others expressing Cre recombinase under the regulation of different promoters (for breeding strategy, see Figure 9):

i. the Acta1 (*Hsa*) promoter, which reconstituted endogenous *Bmal1* in skeletal muscle fiber only. This approach allowed us to produce muscle-RE mice;
ii. the Synaptotagmin10 (*Syt10*) promoter, which reconstituted *Bmal1* in the SCN, along with other brain regions. This approach allowed us to produce the brain-RE mice [172];
iii. the *Hsa* and *Syt10* promoters simultaneously, which reconstituted *Bmal1* in brain and skeletal muscle, giving reconstituted/reconstitued (RE/RE) mice.

Total *Bmal1* KO and wild-type (WT) mice were also used as controls.

A summary of the animal models used can be found in Figure 11.

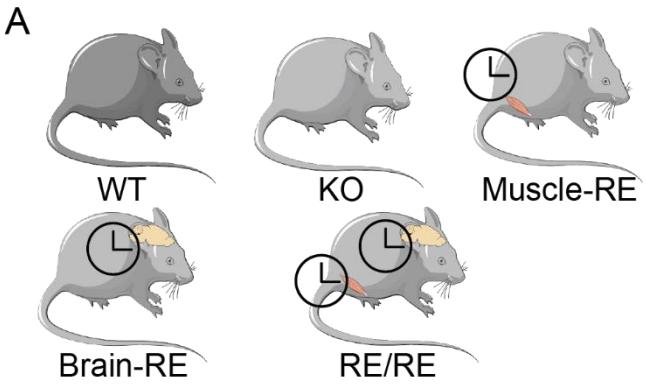

Figure 11. **Mouse models used in the study.** A) (1) WT (*Bmal1-stop*FL$^{wt/wt}$), (2) KO (*Bmal1-stop*FL$^{f/f}$ *Hsa*-Cre$^{wt/wt}$ *Syt10*-Cre$^{wt/wt}$), (3) Muscle-RE (*Bmal1-stop*FL$^{f/f}$ *Hsa*-Cre$^{tg/wt}$), (4) Brain-RE (*Bmal1-stop*FL$^{f/f}$ *Hsa*-Cre$^{wt/wt}$ *Syt10*-Cre$^{tg/wt}$) and (5) RE/RE (*Bmal1-stop*FL$^{f/f}$ *Hsa*-Cre$^{tg/wt}$ *Syt10*-Cre$^{tg/wt}$).

As it is known that KO mice present premature aging, we wanted to assess whether the rescue of *Bmal1* in muscle or brain prevents this premature aging phenotype in skeletal muscle. We first characterized these mice models at two different ages: 10 weeks (when total KO mice do not present signs of premature aging) and 26 weeks (when they present evident signs of premature aging as lower body weight, cataracts, sarcopenia, and/or calcification and ossification of hind limb joints) [104]. When comparing the muscle phenotype of WT and KO mice at these two ages, we observed signs of muscle deterioration already in 10-week-old KO mice. These included an increased collagen accumulation (fibrosis) in tibialis anterior (TA) muscle (Figure 12A). More pronounced signs of muscle deterioration were present in KO mice from 10 to 26 weeks, such as the presence of small embryonic myosin heavy chain (eMHC)-expressing fibers and central-nucleated fibers (CNF) (both indicators of muscle damage), overt fibrosis, and infiltrating inflammatory cells (Figure 12A-D). These results indicate that the general lack of *Bmal1* expression in all tissues affected negatively to the skeletal muscle phenotype.

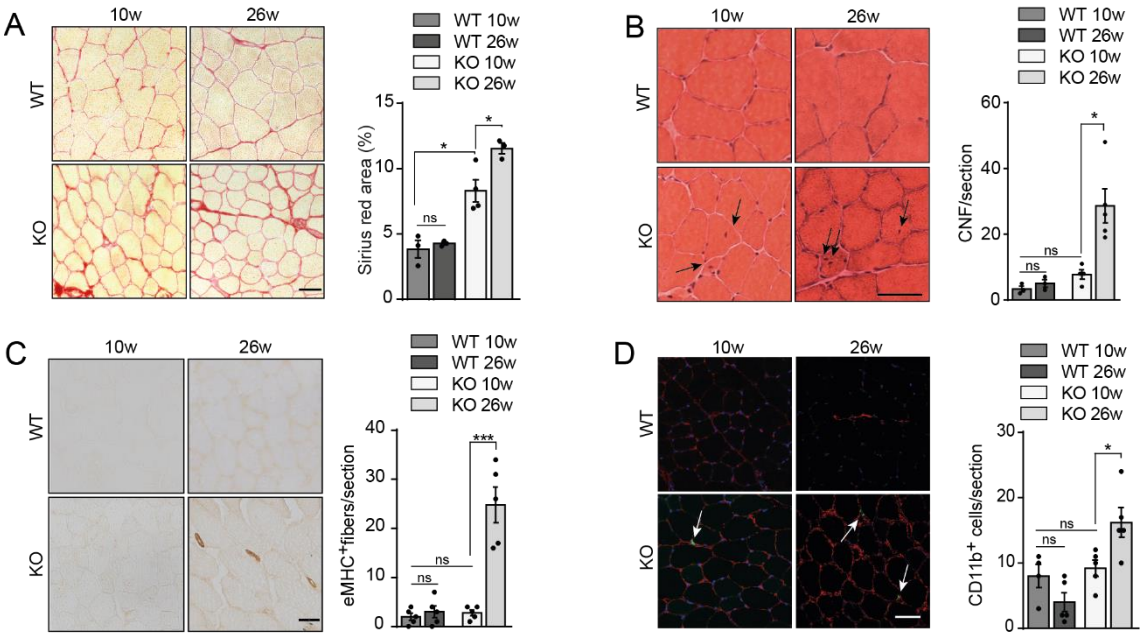

Figure 12. KO mice present muscle premature aging. Increased sarcopenia features in TA muscles of old *Bmal1* KO mice, showing: A) increased collagen deposition by Sirius red staining; B) the presence of centrally nucleated fibers (CNF); C) embryonic myosin positive (eMHC$^+$) fibers; and D) infiltrating myeloid CD11b$^+$ cells. Scale bars: 50 μm. Results are mean ± s.e.m.; *P < 0.05, **P < 0.01, ***P < 0.001 (*t*-test; two-tails) ns, non-significant.

We then analyzed the muscles of the other mutant mice at 26 weeks of age, the timing in which we observed a more severe phenotype in muscles from KO mice. Rescuing *Bmal1* expression only in skeletal muscle or brain did not rescue these muscle aging traits, as they remain significantly higher compared to WT control mice (Figure 13A-B). However, double reconstitution (brain and skeletal muscle, RE/RE mice) recovered the sarcopenic phenotype, as shown by the rescue in the numbers of eMHC-expressing fibers, CNF, levels of Sirius red staining, and the number of infiltrating inflammatory cells as compared to WT mice (Figure 13A-B). Moreover, the atrophy of type IIB fibers (fast twitch, glycolytic; the specific fibre type mostly affected by atrophy during muscle aging) was prevented in RE/RE mice, but not KO, muscle-RE or brain-RE (Figure 13A-B). Finally, RE/RE mice presented also the recovery of muscle force, which was similar to the WT group (Figure 13B). These results demonstrate that the central:peripheral clock communication (brain:muscle) is required for the maintenance of muscle physiology and also to prevent its premature aging.

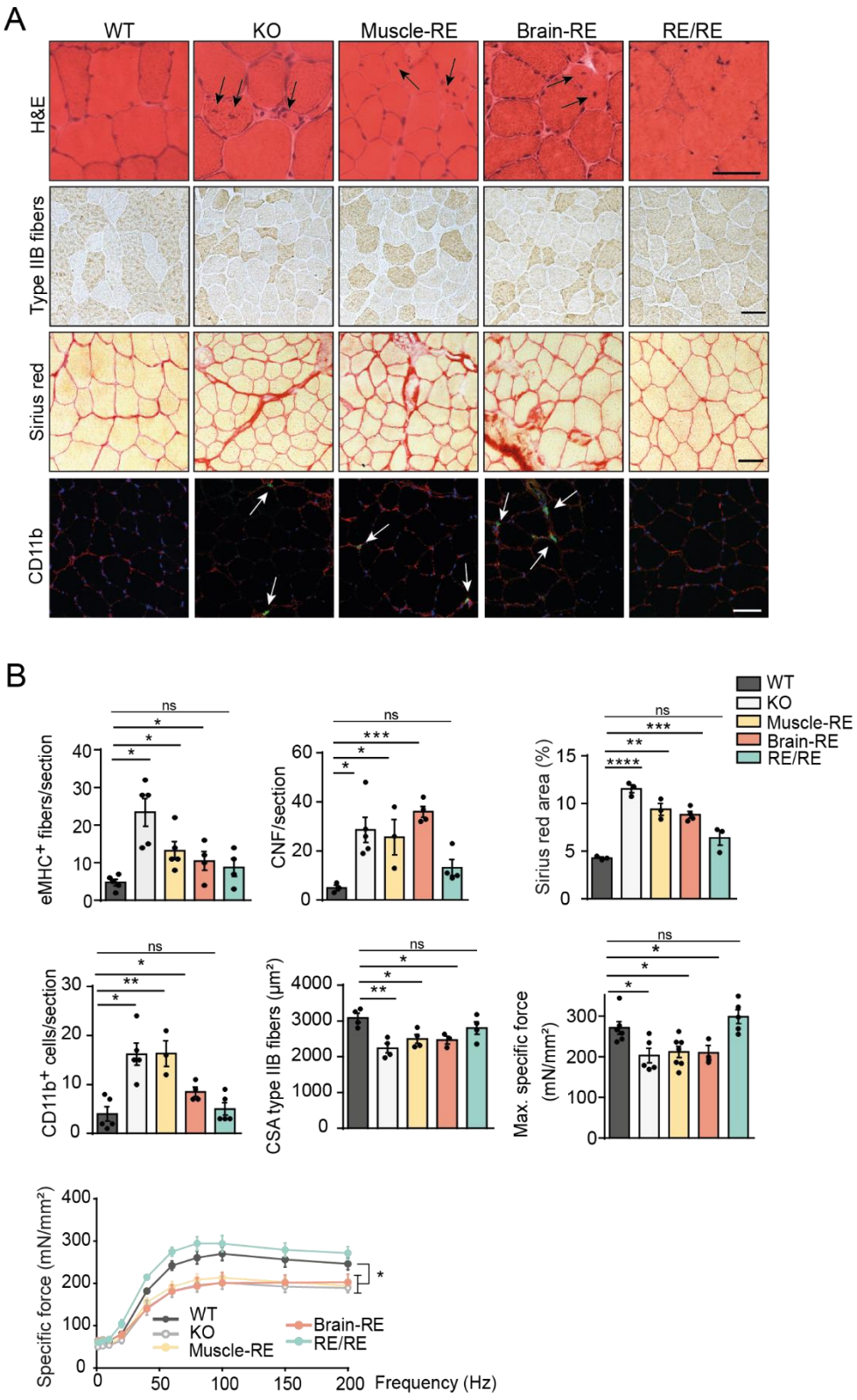

Figure 13. Brain and muscle clocks are necessary and sufficient to restore functional skeletal muscle. A) Representative images of hematoxylin and eosin (H&E), type IIB fibers immunostaining, interstitial collagen by Sirius red, and infiltrating inflammatory CD11b^{+} cells immunostaining in cryosections of TA muscle of the different mouse models at 26 weeks of age. B) Quantification of fibers expressing embryonic myosin, CNF, collagen content by Sirius red

staining, infiltrating inflammatory CD11b^{+} cells, and cross-sectional area (CSA) of fast type IIb fibers in TA muscles of the different mouse models at 26 weeks of age. Maximal specific isometric tetanic force and force-frequency curves of *extensor digitorum longus* (EDL) muscles of the different mouse models are shown. Scale bars: 50 μm. Results are displayed as mean ± s.e.m.; P values are from *t*-test (two-tailed). Force-frequency curves, two-way ANOVA; *P < 0.05, **P < 0.01, ***P < 0.001, ****P < 0.0001, ns, non-significant.

As skeletal muscle plays an important role in body metabolism and locomotion, we also analyzed the metabolism and behaviour of the various animal models during light/dark cycles at ~22 weeks of age. KO mice did not show any rhythmic pattern in their activity, oxygen consumption, energy expenditure, or glucose and lipid oxidation, in accordance with previous studies [81,82,173] (Figure 14A). Muscle-RE mice did not recover either the rhythmicity of metabolic cycles or the locomotor rhythms (Figure 14A). Importantly, brain-RE and RE/RE mice presented circadian patterns of activity/inactivity and metabolic parameters, being more active during the dark phase, from ZT12 to 0 (Figure 14B). This indicates that the central clock has the autonomy to drive these rhythmic patterns in the mice, even at advanced stages of their life. However, brain-RE presented profound signs of sarcopenia, which confirms that muscle alterations in this model (Figure 13) were not due to a lack of activity in the mice (which causes atrophy). In contrast, it confirms that the muscle clock is necessary to maintain tissue homeostasis.

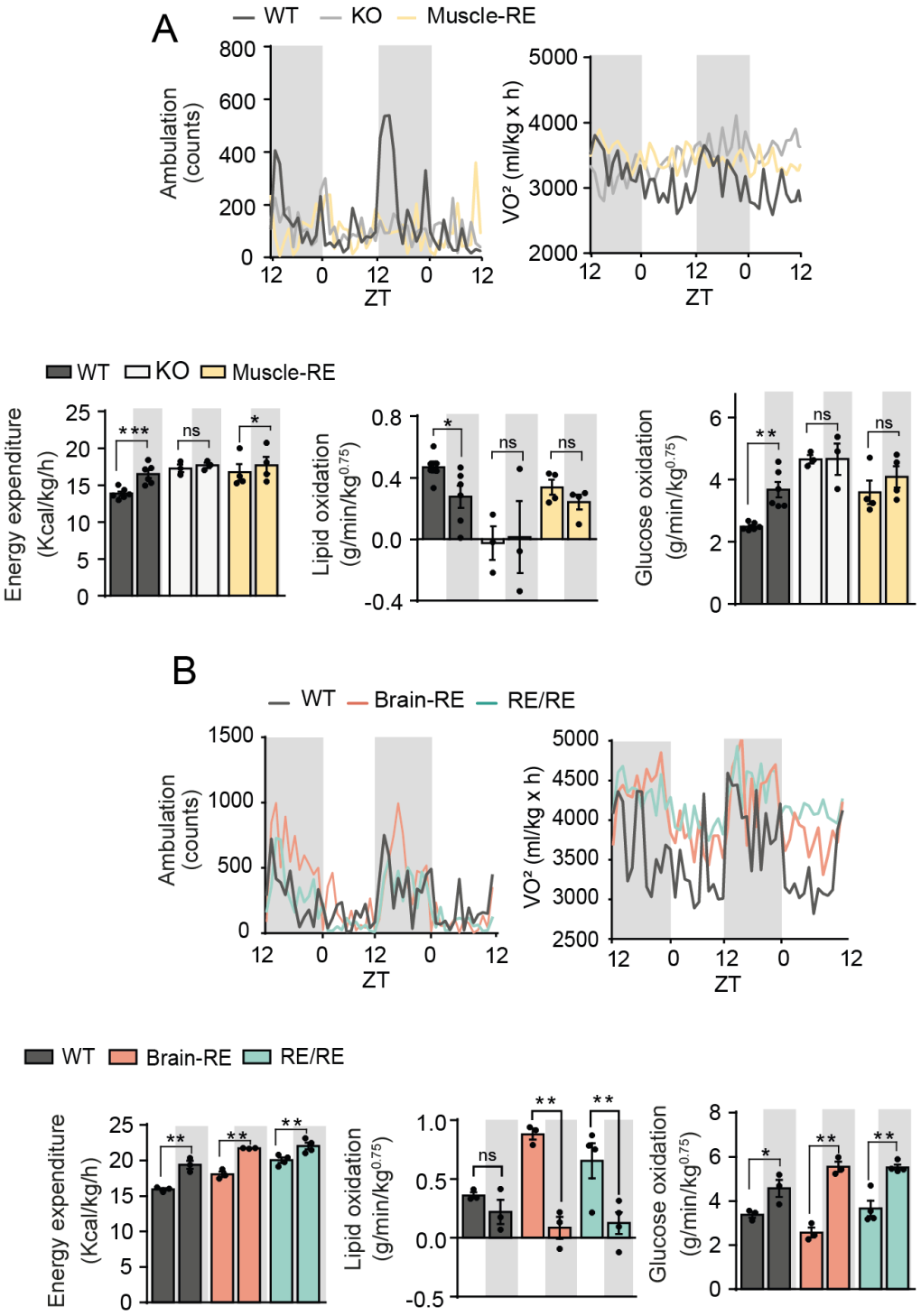

Figure 14. SCN clock is necessary and sufficient to restore circadian behavior in otherwise clock-less mice. A) Activity patterns, oxygen consumption (VO_2), and metabolic parameters of WT, KO, and muscle-RE mice at 20–23 weeks of age. B) Activity patterns, VO_2, and metabolic parameters of WT, brain-RE, and RE/RE mice at 20-23 weeks of age. Results are displayed as mean ± s.e.m.; *P* values are from *t*-test (one-tailed). **P* < 0.05, ***P* < 0.01, ****P* < 0.001, ns, non-significant.

Prompted by these findings, we compared the lifespan of the different models. KO mice start dying at 26 weeks of age [104]. All genetic models still displayed a reduced lifespan compared to WT: at 50 weeks of age, 100% of the mutants had died but all WT mice were still alive. However, we report a small but significant increase in the lifespan of RE/RE and muscle-RE mice as compared to KO (Figure 15A). This suggests that the muscle clock is sufficient to extend the lifespan of the mice to a limited degree. However, other peripheral clocks are required to make a more prominent change in this parameter.

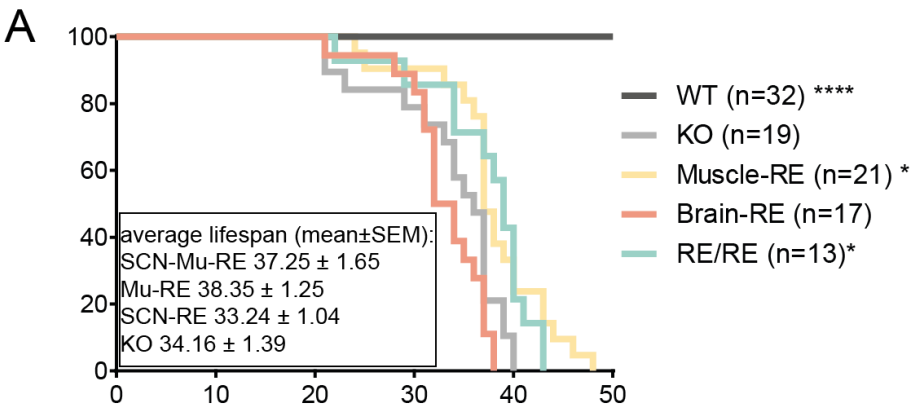

Figure 15. Muscle clock is sufficient to produce a short extension in lifespan. A) Survival curves of WT, KO, muscle-RE, brain-RE, and RE/RE mice. Mantel-Cox test, compared to KO. *$P < 0.05$, ****$P < 0.0001$.

1.2 Circadian transcriptome in the different mouse models

After observing that restoration of brain and muscle clocks prevented muscle premature aging, we aimed to describe the muscle circadian gene expression of the different genetic models to understand which transcriptional changes are linked to the different phenotypes during premature aging. For that, we obtained muscles from WT, KO, muscle-RE, brain-RE, and RE/RE mice at 10 and 26 weeks of age. To detect circadian changes in gene expression, we collected the samples every 4 hours over 24 hours (n=4 mice per timepoint) and then analyzed them by RNA-sequencing (RNA-seq). With this approach, we had 6 different ZT, starting when the lights turn on (ZT0), and finishing 4 hours before the new light cycle starts (ZT20).

At both ages, analysis of PCA showed that muscle-RE and RE/RE samples were clustering closer to WT than to KO samples. However, this was not the case for the brain-RE muscles, indicating that muscle clock restoration was important for the general recovery of muscle gene expression (Figure 16A & 17A).

Next, we used the Jonckheere-Terpstra-Kendall (JTK) algorithm [162] to detect circadian transcripts in each genotype. First, we analyzed the expression of core clock genes. Although *Bmal1* was detected by RNA-seq in KO muscles (Figure 16B), the origin of this signal came from aberrant transcripts of exonic regions precedent to exon 5, the first one being translated (see Figure 8). As expected, BMAL1 protein was not detected in muscle tissue from KO mice (Figure 16C). In muscles from mice of both ages, muscle-RE presented a recovery of the expression levels of some core clock genes (i.e. *Bmal1, Per2-3,* and *Nr1d2*) (Figures 16B & 17B). Moreover, this recovery was also confirmed for the BMAL1 protein at 10 weeks of age (Figure 16C). However, most of these genes were not oscillating (i.e., *Bmal1, Per1-3, Cry1-2, Rorc,* and *Nr1d1*) at any age, indicating that the oscillatory capacity of the core machinery in skeletal muscle is non-autonomous (e.g., it depends on signals coming from other tissue clocks). Nevertheless, the gene *Dbp* (considered a key clock output gene), showed a rhythmic expression in muscle-RE compared to KO muscles at 10 weeks, despite having a lower amplitude than in WT group (Figure 16B). This suggests that the sole presence of the clock in muscle sufficed to induce a circadian output, independently of robust oscillations in core clock genes. In brain-RE muscles, only *Per* and *Cry* genes showed rhythmic expression (Figure 16B & 17B), which indicates that their oscillation in muscle is determined by the brain independently of muscle BMAL1. In contrast, in muscles from RE/RE mice, all the core clock components oscillated with period, phases, and amplitudes similar to WT mice at both ages (Figure 16B & 17B). These results suggest that the brain:muscle node is necessary and sufficient to drive the oscillation of the muscle clock machinery.

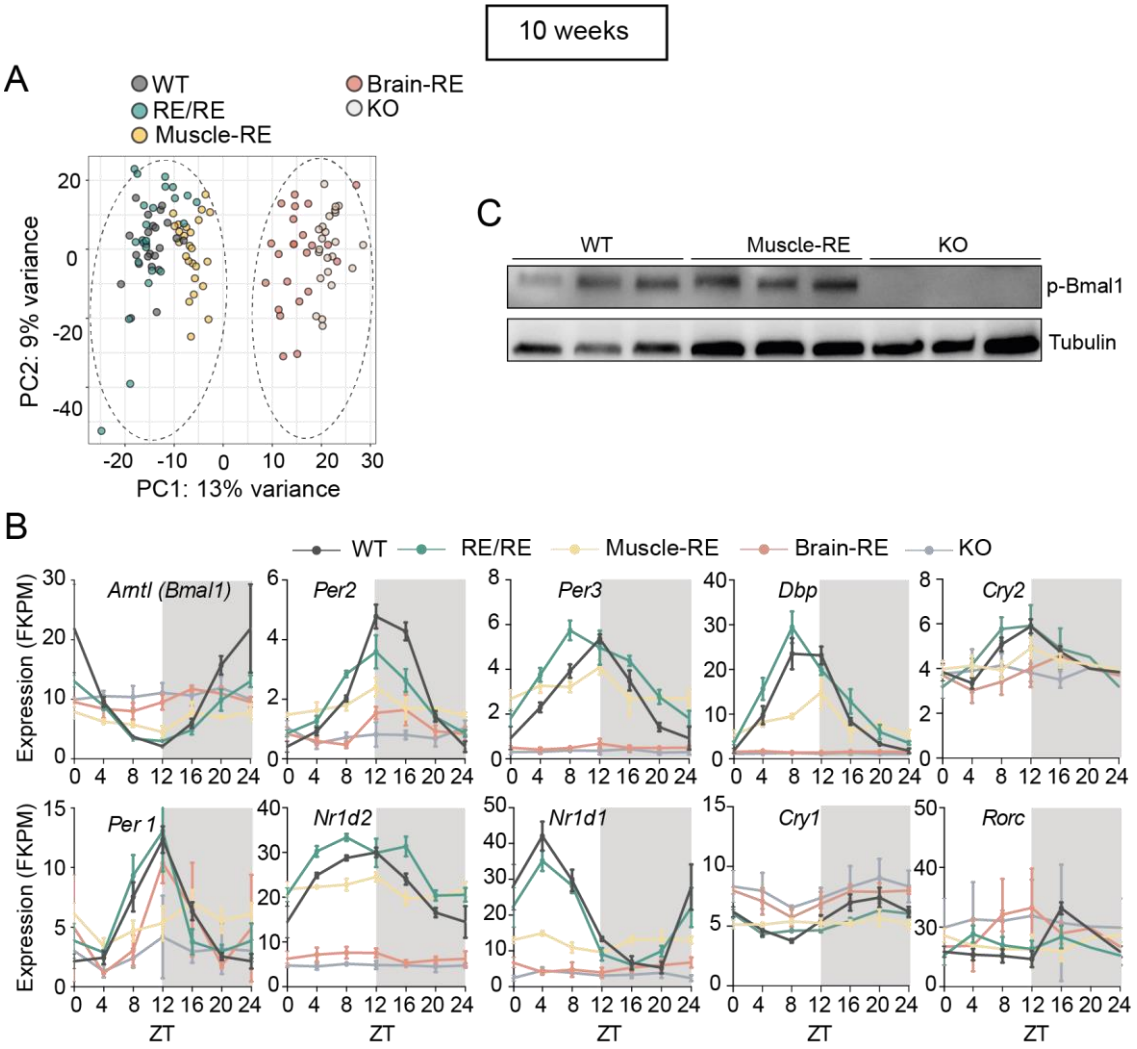

Figure 16. The muscle clock is non-autonomous, and brain:muscle clock interactions drive core clock machinery, rhythmic functions, and correct phase at 10 weeks of age. A) PCA of the full transcriptome of TA muscle from WT, RE/RE, muscle-RE, brain-RE, or KO young (10- to 12-week-old) mice. B) Abundance profiles of core clock genes in WT, RE/RE, muscle-RE, brain-RE, or KO young mice under LD entrainment; n = 3–4 mice at each time point. Data are presented as mean ± SD. C) Levels of BMAL1 protein in skeletal muscle of WT, muscle-RE and KO mice.

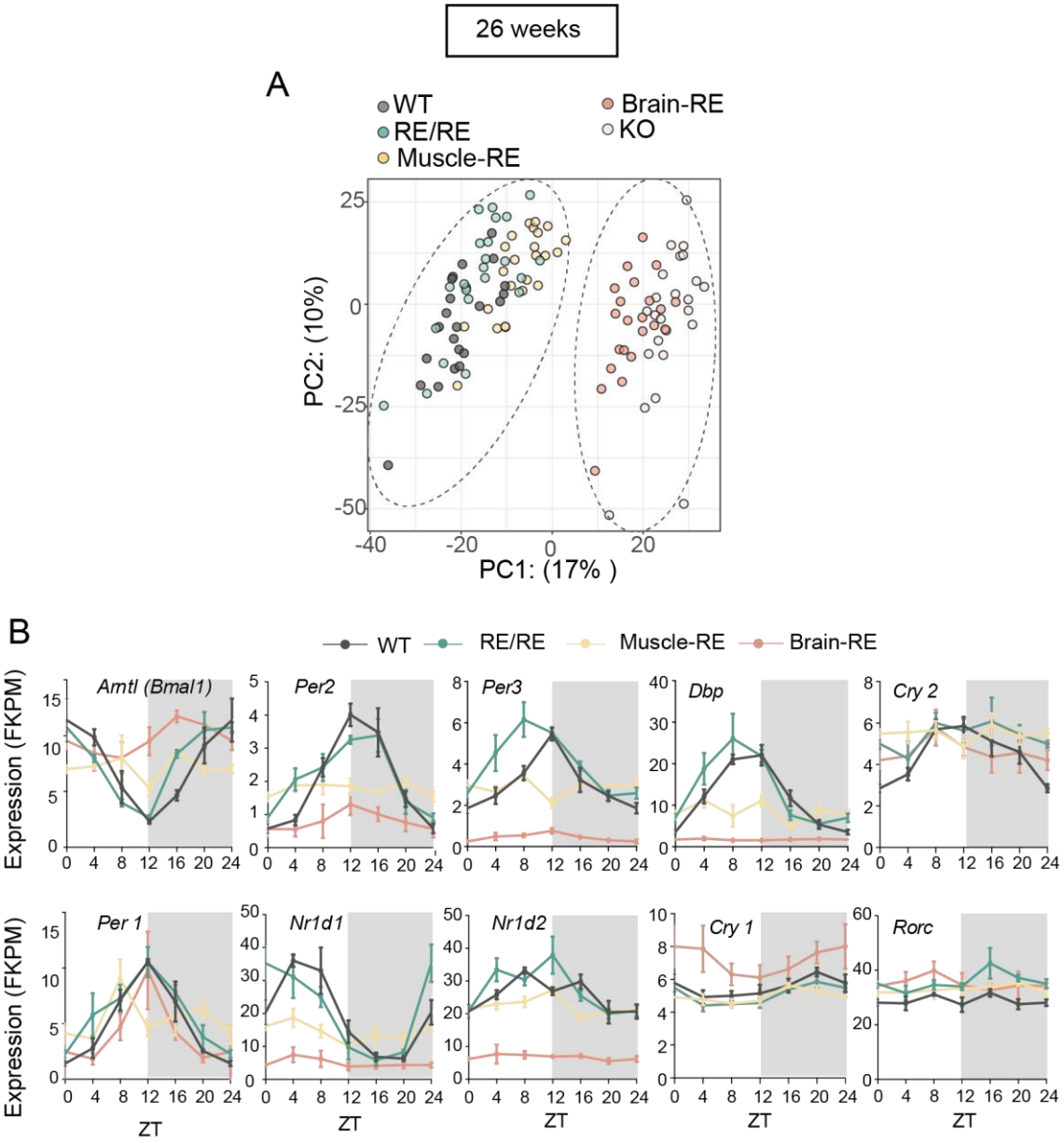

Figure 17. Brain:muscle clock interactions drive core clock machinery, rhythmic functions, and correct phase also at 26 weeks of age. A) PCA of the full transcriptome of TA muscle from WT, RE/RE, muscle-RE, brain-RE, or KO prematurely aged (24- to 27-week-old) mice. B) Abundance profiles of core clock genes in WT, RE/RE, muscle-RE, brain-RE, or KO young mice under LD entrainment; n = 3–4 mice at each time point. Data are presented as mean ± SD.

After examination of the core clock machinery, we examined the whole circadian transcriptome of each genotype at 10 weeks of age. Only ~7% of the rhythmic transcripts in WT muscles were also present in muscles of muscle-RE mice (and not of KO mice) (Figure 18A). This indicates that the expression of this small fraction of genes depended directly on the muscle clock. These muscle-autonomous rhythmic genes (e.g., that did not require the central brain clock) (n = 112) presented different phases in muscle-RE compared to WT, with a peak of expression between ZT16-18 (Figure 18B-C). They also

had lower amplitude compared to WT (Figure 18D). This group of muscle BMAL1 autonomously-driven genes was involved in biological functions related to stress and inflammatory pathways (such as sumoylation of DNA replication and UV response, and Toll-like receptor and interleukin signaling), basic cell transcription, and circadian regulation (Figure 18E).

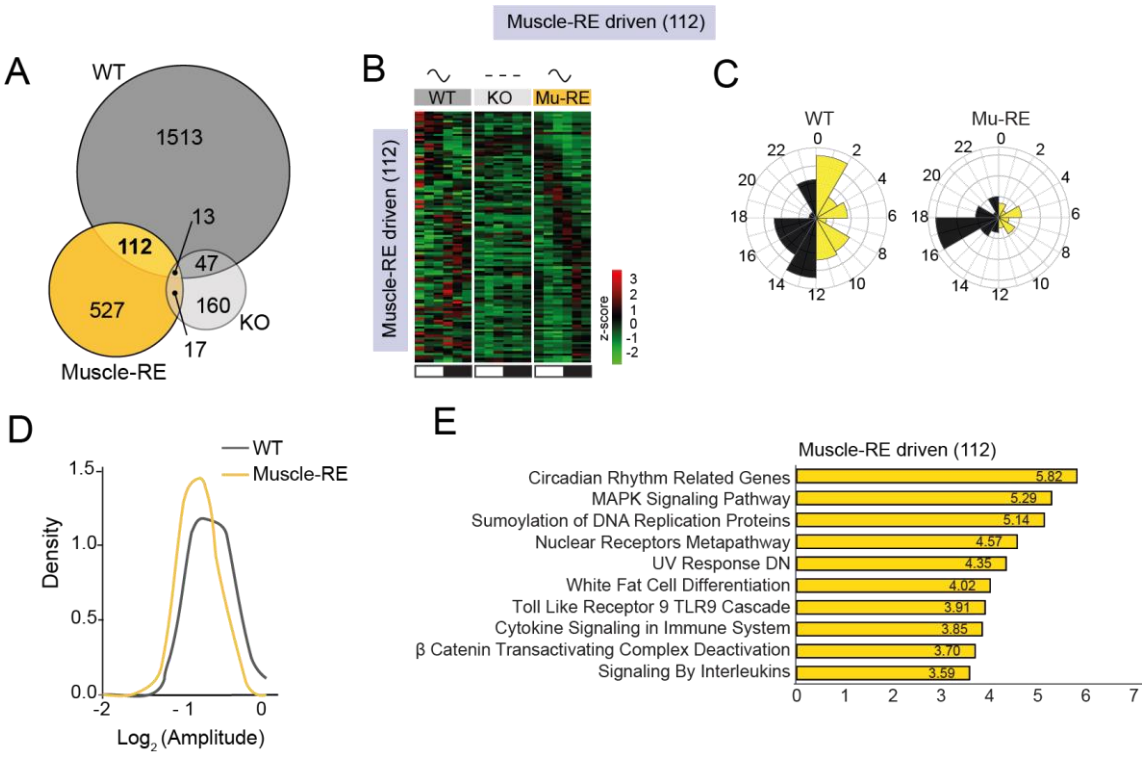

Figure 18. Muscle clock is non-autonomous and drives the rhythmicity of a small set of genes. A) Venn diagram showing intersections of genes oscillating from WT, KO and muscle-RE at 10 weeks of age (JTK_CYCLE, adjusted $P < 0.05$). B) Phase-sorted expression heatmap of 112 autonomous genes that oscillated only in WT and muscle-RE (Mu-RE), but not in KO, young mice; JTK_CYCLE, adjusted $P < 0.05$. C) Circular histogram plots of the peak phase of genes in B). D) Density plot showing amplitude comparison of genes in B); Welch's t-test, *WT versus Mu-RE, $t = 4.41$, $P = 0.00002$. E) Bar plot showing selected canonical pathways and hallmarks enrichment analysis of the indicated sets of genes; MSigDB FDR < 0.05. GO biological process and KEGG pathway enrichment analysis of the same sets.

Strikingly, a high fraction of WT rhythmic transcripts also oscillated in brain-RE muscles (~33% at 10 weeks of age) (Figure 19A). However, the phase of this group of genes (n = 560) was strongly altered, with their peak of expression between ZT14-18 (Figure 19B-C). Moreover, the amplitude of these genes was slightly reduced (Figure 19D). These brain-related genes were enriched in several signal transduction pathways associated with stress responses and circadian processes (Figure 19E).

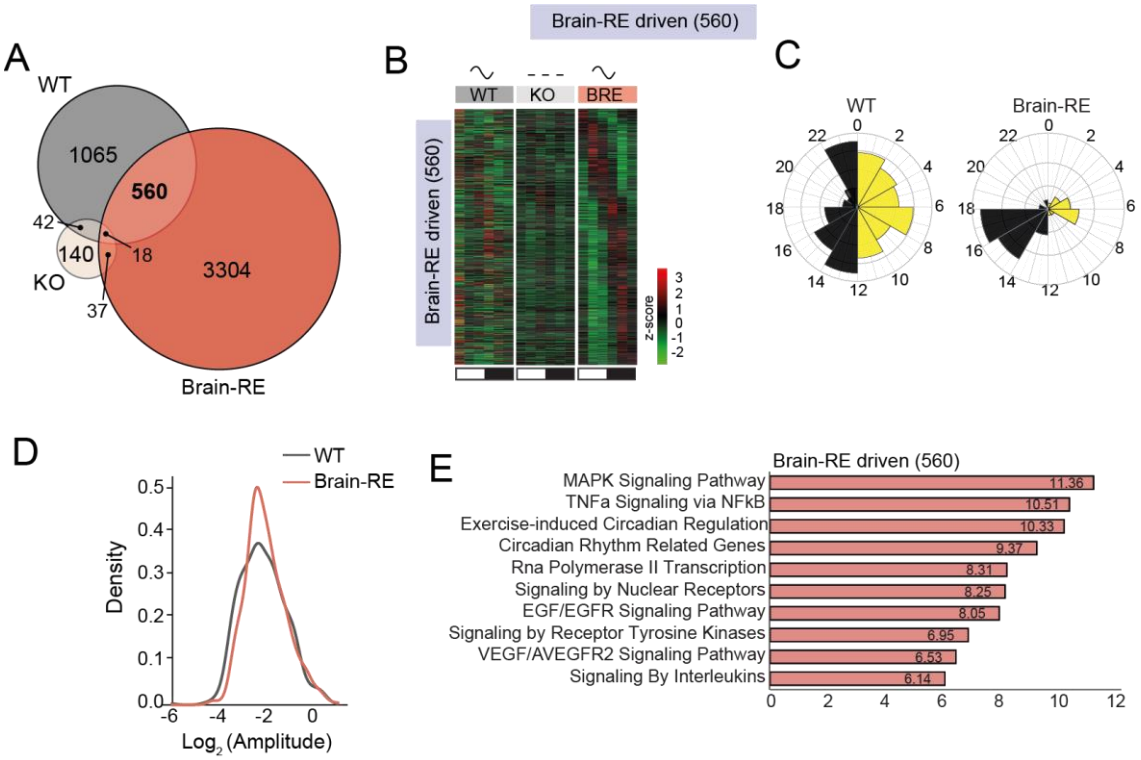

Figure 19. Brain clock restores the rhythmicity of a specific set of genes. A) Venn diagram showing intersections of genes oscillating from WT, KO, and brain-RE at 10 weeks of age (JTK_CYCLE, adjusted P < 0.05). B) Phase-sorted expression heatmap of 560 brain-dependent genes that oscillated only in WT and brain-RE (BRE), but not in KO, young mice; JTK_CYCLE, adjusted P < 0.05. C) Circular histogram plots of the peak phase of genes in (B). D) Density plot showing amplitude comparison of genes in B); Welch's *t*-test, not significant. E) Bar plot showing selected canonical pathways and hallmarks enrichment analysis of the indicated sets of genes; MSigDB FDR < 0.05. GO biological process and KEGG pathway enrichment analysis of the same sets.

Finally, in RE/RE muscles, the rhythmic transcripts retained from WT (~11% at 10 weeks) (Figure 20A) exhibited normal phase and amplitude distribution (Figure 20B-D), which might be responsible for the prevention of premature aging and homeostatic muscle maintenance. More specifically, genes that only required the brain:muscle module for daily rhythmicity (n = 189) included these with functions in the regulation of muscle growth and proteostasis, including TNFα/NF-κB signaling (negative regulation of myofiber growth), FoxO-mediated transcription regulation (*Akt2, FoxO4*), and PI3K/AKT and mTOR signaling (positive regulation of myofiber growth), autophagy (regulation of myofiber proteostasis) [174], myogenesis (e.g., *Myog,* the master regulator of myogenic differentiation, and *Tcap*) [175], and metabolic functions, such as insulin/glucose and phospholipid metabolism [176] (Figure 20E).

As we detected important muscle pathways being rhythmic and dependent on brain:muscle axis (Figure 20E), we also performed a PSEA analysis to examine the phase distribution of the rhythmic functions in the different models. In WT muscles, these functions were distributed one after the other, as well as in muscle-RE and RE/RE groups. However, in brain-RE muscle, all of these functions were broadly distributed from ZT4 to ZT20 (Figure 20F). In addition, we also observed that the phases of muscle-RE were very different (almost the opposite) from those found in WT. Only in RE/RE these phases were maintained to some extent. This again suggests that central and peripheral clocks' restoration is sufficient to drive muscle rhythmic functions at their proper time.

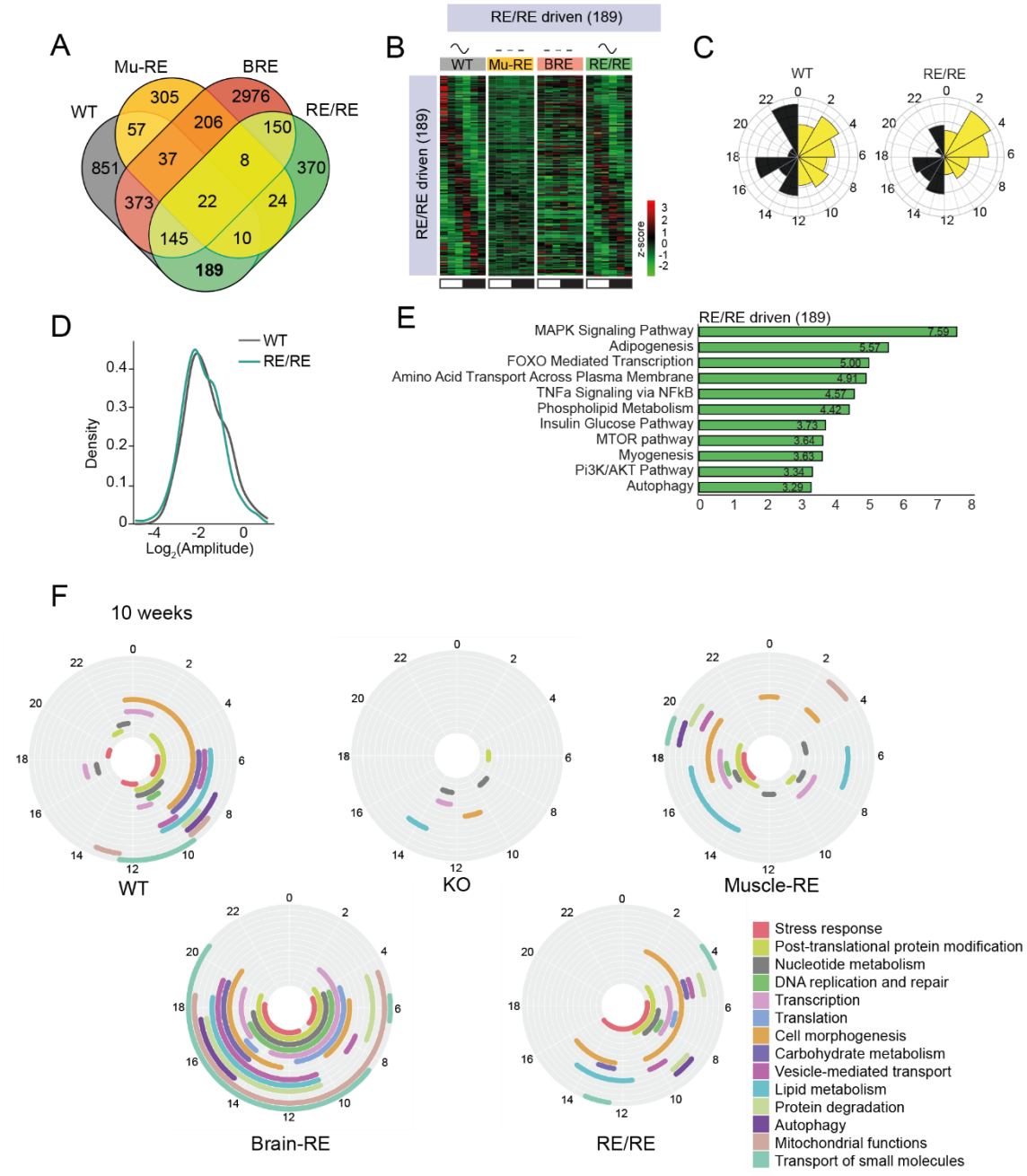

Figure 20. Brain:muscle clock interactions drive core clock machinery and rhythmic homeostatic muscle functions in the correct phase. A) Venn diagram showing intersections of genes oscillating from WT, muscle-RE (Mu-RE), brain-RE (BRE) and RE/RE at 10 weeks of age (JTK_CYCLE, adjusted $P < 0.05$). B) Phase-sorted expression heatmap of 189 RE/RE driven genes that oscillated only in WT and RE/RE, but not in Mu-RE or BRE, young mice; JTK_CYCLE, adjusted $P < 0.05$. C) Circular histogram plots of the peak phase of genes in (B). D) Density plot showing amplitude comparison of genes in B); Welch's *t*-test, not significant. E) Bar plot showing selected canonical pathways and hallmarks enrichment analysis of the indicated sets of genes; MSigDB FDR < 0.05. GO biological process and KEGG pathway enrichment analysis of the same sets. F) Circular 24-hour phase distribution of aggregated muscle tissue–oriented functional

categories from WT, KO, muscle-RE, brain-RE, or RE/RE mice at 10 weeks of age; PSEA, total rhythmic genes, Kuiper Q-value (vs. uniform) < 0.05.

After having dissected the role of brain:muscle clocks and the possible transcriptional mechanisms that prevented muscle aging, we next investigated which rhythmic functions were not dependent on brain and muscle clocks. About 50% of oscillating genes were only rhythmic in WT muscles at 10 or 26 weeks, indicating that brain:muscle module is not sufficient to restore the circadian expression of these genes and that other peripheral clocks are required (Figure 21A). These genes requiring other peripheral:muscle clock communication (n = 851) were related to a variety of processes including protein phosphorylation, cell-cell contact, and signal transduction cascades (i.e. focal adhesion or EGF and second messenger signaling) and pathways involved in muscle homeostasis, such as thyroid hormone, responses to oxygen levels (hypoxia), and immune system regulation [176–179] (Figure 21B).

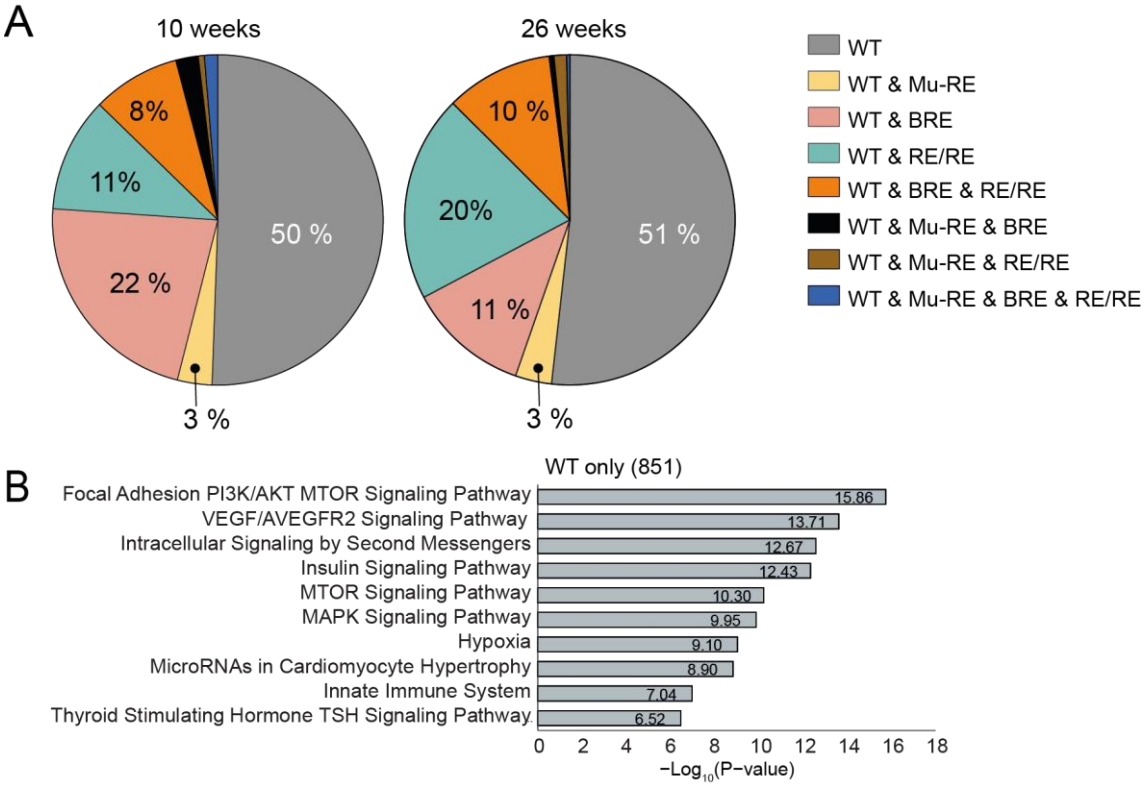

Figure 21. Half of the rhythmic transcripts require other tissue clocks to restore their oscillatory expression. A) Pie chart showing the proportion of rhythmic genes intersections between WT, RE/RE, muscle-RE (Mu-RE), or brain-RE (BRE) mice at 10 or 26 weeks of age as a percentage of total rhythmic genes in WT (JTK_CYCLE, adjusted *P* < 0.05). B) Bar plot showing selected canonical pathways and hallmarks enrichment analysis of the indicated sets of genes; MSigDB, FDR < 0.05.

In summary, the results of this section indicate that brain:muscle clocks module is the minimal system that generates signals to both regulate muscle essential daily homeostatic functions and prevent muscle sarcopenia. However, they also highlight the importance of other peripheral clocks to accomplish the circadian gene program and support key physiological functions in muscle.

1.3 The implication of brain and muscle clocks on glucose homeostasis

Transcriptomic data suggested that pathways which are important for muscle homeostasis are rhythmic. Among these, pathways related to glucose and insulin signaling were dependent on brain:muscle clocks (Figure 20E). It is known that muscle plays an important role in glucose homeostasis in the body and that there is insulin resistance and hyperinsulinemia during aging. Clock mutants that suffer premature aging (including *Bmal1*-KO) present hyperglycemia [180,181]. Thus, we hypothesized that restoring brain and muscle clocks could alleviate the hyperinsulinemia observed in KO during the last stages of mice. To investigate this, we fasted the mice for 6 hours starting at the beginning of the light cycle (ZT0) and then performed an oral glucose tolerance test (OGTT) at ZT6 on WT, KO, brain-RE, muscle-RE, and RE/RE mice at 10 or 26 weeks of age.

At 10 weeks, only brain-RE mice presented glucose tolerance levels that were similar to WT mice (Figure 22A), as expected based on previous reports [172]. However, at 26 weeks, brain-RE mice presented glucose intolerance that was similar to KO mice. In contrast, this phenotype was rescued in RE/RE mice at 26 weeks of age, with levels similar to WT mice (Figure 22B).

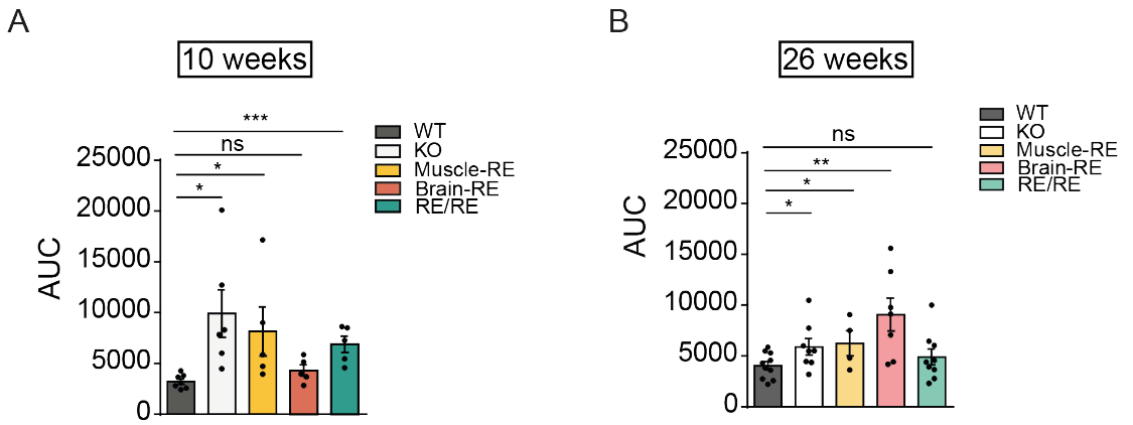

Figure 22. Glucose tolerance of WT, KO, muscle-RE, brain-RE, and RE/RE mice at 10 or 26 weeks of age. Mice were first fasted for 6 hours, and then glucose was administered orally. Blood glucose after administration is represented by the area under the curve (AUC) for (A) 10 and (B) 26 weeks. Results are displayed as mean ± s.e.m.; *P* values are from *t*-test (two-tailed). **P* < 0.05, ***P* < 0.01, ****P* < 0.001, ns, non-significant.

1.4 The muscle clock acts as a gatekeeper and represses brain clock signals to adapt circadian functions to muscle needs

Overall, we identified four types of rhythmic expression of transcripts: (1) muscle clock-autonomous (Figure 18E), (2) dependent on brain clock (Figure 19E), (3) dependent on both brain and muscle clocks (Figure 20E), and (4) dependent on clocks in other tissues (Figure 21B). We were intrigued by the unique and large group of genes that were rhythmic exclusively in brain-RE muscles (n = 2976) (Figure 23A). The circadian transcriptome of these muscles was composed of almost three times more rhythmic genes than in WT muscles (Figure 23B). However, these genes had decreased amplitudes and misaligned oscillation phases (Figure 23C-D). In contrast to the two expression peaks found at the beginning of the light and dark phases in WT circadian transcriptome (Figure 23E) [121], most of the rhythmic transcripts in brain-RE mice peaked between ZT16 to ZT18 (Figure 23E). These brain-related transcripts had a role in basic molecular processes (such as translation, nucleotide metabolism, protein localization, protein degradation, and mRNA splicing) and basic cellular processes (such as mitochondrial function and apoptosis), in addition to pathways associated with stress (Figure 23F). We hypothesize that their inappropriate time of expression may be adverse for muscle tissue, which in turn causes its deterioration. Remarkably, the addition of muscle clock (in the RE/RE mice) was sufficient to normalize both the altered alignment and the exaggerated number of rhythmic genes observed in the muscle of brain-RE (Figure 23B, D, and E). These results indicate that the muscle clock is necessary to gate

and restrain the expression of many brain-regulated circadian genes in muscle, thereby supporting normal tissue physiology.

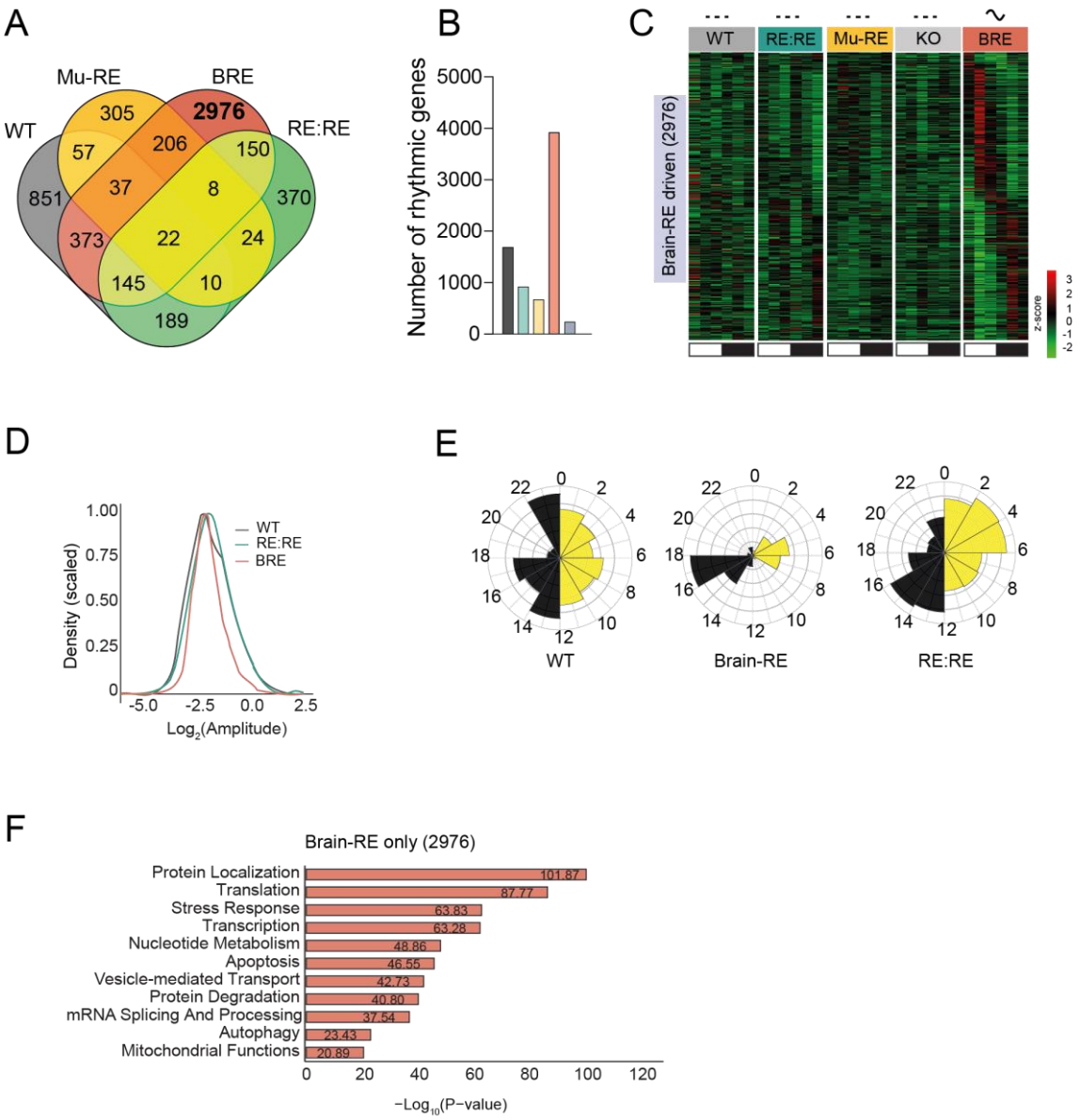

Figure 23. **Gating of muscle tissue rhythmic functions and phase by the peripheral muscle clock.** A) Venn diagram showing intersections of genes oscillating in WT, muscle-RE (Mu-RE), brain-RE (BRE), and RE/RE young mice; JTK_CYCLE, adjusted $P < 0.05$. B) Number of rhythmic genes in WT, RE/RE, muscle-RE, brain-RE, and KO young mice; JTK_CYCLE, adjusted $P < 0.05$. C) Phase-sorted expression heatmap of 2976 genes oscillating only in brain-RE young mice but not in WT, RE/RE, or muscle-RE young mice. D) Density plot showing total rhythmic transcripts (JTK_CYCLE, adjusted $P < 0.05$) amplitude comparison; Welch's t-test, *WT versus BRE, t = 6.45, P = 1.34E-10; WT versus RE/RE, not significant. E) Circular histogram plots of the peak phase of genes oscillating in WT, brain-RE, or RE/RE young mice; JTK_CYCLE, adjusted $P < 0.05$. F) Bar plot showing functional enrichment of the brain-RE–only genes; gProfiler, FDR < 0.05. Canonical pathways and hallmarks enrichment analysis.

As skeletal muscle strongly relies on mitochondrial activity to produce energy and sustain physiological functions [182], we examined the genes related to mitochondrial functions that were rhythmic only in brain-RE muscles (Figure 23F). Using MitoCarta [168], we identified the genes that were mitochondrial-related and rhythmic only in brain-RE mice (n = 373), WT mice (n = 78), or RE/RE mice (n = 32). Enrichment analysis showed that these rhythmic genes found in brain-RE were involved in the TCA cycle, mitochondrial biogenesis and respiration, and fatty acid oxidation among others (Figure 24A). In accordance with the gatekeeper function of muscle clock over the brain-regulated genes, these functional categories were not detected as rhythmic in RE/RE muscles. These observations suggest that the muscle clock is responsible for maintaining mitochondrial functions at the appropriate time window, filtering the signals that come from the central clock.

To analyze whether this elevated number of rhythmic genes related to mitochondrial function had a repercussion on mitochondrial physiology of brain-RE muscles, we assessed the health status of muscle mitochondria in the different mouse models at 26 weeks of age. For this, we transfected muscles *in vivo* with a MitoTimer reporter (which encodes a mitochondria-targeted switchable fluorescent protein that emits as green when mitochondria are newly synthesized and shifts to red if oxidized) [183,184]. KO and brain-RE transfected myofibers showed an accumulation of red (damaged) mitochondria, in contrast to WT muscles (Figure 24B). Notably, MitoTimer-transfected myofibers from muscle-RE mice showed a decrease in red:green ratio of fluorescence as compared to KO mice, although this decrease was not significant. However, it could indicate that muscle clock is at least in part responsible of preserving mitochondrial integrity. Remarkably, the intensity of MitoTimer-transfected RE/RE and WT myofibers were similar (Figure 24B), suggesting that brain:muscle communication sufficed to maintain muscle mitochondrial physiology. Further, there was a correlation between the maintenance of muscle metabolism and homeostatic functions and the mitochondrial wellness observed in RE/RE mice. Taking into account that dysfunctional mitochondria trigger sarcopenia during aging [185,186], we suggest that the gatekeeper function of muscle clock ensures the correct timing of daily metabolic and homeostatic functions in muscle and prevents its premature aging.

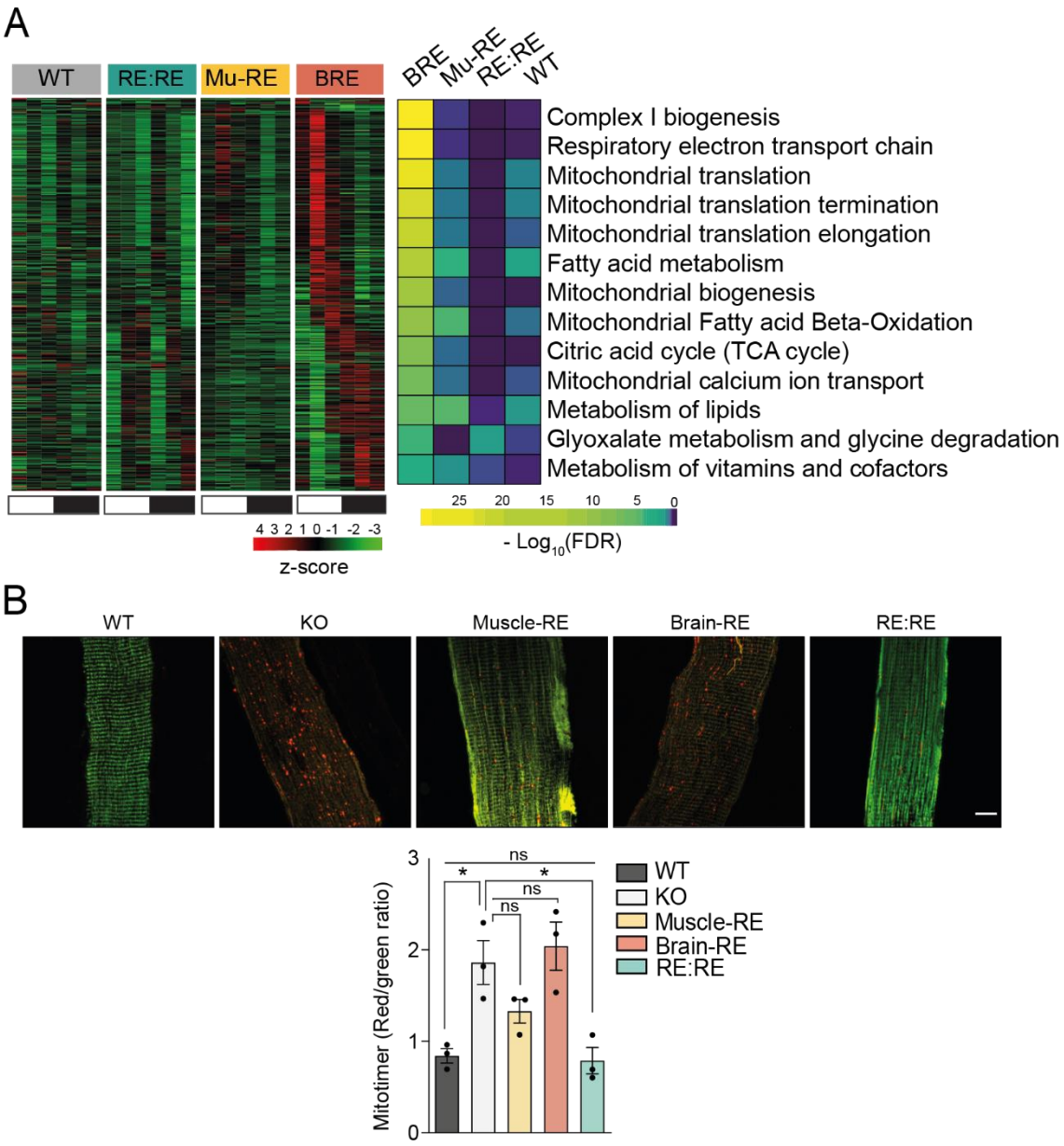

Figure 24. Mitochondrial functions aberrantly rhythmic in brain-RE muscles are corrected by muscle clock influencing mitochondrial wellness. A) Phase-sorted expression heatmap (left) of 368 MitoCarta genes that oscillate in brain-RE young mice; JTK_CYCLE, adjusted $P < 0.05$. B). *In vivo* expression of the mitochondrial stress reporter MitoTimer in myofibers of tibialis anterior muscles of young mice of the indicated genotypes. Representative confocal images are shown. Enhanced red fluorescence was detected in KO, brain-RE, and muscle-RE mice, as compared to WT and RE/RE mice. Scale bars, 10 μm. Quantification of oxidized (red)/unoxidized (green) ratio. Results as mean ± SEM; *$P < 0.05$; ns, non-significant.

2. Dissecting the brain:muscle clock communication

2.1 Adrenal hormones as mediators of brain:muscle clock communication

The mouse models that we have generated in this work have helped us to understand the role of skeletal muscle and brain clocks in regulating muscle function and physiology. After understanding the importance of their communication, we investigated how this connection between the two clocks occurs mechanistically. Our transcriptomic data indicates that RE/RE-dependent rhythmic genes contribute to functions that may be directly related to the effect of adrenal hormones on the muscle (Figure 20E): pathways related to protein balance (FOXO, mTOR, and Pi3K/AKT pathways) and glucose uptake by insulin are related to glucocorticoids (GC) signaling [187]; and pathways related to adipogenesis, phospholipid metabolism and glucose uptake are related to catecholamines (noradrenaline [NADR] and adrenaline [ADR]) function [188]. SCN influences the HPA axis, through autonomic innervation of the adrenal gland, having a role in the regulation of the circadian release of these hormones [189]. Moreover, the ablation of the adrenal glands, or the lack of *Bmal1* expression in them, causes circadian deregulation in some peripheral clocks [190,191]. Therefore, it is possible that some adrenal-derived blood-borne cue mediates the communication between central and muscle clocks.

To examine this hypothesis, we checked the day/night oscillations in blood adrenal hormones from the different mouse models at 10 weeks of age. We examined the rhythmicity of GC secretion, as they are already described to interact with the core clock machinery [99,100]. We observed that only WT, brain-RE, and RE/RE mice were able to sustain this rhythmicity (Figure 25A), suggesting that the central clock is necessary and sufficient to promote the rhythmic secretion of this hormone through the adrenal gland. This supported the hypothesis that adrenal rhythmic hormones could be mediators of the information transmitted from the central to the muscle clock.

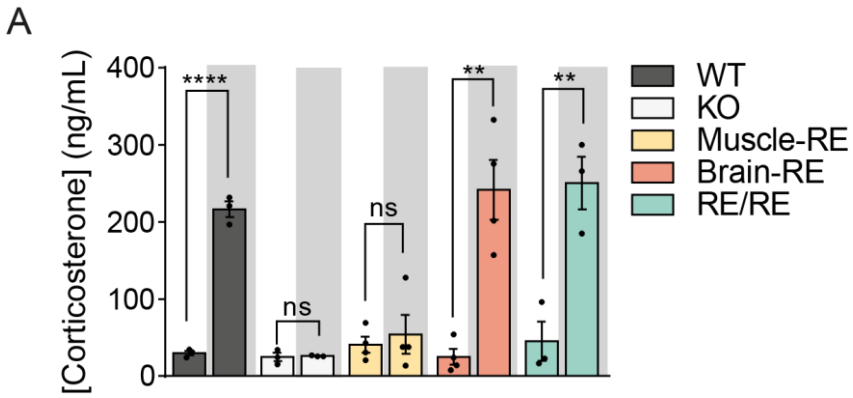

Figure 25. Plasma levels of GCs in the different models. A) Plasma levels at the beginning of the light phase (ZT0) and dark phase (ZT12) of the different models. Results are displayed as mean ± s.e.m.; *P* values are from *t*-test (two-tailed). ***P* < 0.01, *****P* < 0.0001, ns, non-significant.

Supported by these results, we subjected WT mice to bilateral adrenalectomy and examined its impact on muscle clock (Figure 26A). We collected muscles from adrenalectomized (ADX) and sham-operated mice (sham-ADX) at ZT0 and ZT12. After confirming the absence of glucocorticoids in ADX mice (which certified that there were not any residual fragments of the adrenal gland) (Figure 26B), we performed RNA-seq to analyze the muscle transcriptome. For this, we used limma [161] to detect the day/night differentially expressed genes in each condition. Our RNA-seq analysis suggested that the fold-change in the day/night expression of core clock genes was lower when WT mice were subjected to adrenalectomy (Figure 26C). In fact, the genes *Clock* and *Per1* were not detected as day/night differentially expressed in ADX group (Figure 26C). These results indicate that the ablation of adrenal glands has a direct impact on muscle clock in WT conditions.

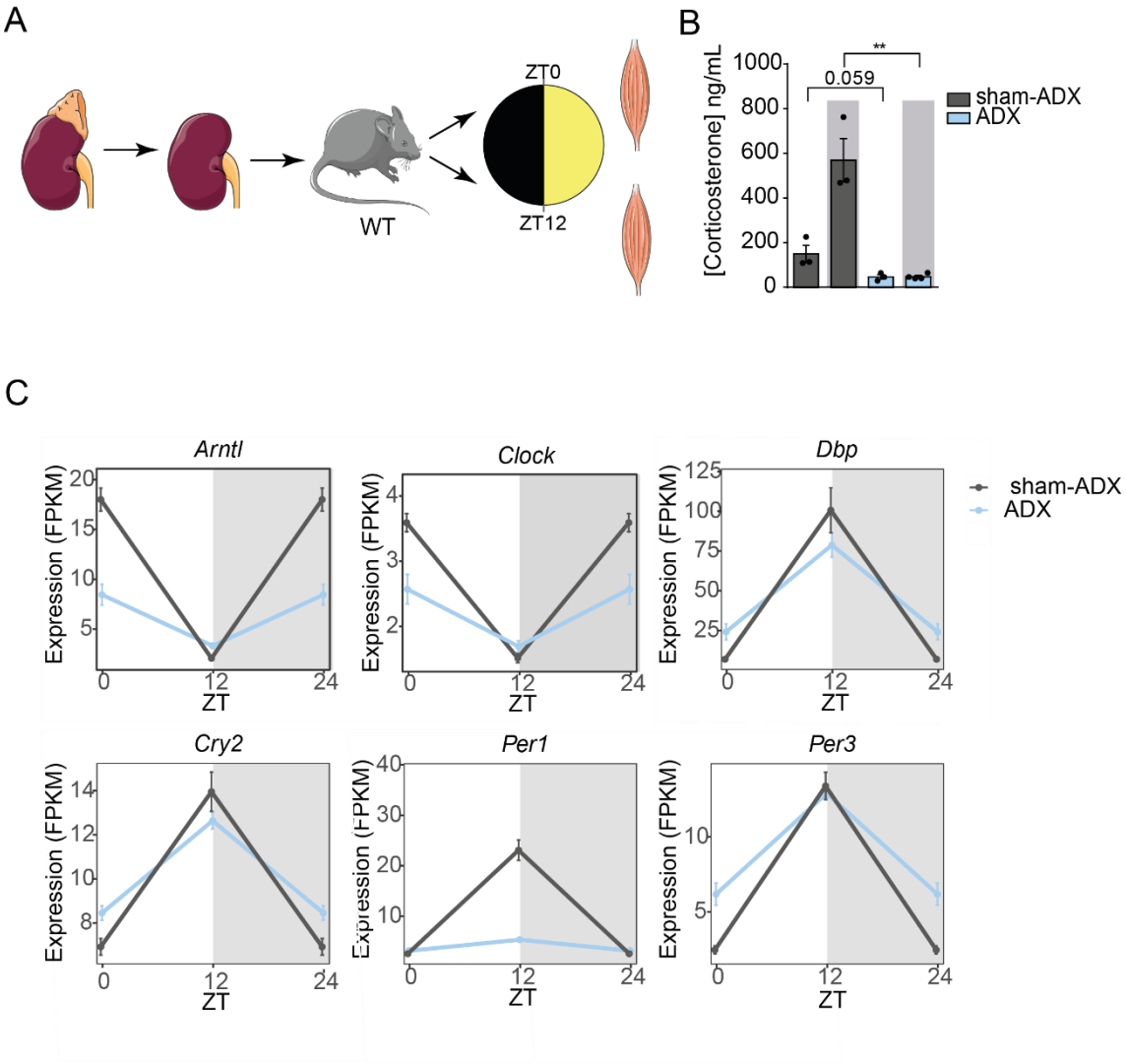

Figure 26. Adrenalectomy decreased the day/night fold change expression of core clock genes in wild-type mice. A) Scheme of adrenalectomy procedure. After bilateral ADX, muscle were harvested at ZT0 and ZT12 to perform RNA-seq. B) Corticosterone levels of sham-ADX and ADX mice at ZT0 and ZT12. Results are displayed as mean ± s.e.m.; *P* values are from t-test (two-tailed). ***P* < 0.01. C) Abundance profiles of core clock genes in sham-ADX and ADX WT mice; n = 3–4 female mice at each time point, from 9 to 12 weeks of age. Data are presented as mean ± SD. For visualization, ZT0 was duplicated (ZT24).

To confirm that this effect in clock machinery was directly related to the absence of brain and muscle communication, we performed adrenalectomy also in RE/RE mice. Muscle samples from these mice, taken at ZT0 or ZT12, were analyzed by RNA-seq. Although the RE/RE-sham group presented core clock genes differentially expressed between day and night, these differences were lost in the RE/RE-ADX group (Figure 27A). These results confirmed the role of the adrenal gland in mediating the communication between SCN and muscle.

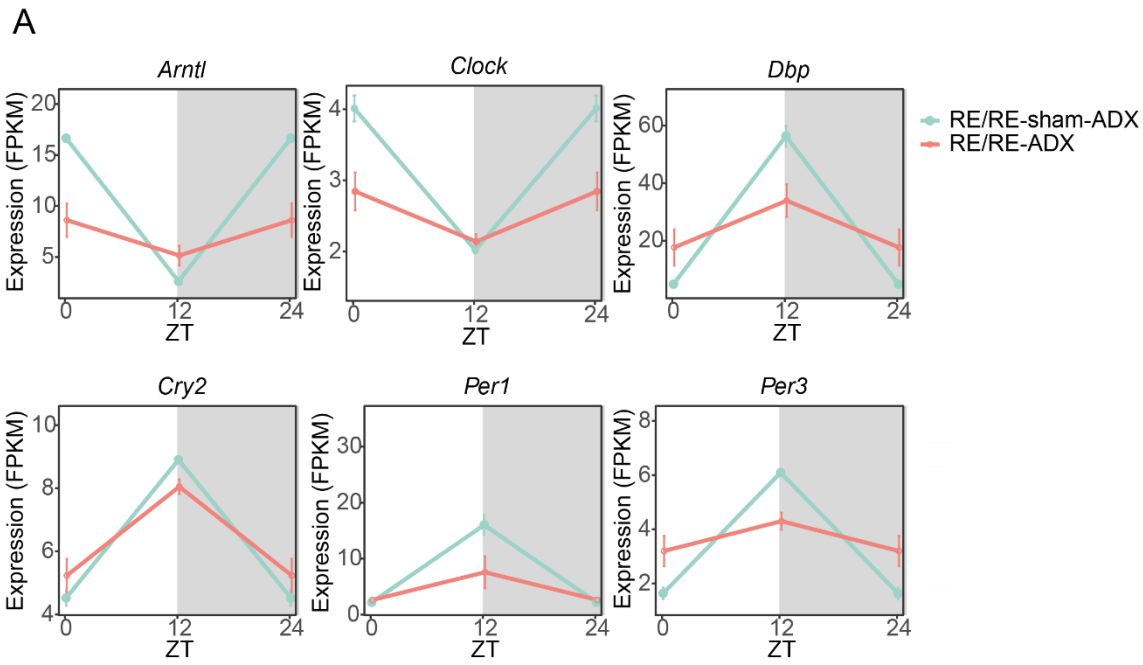

Figure 27. Adrenalectomy abolishes the rhythmicity of core clock genes in RE/RE mice. Abundance profiles of core clock genes in sham-ADX and ADX WT mice; n = 3–4 female mice at each time point. Data are presented as mean ± SD. For visualization, ZT0 was duplicated (ZT24).

We next evaluated which hormone secreted by the adrenal gland was responsible for the oscillation of muscle clock. Apart from sexual hormone precursors, the adrenal gland secretes mainly catecholamines, glucocorticoids (having several destinations in the body), and mineralocorticoids (as aldosterone, with the kidney as the main target organ) [192–194]. As catecholamines and glucocorticoids secretion into the blood is rhythmic, and the peak of secretion occurs at the beginning of the dark phase in mice [195], we injected intraperitoneally dexamethasone (a synthetic glucocorticoid, DEX) or adrenaline (ADR) in WT-ADX mice at the beginning of the dark phase, when adrenal hormones are normally secreted. After 10 consecutive days of injection, we sacrificed the mice at ZT0 or ZT12. Then, we subjected muscles to RNA-seq and analyzed the day/night differentially expressed genes in the different groups. The results of this analysis indicated that both hormones have a role in the day/night oscillation of core clock machinery, although they have a different impact on specific genes (Figure 28A). For example, the effect in *Bmal1* expression was similar between both treatments, but *Per1* showed a decreased rhythmicity upon DEX injection, although the levels of expression were recovered. With ADR, the level of expression of this gene during the night was higher compared to sham-ADX, however, the rhythmicity was recovered. With *Cry2,* ADR injection recovered both day/night levels of expression, although DEX produced a constant upregulation of this transcript.

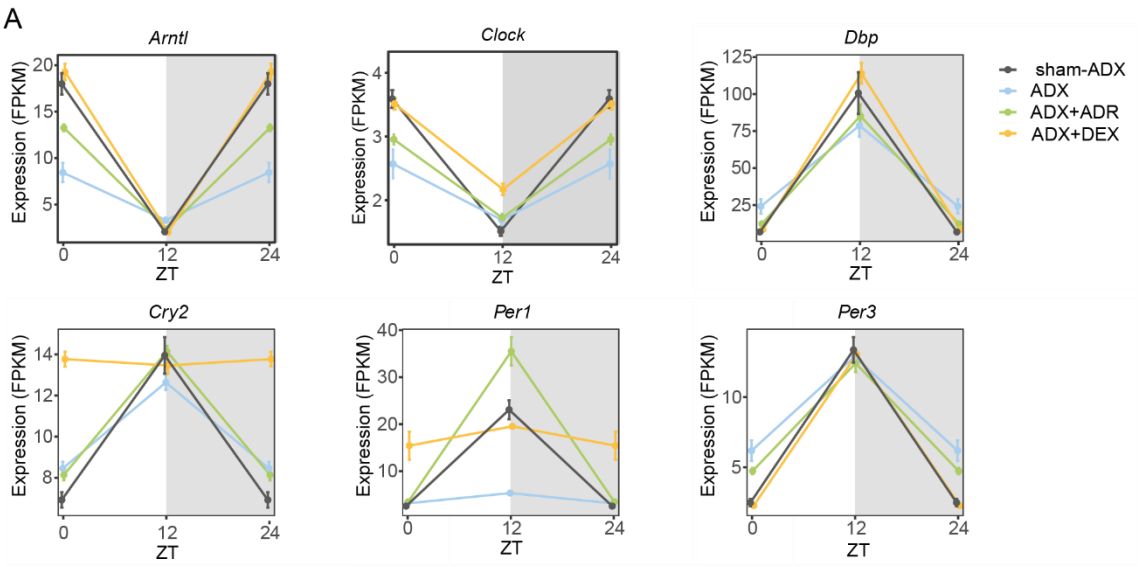

Figure 28. Core clock gene expression is affected by dexamethasone or adrenaline treatment. A) Abundance profiles of core clock genes in sham-ADX and ADX WT mice under DEX or ADR treatment; n = 3–4 female mice at each time point. Data are presented as mean ± SD. For visualization, ZT0 was duplicated (ZT24).

These results lead us to conclude that the adrenal gland is a major mediator of SCN and muscle communication, in part through the secretion of catecholamines and glucocorticoids and that both hormones have a non-replaceable effect on the regulation of muscle core clock machinery.

2.2 Time-restricted feeding (TRF) can substitute the central clock to some extent to drive daily homeostatic muscle functions

We have already described that the reconstitution of central and muscle clocks is necessary and sufficient to restore the rhythmicity of basic muscle functions in *Bmal1* deficient mice. In addition, we have identified GCs and ADR as potential mediators of brain:muscle clock communication. Apart from hormonal signaling, it is also known that brain clock generates feeding/fasting rhythms that help to align all the clocks in the body [130]. Feeding rhythms are powerful *Zeitgebers* for skeletal muscle and other peripheral tissues and can have a dominant effect on the central clock in its role of synchronizing peripheral tissues when central clock and feeding rhythms are not aligned [121,196]. For instance, scheduled feeding during the active phase of WT mice can improve metabolic rhythms in peripheral tissues of central clock-deficient mice [134].

We thus hypothesized that feeding rhythms and central clock can have overlapping functions in controlling rhythms of muscle clock. To study this question, we subjected WT, KO, and muscle-RE mice to two different conditions:

i. Time-restricted feeding (TRF): food is just available during 9-10 hours in the dark phase when WT mice are active. This regime was started when mice were 10 weeks old, for 16 weeks.
ii. *Ad libitum* feeding (ALF): food is always available.

Once mice reached 26 weeks of age, muscle samples were collected every 4 hours for 24 hours and subjected to RNA-seq (Figure 29A). JTK algorithm detected most of the core clock genes oscillating rhythmically in muscle-RE/TRF compared to muscle-RE/ALF mice (e.g., *Bmal1*, *Per3*, and *Nr1d1*), as well as *Dbp* (Figure 29B). The amplitude of these genes was similar to WT/ALF, although the phase was slightly advanced (Figure 29B-C). This demonstrates that TRF can drive the muscle core clock machinery in muscle-RE mice independently of a central clock.

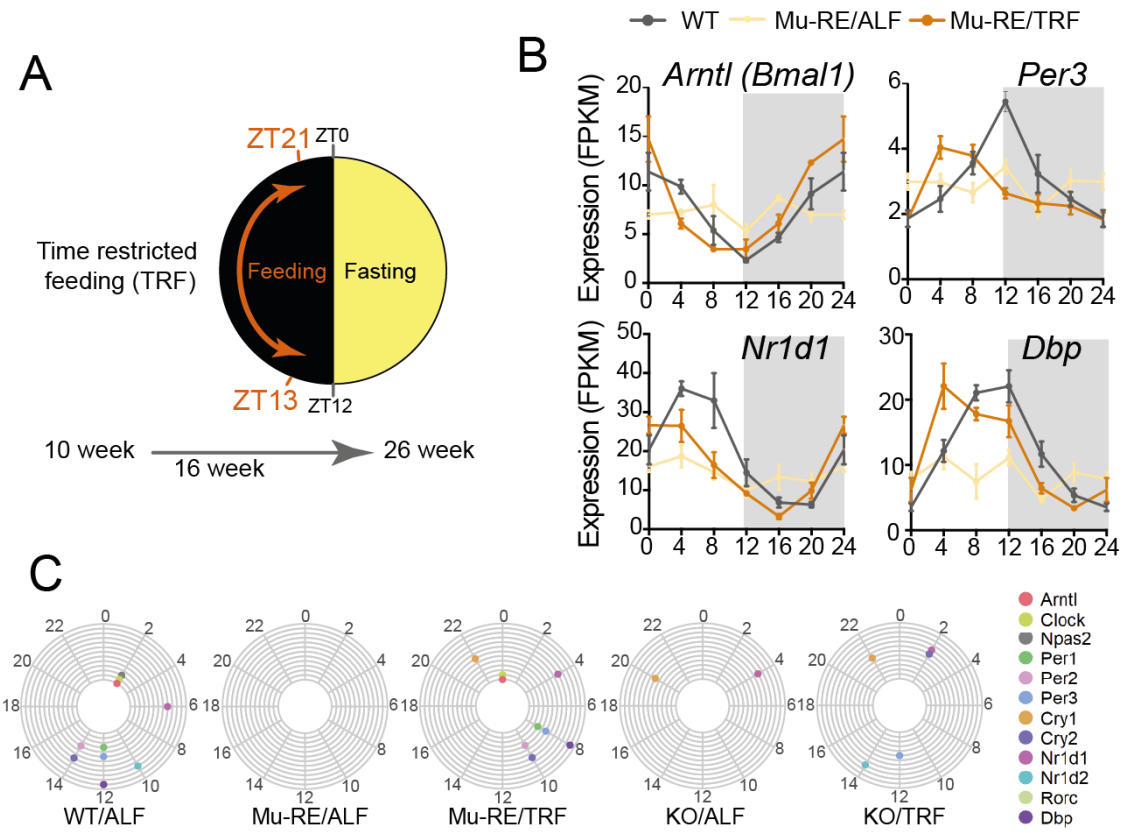

Figure 29. Effect of time-restricted feeding (TRF) on muscle core clock genes. Schematic outline of the time-restricted feeding (TRF) protocol used for WT, muscle-RE, or KO mice, as indicated. Young (9- to 10-week-old) mice were fed only during the active time (dark phase) for

about 9 or 10 hours; muscle was collected after 16 weeks of either TRF or *ad libitum* feeding (ALF). No food was available during the rest time (light phase) during the entire experiment. B) Analyses of WT/ALF, muscle-RE/ALF, or muscle-RE/TRF mice by abundance profiles of core clock genes. C) Circular plots showing peak phase distribution of rhythmic core-clock genes oscillating in WT/ALF, muscle-RE/ALF, muscle-RE/TRF**,** KO/ALF, or KO/TRF mice at 26 weeks of age (JTK_CYCLE, adjusted $P < 0.05$).

PCA plots showed that muscle-RE/TRF clustered with WT/TRF, but not with KO/TRF. (Figure 30A). Moreover, the circadian transcriptome in muscle-RE/ALF mice showed a lower amplitude compared to WT, and this was restored upon TRF (Figure 30B). As examples of important muscle genes that recovered rhythmicity upon TRF, we observed that the master regulator of myogenesis *Myod1* and downstream-regulated gene *Tcap* [114] regained rhythmicity in muscle-RE/TRF (Figure 30C). These observations suggest that feeding/fasting rhythms help to provide not only rhythmicity to the core clock machinery but also coherence at the level of the entire muscle transcriptome.

We also inquired about the functions that were dependent on muscle clock and feeding rhythms (and therefore not present in muscle-ALF, and common between muscle-RE/TRF and WT/ALF, n = 184) and those that were muscle-RE/TRF-driven and dependent on brain:muscle clock communication (*n* = 88) (i.e., common between muscle-RE/TRF, WT/ALF and RE/RE/ALF) (Figure 30D). We found that feeding rhythm–dependent genes that required muscle clock were related to important muscle functions, such as lipid metabolism and muscle growth/atrophy regulation (e.g., genes related to glucocorticoid receptor pathways, TNFα/NF-κB, and the p38 MAPK pathways), as well as circadian regulation (Figure 30E). Importantly, the core clock factors *Bmal1, Per1, Per2, Nr1d1, Dbp,* and *Clock*, as well as the myogenic regulator *Myod1*, were among the transcriptional regulators that required brain:muscle communication and that were also driven by TRF in muscle-RE condition, showing overlapping functions of the central clock and the feeding rhythms (Figure 30F). In conclusion, TRF can (at least in part) substitute SCN-derived signals.

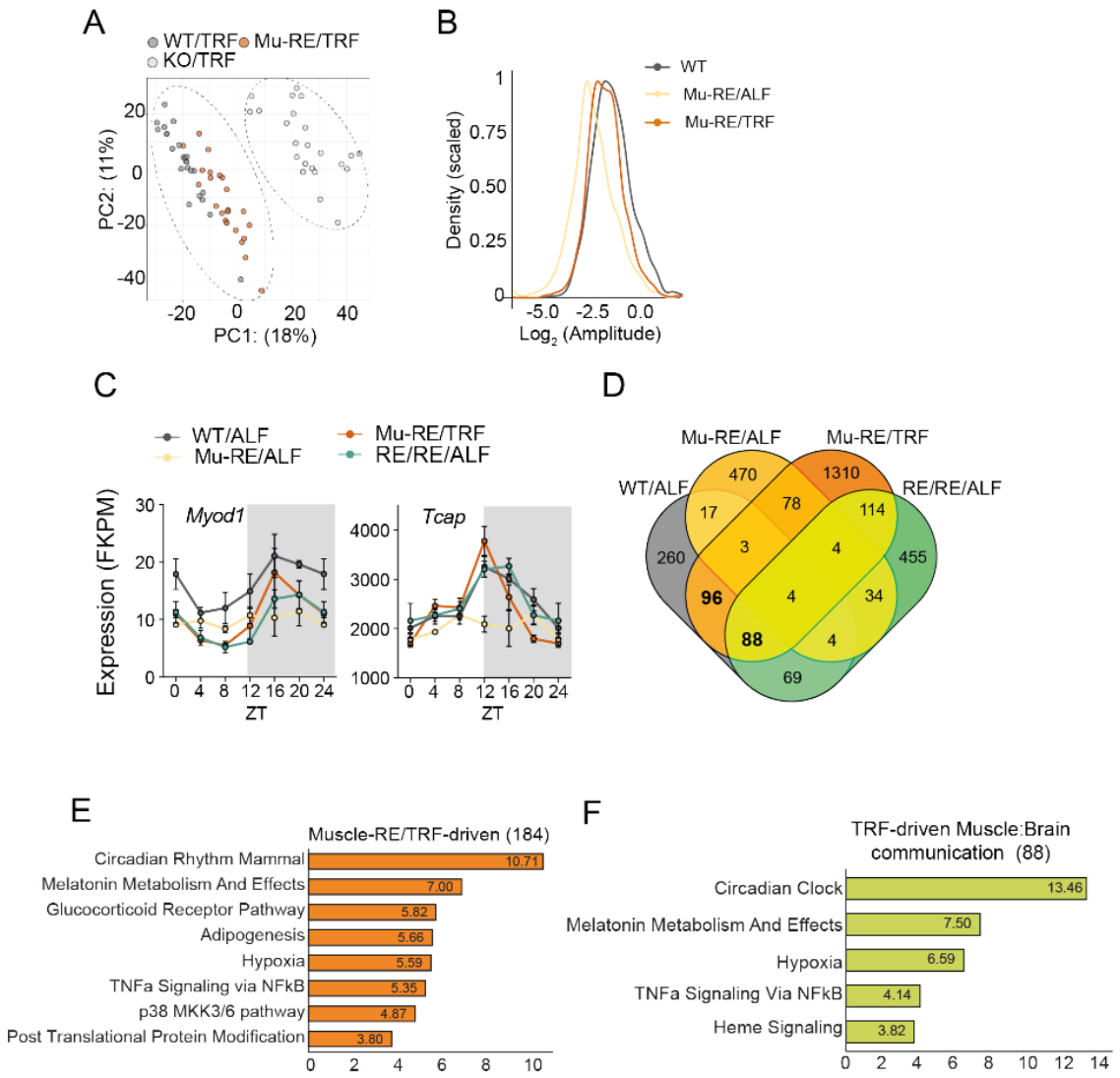

Figure 30. Effect of time-restricted feeding (TRF) on muscle circadian transcriptome. A) PCA of the full transcriptome of WT/TRF, muscle-RE/TRF, and KO/TRF. B) Density plot comparing total rhythmic transcript (JTK_CYCLE, adjusted $P < 0.05$) amplitudes; Welch's *t*-test, *WT versus Mu-RE ALF, t = 11.13, P = 3.16E-27; **WT versus Mu-RE TRF, t = 5.97, P = 3.42E-09. C) Abundance profiles of the indicated genes in WT/ALF, WT/TRF, muscle-RE/TRF and RE/RE/ALF genes in 26-week-old mice. D) Venn diagram showing intersections of genes oscillating in WT/ALF, muscle-RE/ALF, muscle-RE/TRF and RE:RE/ALF mice, but not in KO/TRF (not included in Venn diagram for simplification); JTK_CYCLE, adjusted $P < 0.05$. E and F) Bar plot showing selected canonical pathways and hallmarks enrichment analysis of the indicated sets of genes; MSigDB, FDR < 0.05.

Next, we addressed how these similarities between WT/TRF and muscle-RE/TRF in the transcriptomic profile impacted the physiology of the animal. In terms of behavior, TRF induced activity cycles both in KO and muscle-RE mice. Notably, muscle-RE mice increased their movement some minutes before food was available as compared to WT

mice (Figure 31A), suggesting although TRF was able to rescue the amount of movement of the mice, it was not fully capable of aligning it with the start of the dark phase only when muscle clock is present. However, this did not happen in RE/RE mice (Figure 14B). In addition, rhythms of RER and VO_2 were also rescued as well as the oscillation in the lipid and glucose oxidation (Figure 31B-D), similar to what is shown in other clock-compromised mouse models [134,173]. This restoration of metabolic rhythms was not an indirect effect of underlying caloric restriction, as mice increased food consumption but decreased body weight after five weeks of TRF (Figure 31E, F). Finally, we also observed that TRF moderately extended the lifespan of both KO and muscle-RE mice (by 6% and 12%, respectively) (Figure 31G). Thus, we can conclude that TRF has beneficial effects at the organism level.

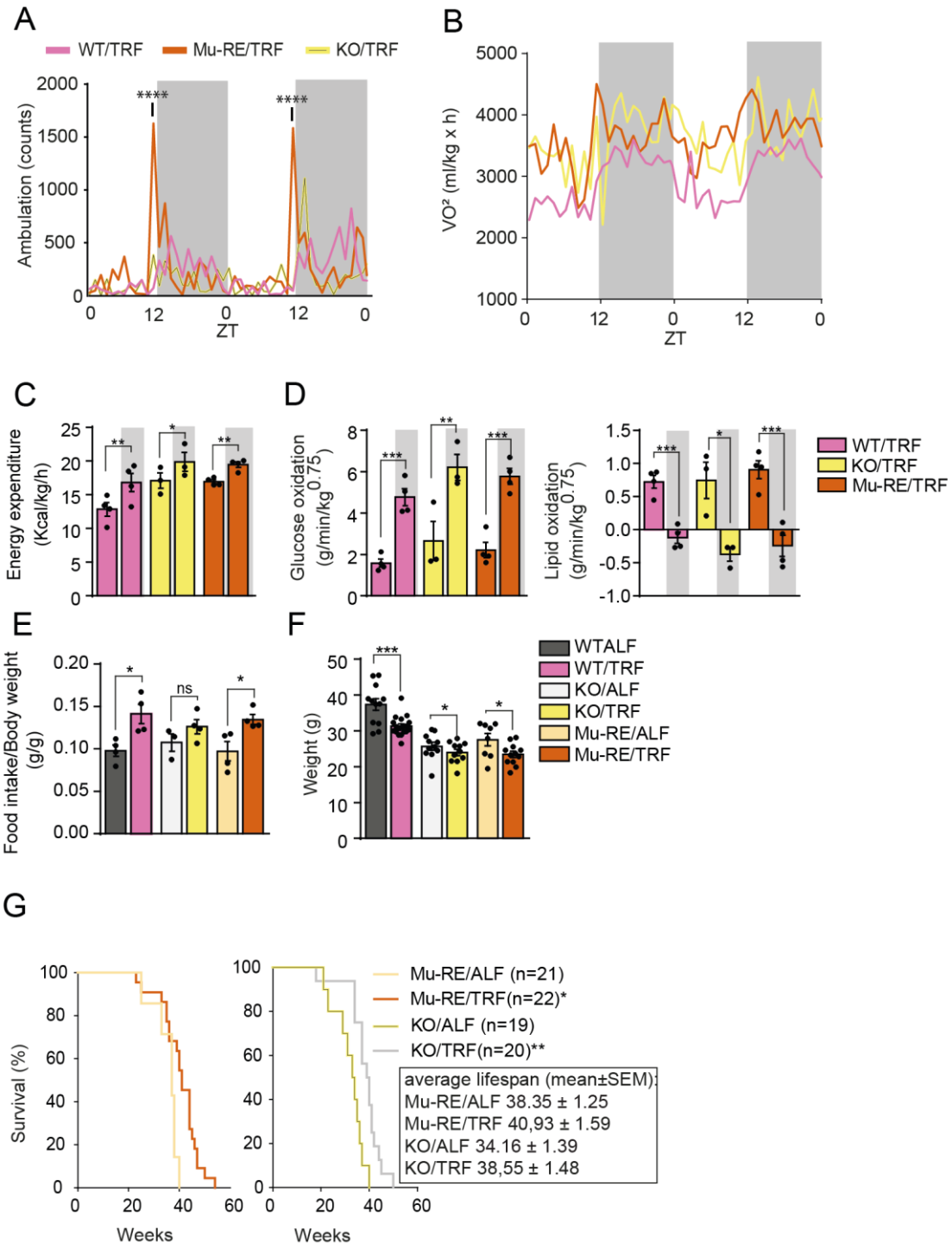

Figure 31. Feeding/fasting rhythms restore animal rhythmic behavior and prolong lifespan. A-D) Activity and metabolic parameters in young and aged mice after TRF, showing: A) locomotor activity pattern; B) oxygen consumption; C) energy expenditure; D) glucose and lipid oxidation graph. E) Normalized food intake of each mouse genotype after 5 weeks of the experiment. F) Body weight at the end of the experiment. G) Survival curves of muscle-RE/ALF, muscle-RE/TRF, KO/ALF, and KO/TRF mice. Results are displayed as mean ± s.e.m.; *P* values are from *t*-test (one-tailed) except for locomotor activity: two-way ANOVA with multiple comparisons (WT/TRF as a control; Significance shown between muscle-RE/TRF and WT/TRF when food is not

available); Survival curve: Mantel-Cox test, compared to the same genotype under ALF. *$P < 0.05$, **$P < 0.01$, ***$P < 0.001$, ****$P < 0.0001$.

We then asked whether feeding rhythms were also having a beneficial effect on muscle physiology in an independent manner of the central clock. TRF rescued some aging traits in muscle only in muscle-RE mice after TRF (but not in KO mice), proving the power of the combination of autonomous clock and TRF even when central clock was not present. These traits included i) reduced fibrosis from muscle-RE/ALF to muscle-RE/TRF (Figure 32A) and ii) improved mitochondrial wellness reaching WT levels (Figure 32B), both of which are key factors for preventing premature aging. We also found that the number of CNF was significantly lower in KO/TRF and muscle-RE/TRF mice as compared to their ALF counterparts (Figure 32A), indicating that TRF has a beneficial effect on muscle independently of muscle clock for specific traits. However, other traits were not recovered under TRF in muscle-RE mice, such as the number of eMHC positive fibers (Figure 32A), CSA of type IIb fibers (Figure 32C), and *ex vivo* force of EDL (Figure 32D).

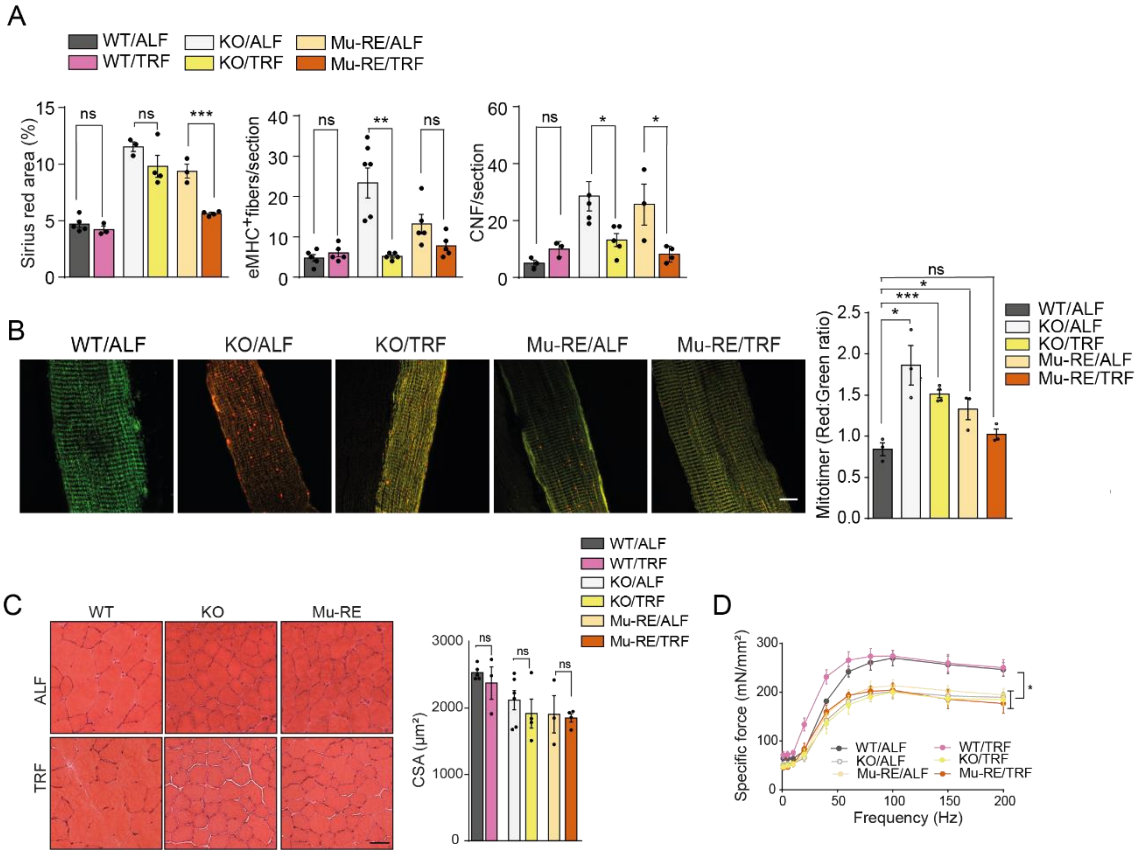

Figure 32. TRF has a positive effect on muscle physiology of clock mutants. A) Quantification of collagen deposition by Sirius red staining, with the number of eMHC⁺ fibers, and centrally nucleated fibers (CNFs) in TA muscle from WT, KO, or muscle-RE mice under ALF or TRF conditions. B) Representative images and quantification of in vivo MitoTimer reporter

expression in myofibers of TA muscles of the indicated mice genotypes and treatments to assess mitochondria stress. Oxidized (red)/unoxidized (green) ratio was quantified. *P* values are from *t*-test *$P < 0.05$, ***$P < 0.001$; ns, non-significant. C) Representative H&E images and quantification of mean fiber size in TA muscles of WT, KO, and muscle-RE mice under an ALF or a TRF regime. D) Force-frequency curves of EDL muscles of the different experimental groups at about 26-weeks of age.

These results suggest that signals from cyclic feeding or arising from the central clock overlap to some extent in maintaining muscle physiology. However, there are other physiological traits of muscle that require the activity of the central clock, such as the prevention of myofiber atrophy and loss of muscle force.

3. Feeding/fasting rhythms preserve daily functions and prevent sarcopenia in physiologically aged mice

3.1 Age-related circadian gene misalignment in old muscle is prevented by feeding/fasting rhythms

One of the major synchronizers for the periphery is the brain-imposed feeding-fasting cycles [173,196–199]. However, the brain clock deteriorates during physiological aging, and this can exert moderate changes in the intrinsic circadian periods of mice, leading to an aging-dependent decline in the circadian functions of the body [200–203]. We have described in our previous results that TRF can exert a beneficial effect on muscle even when the central clock was not present, recovering some of the brain-driven rhythmic functions. In addition, this effect is greater when muscle clock is restored. Based on these results, we hypothesized that TRF antagonize the effects of the decline of the central clock function during physiological aging and as a result helps to prevent sarcopenia in old animals.

To test this, we subjected adult WT mice (66- to 74-week-old) to TRF for approximately 26 weeks. As a control group, we used young (10- to 12-week-old) mice with ALF (Figure 33A). We performed a circadian RNA-seq to study the changes that occurred at the level of the circadian transcriptome during muscle aging with or without the TRF intervention. A big proportion of rhythmic transcripts of young mice (~76 %) were not present in old muscles. However, 445 genes were *de novo* rhythmic in the aged group (Figure 33B). In addition, old/ALF rhythmic genes presented a lower amplitude compared to young (Figure 33C-D). We also performed PSEA to determine the daily distribution of the circadian functions of muscle. We observed that the rhythmic functions were clustered

specifically at ZT0-ZT6 in old/ALF mice as compared to young/ALF mice (which showed a broader distribution) (Figure 33E). These observations indicated that during aging, muscle undergoes circadian reprogramming. However, this reprogramming is not caused by a change in the expression of the core clock genes, as the core clock machinery remained rhythmic in both ages (Figure 33F). These results correlate with previous findings in muscle/epidermal stem cells and liver from young and old mice [204,205].

Interestingly, when TRF was applied to old mice, it induced the transcription of 327 genes only present in young mice, as well as of 980 new rhythmic genes (Figure 33B), it prevented the loss of amplitude observed in old/ALF rhythmic genes (Figure 33C-D) and avoided the changes in peak distribution of rhythmic functions present in old/ALF (Figure 33E). In conclusion, scheduled feeding/fasting cycles prevent the age-related circadian gene misalignment in old mice and induce a new circadian gene program.

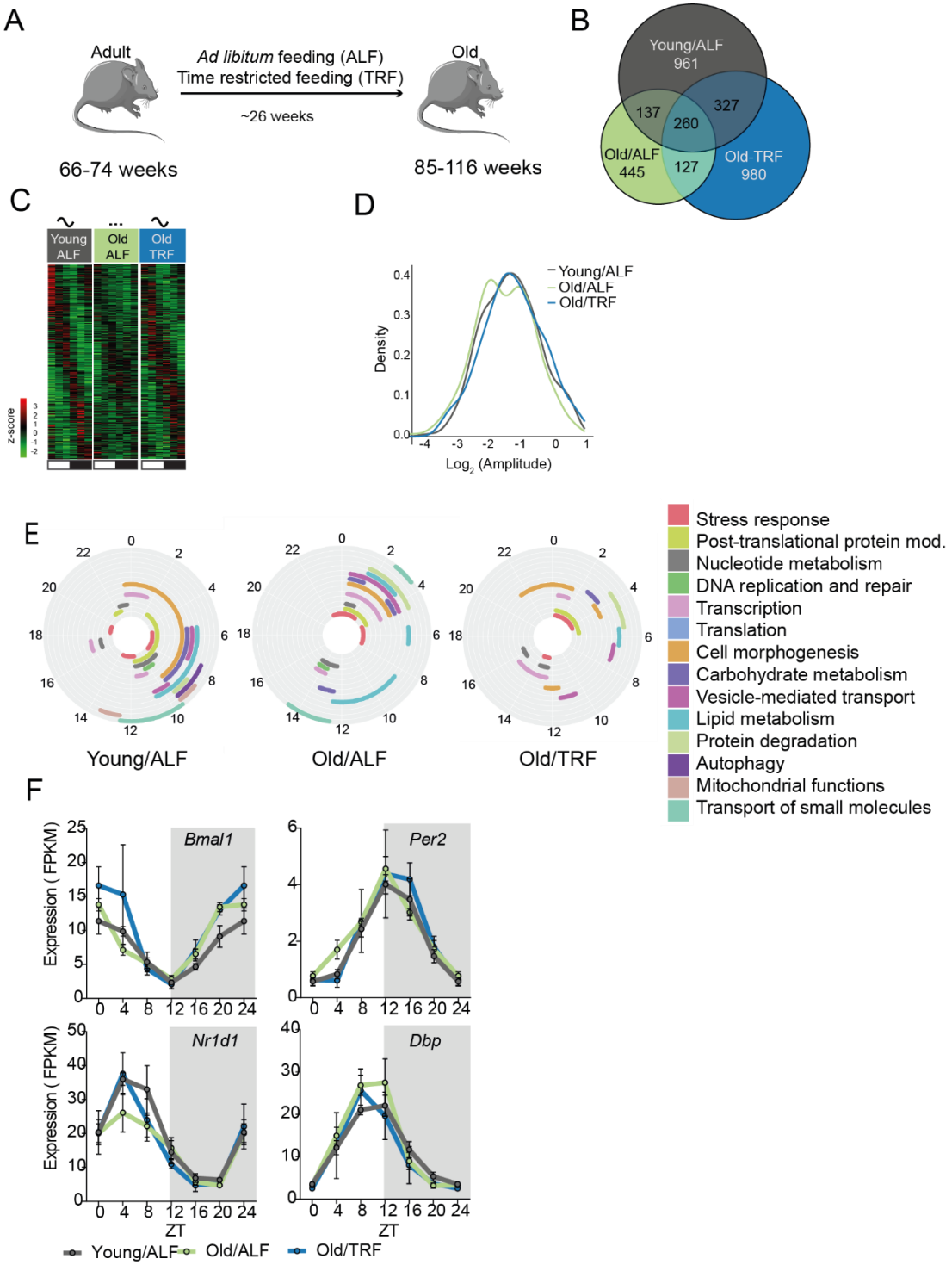

Figure 33. Effect of time-restricted feeding (TRF) on muscle rhythmic output in physiologically aged mice. A) Schematic outline of TRF used in this study for physiologically aged old mice. Old adult wild-type (WT) mice were fed a TRF regime (e.g., food only for 9 to 10 hours during the active phase) or ad libitum feeding (ALF) for ~26 weeks prior to collecting mice muscle samples. n = 24 mice, with 4 mice at each timepoint. The comparison groups were young adult (10- to 12-week-old) WT mice only with ALF, or with ALF plus 16 weeks of TRF (young/TRF). B) Venn diagram showing intersections of genes oscillating in WT mice depending on age and feeding regime, comparing young (10- to 12-week-old)/ALF, old/ALF, and old/TRF mice.

JTK_CYCLE, adjusted $P < 0.05$. C) Phase-sorted expression heatmap of 327 genes that oscillated only in young/ALF and old/TRF WT mice. D) Density plot showing rhythmic transcripts (JTK_CYCLE, adjusted $P < 0.05$) amplitude comparison for 260 genes commonly oscillating in young/ALF, old/ALF, and old/TRF WT mice; Welch's *t*-test, *young/ALF versus old/ALF, t = 2.2, $P = 0.028$; young/ALF versus old/TRF, not significant. E) Circular 24-hour phase distribution of aggregated muscle tissue-oriented functional categories in young/ALF, old/ALF, and old/TRF WT mice (PSEA, Kuiper Q-value (vs. uniform) < 0.05). F) Abundance profiles showing peak phase distribution of oscillating core clock genes in young/ALF, young/TRF (for 26 weeks), and old/TRF mice.

To understand which young (and central and muscle clocks-dependent) circadian functions were maintained by TRF in old, we studied the signature of rhythmic genes shared between muscle-RE/TRF, young RE/RE (ALF), and old WT/TRF mice. These genes (n = 179) (Figure 34A) had very similar phases in the 3 genotypes (Figure 34B) and were enriched in functions related to muscle homeostatic pathways (genes as *Myod1* and *Tcap*), lipid and carbohydrate metabolism, and circadian regulation (Figure 34C). These results reinforce the notion that brain:muscle communication that dampens with aging can be to some extent be restored by TRF via the muscle clock.

We also analyzed the differentially-expressed genes (DEGs) that were common between the physiologically-aged WT mice and all the premature aged models. The common arising functions were important for the maintenance of muscle mass and physiology (e.g., insulin, FoxO, AMPK, or mTOR signaling). The impaired expression of these genes was not present in muscles of either old WT/TRF or young RE/RE (ALF) mice (Figure 34D).

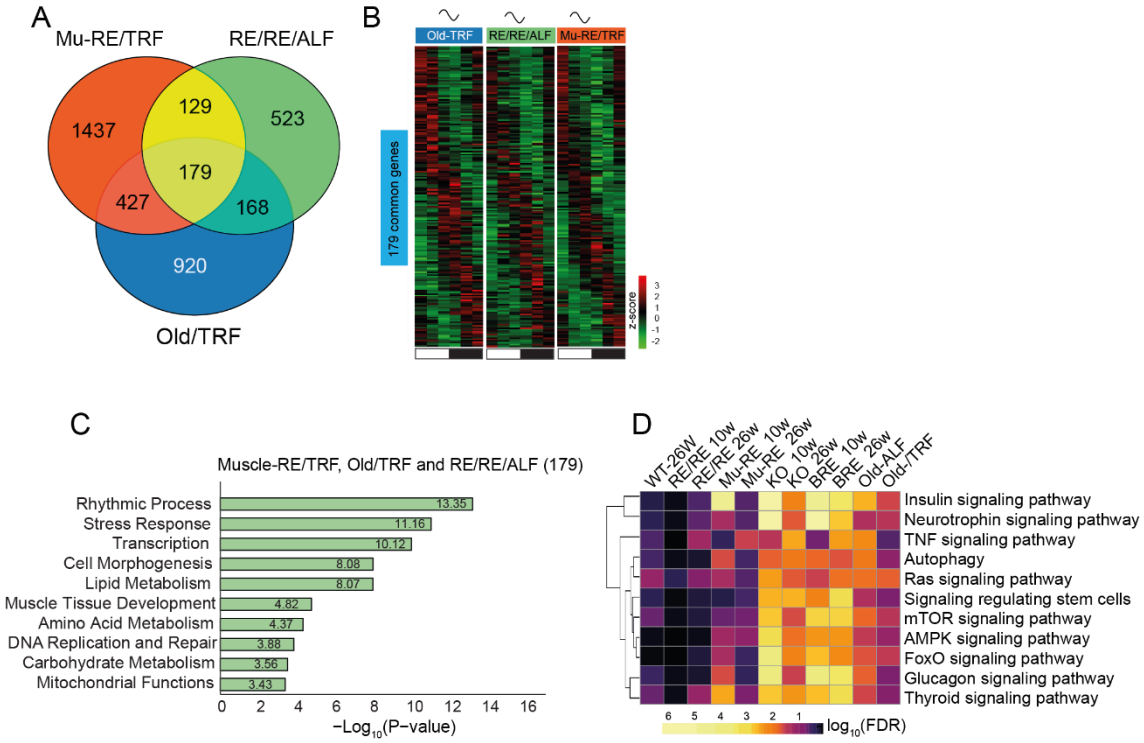

Figure 34. TRF can prevent muscle aging and reprogramming and can maintain brain and muscle clocks-dependent signatures. A) Venn diagram showing rhythmic gene overlap RE/RE/ALF and muscle-RE/TRF at 26 weeks and in old WT/TRF (JTK_CYCLE, adjusted $P < 0.05$). B) Phase-sorted expression heatmap of 179 genes commonly rhythmic in A. C) Bar plot showing selected canonical pathways and hallmarks enrichment analysis of the indicated sets of genes; MSigDB, FDR < 0.05. D) Heatmap showing the significance of KEGG pathway enrichment for differentially expressed genes (DEGs) between the indicated groups and young WT/ALF mice. Only the perturbed pathways (gProfiler, FDR < 0.05) in physiological and premature aging, but not in normal phenotypes, are shown.

These results indicate that TRF prevents the reprogramming of old WT muscle, and that TRF mimics to a certain extent the central clock capacity of driving the muscle clock.

3.2 Sarcopenia is prevented by feeding/fasting rhythms in physiologically old muscles

After observing the effects of TRF at the level of muscle transcriptome in physiologically aged mice, we assessed whether these changes were accompanied by reduced sarcopenia in old muscles. TRF had a strong effect in reducing the atrophy of type IIb fibers, the levels of fat accumulation, and fibrosis in old mice (Figure 35A-B). In addition, muscle force was also preserved, as it was not statistically significant in WT/ALF mice (Figure 35C). Furthermore, TRF prevented the loss of mitochondrial bioenergetics and metabolism in old muscles *in vivo*, as observed by the preservation of succinate

dehydrogenase (SDH) activity (which indicates changes in the overall oxidative capacity of a skeletal muscle) (Figure 35D). In addition, the increase of damaged mitochondria observed with MitoTimer in old/ALF muscles was not present in old/TRF muscles (Figure 35A&D).

Finally, we also compared the locomotor and metabolic rhythms of the mice. The rhythmic locomotor movement was improved in old/TRF mice compared to old/ALF mice, and diurnal rhythmic patterns of RER and VO_2 (oxygen consumption) were also maintained in old/TRF mice (Figure 35E).

In sum, these results are consistent with the observations that arise from the transcriptome, indicating that following a TRF regime can prevent muscle aging in mice.

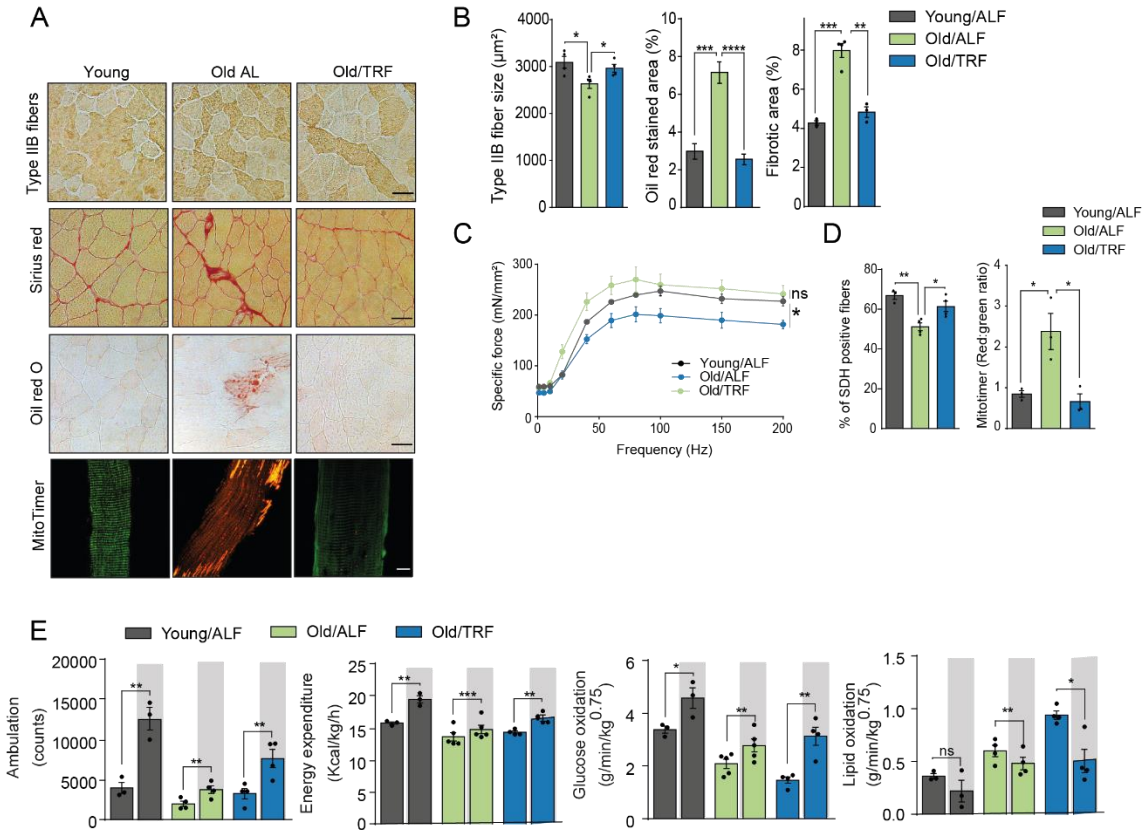

Figure 35. Time-restricted feeding (TRF) effect on muscles and general physiology from old mice. A) Representative pictures of fast type IIb fibers immunostaining, collagen content by Sirius red staining, Oil Red O staining, and MitoTimer reporter and in tibialis anterior muscles of young-WT/ALF, old-WT/ALF, and old-WT/TRF mice. B) Quantification of IIb fibers CSA, lipid content by Oil Red O staining, and collagen deposition of the indicated experimental groups. C) Force-frequency curves of EDL muscles after *ex vivo* isometric stimulation. D) Quantification of myofibers with high mitochondrial enzymatic activity by succinate dehydrogenase (SDH) staining and mitochondrial fitness by the MitoTimer reporter (with the red:green ratio showing

damaged:healthy mitochondria). E) Quantification of the activity patterns, energy expenditure, and lipid and glucose oxidation in mice of the different experimental groups. Scale bars: 50 µm except for MitoTimer, 10 µm. Results are displayed as mean ± s.e.m.; *P < 0.05, **P < 0.01, ***P < 0.001, ****P < 0.0001, ns, non-significant (two-tailed t-test except for force-frequency curves, two-way ANOVA and metabolic parameters, one-tailed t-test).

DISCUSSION

Brain and muscle clocks are required to maintain muscle physiology and to prevent premature aging

Aging is a phenomenon intrinsic to every organism, characterized by a functional decline at the end of life. Among the hallmarks of aging, altered intracellular communication and deregulated nutrient sensing are two factors that can evolve into organ failure and loss of proper inter-tissue communication, which leads the organism towards physiological inconsistency and failure [206,207]. The central clock located in the SCN integrates information from the environment and sends out synchronization cues to clocks in other tissues, which in turn integrate this information to run their daily functions [208]. Moreover, mice with constitutive deletion of the essential clock component *Bmal1* show an accelerated aging phenotype [104]. This indicates that aging and the circadian clock system are highly intertwined. However, at the beginning of this work, we had little knowledge about the relative importance and roles of individual nodes in the circadian clock network, or about how these interdependencies between different clocks change during aging.

Here, we have demonstrated the most basic circadian components that support key aspects of skeletal muscle function in young and old mice. We found that restoration of *Bmal1* expression in myofibers and *Syt10*-positive cells is necessary and sufficient not only for controlling muscle circadian gene expression but also for preserving muscle physiology and reducing signs of muscle aging (sarcopenia). We observed that core clock genes of muscles from young RE/RE mice oscillate with highly similar profiles to WT. Moreover, the restoration of the two clocks is sufficient to drive the rhythmicity of 11% of the WT muscle circadian transcriptome. These genes are involved in essential functions for muscle maintenance, such as the regulation of proteostasis or myofiber growth.

Since the majority of core clock genes expression levels are already restored in the muscles of muscle-RE mice, we can speculate that it is the rhythmic function of the clock, rather than the presence of *Bmal1* alone, which is decisive in the transcriptional and functional rescues we observe in RE/RE. In line with the lack of core clock genes oscillations in muscle-RE mice, there is a restoration of only 7% of the muscle circadian transcriptome at 10 weeks of age, including genes involved in stress and inflammatory responses. These results are similar to the circadian transcriptome of gastrocnemius muscle from muscle-RE mice [209]. Although in gastrocnemius muscle, there was slight oscillation of the core clock genes (but with amplitudes that are far away from WT), the total recovery of the circadian transcriptome remains very poor in both muscles [209]. In

contrast to muscle, the autonomous clock of skin and liver shows clearer evidence of oscillation, as most core clock genes were found to oscillate, albeit with a 2-4 h phase advance compared to WT condition when only skin or liver clocks were restored. Each autonomous clock drives 13% and 11% of their circadian transcriptome, respectively [82,210], regulating functions such as the correct timing of cell cycle to avoid radiation damage during cell division in the case of skin, and glycogen metabolism in the case of liver [82,210], pointing to a higher degree of autonomy of these peripheral clocks compared to muscle. Although we have shown that the brain clock contributes to a substantial recovery of the circadian transcriptome in muscle, the effects of central clock on other peripheral clocks (such as in liver and skin) remain unknown.

We also observed that 50% of the WT circadian transcriptome is not recovered in RE/RE muscles. This means that there is a big proportion of the circadian muscle physiological functions that require the restoration of other peripheral clocks. This fits well with recent data demonstrating that when BMAL1 is absent from skeletal muscle but present in the rest of the body (including the SCN), the liver circadian transcriptome is affected [173]. Hence, in addition to central:peripheral clock communication, there is growing evidence that peripheral clocks are also capable of signaling to each other and that this signaling is required to ensure proper body physiology. Regarding the effect of muscle clock in other peripheral tissues apart from liver, *Bmal1* restoration in muscle regulates sleep and recovers the amount of total movement of animals (functions require brain activity) [211,212], although we have not detected this improvement in our muscle-RE. The reason could be the continuous expression of *Bmal1* in the models of the mentioned studies, as the gene was under the control of human α-actin-1 promoter. In our case, it was expressed under its own promoter.

These differences found in the muscle circadian transcriptome of our models were translated into the physiology of the tissue. KO, muscle-RE and brain-RE (none of them showing proper oscillation of their core clock genes) showed signs of muscle aging, that were present at 10 weeks of age, but were aggravated at 26 weeks of age. However, expression of *Bmal1* in myofibers and in brain was sufficient to prevent them. Indeed, it had a direct impact on muscle force, being completely recovered in RE/RE mice even in 26-weeks-old mice. This restoration of muscle phenotype was not because of a recovery in the amount of total movement observed in RE/RE (lack of movement drives to muscle atrophy), as rhythmic brain-RE mice, which also exhibit locomotor rhythms and activity levels comparable to WT, had evident signs of sarcopenia. We have therefore concluded that central and muscle clocks restoration has a powerful effect on preventing sarcopenia

in a model that constitutively lacks *Bmal1.* In contrast, in the skin from skin-RE (where the rhythmicity of core clock genes is present), the rescue of the autonomous clock was sufficient to significantly reduce the premature skin aging occurring in KO mice, shown by a reduction of the thickness of the cornified layer present in 30-weeks-old mice [81]. We can then speculate that the rhythmicity of the core clock genes is important not only for the recovery of the circadian transcriptome but also for the maintenance of the tissue.

One limitation of our study was the fact that our *Bmal1* KO is conventional, such that *Bmal1* is absent throughout an animal´s lifetime, rather than inducible deletion at a given point. Studies showed that premature aging of KO adult mice is not present when *Bmal1* is expressed until 3 months of age[213]; therefore, it is an open question at which specific developmental timepoint *Bmal1* is regulating lifespan. In line with this study, it has been shown that the reduced *ex vivo* force present in gastrocnemius muscles of 5-months-old muscle-specific and constitutive *Bmal1*-KO was recovered when *Bmal1* was eliminated in 2-months-old mice [112]. Thus, it could be possible that the aging phenotype observed in KO is due to the lack of *Bmal1* during developmental stages, and that the rescue of *Bmal1* during this precise time window in muscle and brain is required to prevent premature muscle aging.

<u>The muscle peripheral clock has a gatekeeping role over signals from the central clock</u>

We have observed a limited capacity of the muscle autonomous clock to generate rhythmicity in gene expression. In contrast, in muscles from brain-RE model, the number of oscillatory genes was three-times more than those found in WT muscles, although core clock genes were not oscillating. This number was drastically reduced in RE/RE conditions. These observations point to an ability of brain clock to drive a muscle circadian output that is independent of muscle clock, and that the autonomous muscle clock is playing a key role in gating these signals coming from the brain clock. This gating function of muscle autonomous clock is needed to restore tissue physiology.

Supporting our data in muscle, a recently published work in brain-RE mice shows that in the absence of other clocks, there are a large number of *de novo* rhythmic serum metabolites (174/298 total) that are not oscillating in WT mice [172]. This substantial number of cyclic metabolites suggests that the brain generates a broad number of circulatory metabolic rhythms, but that input from peripheral clocks is required to modulate and fine-tune these signals coming from the central clock. Considering brain-RE muscles, we have observed new circadian functions that were not present in WT as

well as mistimed expression of the circadian genes shared between brain-RE and WT. Recovering brain and muscle clocks corrected the phase of homeostatic processes, such as mitochondrial function and autophagy. Performing these functions at the right time is important for the muscle, as it completely depends on mitochondria in situations of high energy demand, and altering these functions drives sarcopenia [182,214,215]. Similar results have been found in the skin, where the brain-specific restoration of *Bmal1* causes the daytime expression of early cell cycle genes [216]. This is detrimental to the homeostasis of skin, as this is the moment of the day in which the tissue is more exposed to DNA-damaging conditions which could cause mutations during DNA replication. In WT mice and mice with *Bmal1* expressed only in brain and skin, the phase of genes involved in DNA replication is corrected, which minimizes DNA damage [217].

In this study, we have also observed that the brain clock has a role in controlling body glucose homeostasis. In previous reports, brain-RE was shown to exhibit a WT response to oral glucose tolerance tests in young mice, which was lost in muscle-RE [172]. Here, we show that RE/RE mice did not improve glucose tolerance at this age. In contrast, in young mice, glucose tolerance can be restored with the joint actions of liver and muscle clocks together with feeding/fasting rhythms [209], indicating that feeding/fasting cycles generated by the brain clock are the required signal to sustain glucose homeostasis, together with synchronized liver and muscle clocks. Simultaneous brain and muscle clock restoration could be detrimental to a clockless and asynchronous liver, which may be why glucose tolerance is not restored to WT levels in RE/RE mice. However, this scenario changes during premature aging. 26-weeks-old RE/RE mice show similar glucose tolerance to WT (and brain-RE does not). It is possible that exhaustion of brain clock in the last stages of the lives of mice [201,218], harms glucose tolerance of aged brain-RE mice. In this scenario, muscle clock reconstitution seems to be beneficial, as RE/RE mice completely recovered WT levels of blood glucose. This indicates that in this specific moment of life, only brain and muscle clocks are required to support systemic glucose tolerance.

Signaling from the adrenal gland maintains the communication between the brain and muscle clocks

An unsolved question is how the brain interacts with muscle clock. Adrenal glands have been suggested as possible connectors between the central and peripheral oscillators, because their removal altered the rhythmicity of peripheral clocks, but not that of the

central clock in WT mice [132,190,191]. However, their specific roles in communicating brain and muscle clocks have not been explored in detail. We observed that glucocorticoid secretion rhythms by the adrenal glands were preserved in RE/RE and brain-RE mice, but not in KO or muscle-RE mice, meaning that the brain clock was sufficient to sustain these hormonal oscillations into the bloodstream and that the adrenal gland (even without a functional clock) could mediate central and muscle clock communication.

Although this part of the study was limited to the analysis of two-time points (ZT0 and ZT12), the day/night fold-change expression of muscle core clock genes was reduced when the adrenal glands were not present in WT mice. Moreover, these day/night differences were abolished in RE/RE muscles, indicating a mediator role of adrenal hormones in driving the expression rhythmicity of core clock genes in muscle. Previous studies have analyzed the effect of adrenalectomy on the circadian transcriptome of other peripheral tissues. In white adipose tissue adipokine genes lost their daily rhythmicity, and the expression of the core clock gene *Per1* became flat[191]; in liver, *Per1* is also the most sensitive core clock gene after the removal of adrenal glands. In other tissues (such as jejunum, kidney cortex, and splenocytes), the effect depended on the specific clock gene. For example, *Dbp* has a reduced amplitude in kidney and is phase delayed in jejenum [190]. We observed that in skeletal muscle from adrenalectomized mice the expression of *Per1* was dramatically affected, as observed in fat and liver. Accordingly, muscle *Per1* levels were very sensitive to dexamethasone or adrenaline administration. However, the effect of each treatment was different, as dexamethasone recovered the level of expression, but the day/night differential expression was recovered only after adrenaline administration at the beginning of the dark phase.

In the mentioned previous studies, the effect of adrenalectomy on peripheral tissues has been directly attributed to glucocorticoids. However, the adrenal gland secretes several rhythmic hormones, such as aldosterone or catecholamines [219,220]. Although aldosterone has the kidney as its main target, adrenaline when secreted into the bloodstream targets several organs, including the skeletal muscle. Catecholamines play an important role in muscle having a direct effect on its contraction and relaxation capacity [221] and are responsible for the stress-induced increase in skeletal muscle force [222] regulating directly the muscle performance throughout the day. Here, we show that each treatment affects each clock gene differentially, meaning that both hormones (and not only corticosteroids) participate in the control of the expression of clock genes in muscle. Something similar may be happening to other peripheral clocks, an issue that remains largely unexplored.

Therefore, we suggest that the simultaneous presence of both hormones may control both the levels and the rhythmicity of core clock genes in muscle.

Feeding/fasting cycles can drive some daily homeostatic functions in muscle

Apart from external light-dark cycles, exercise or feeding time can modulate peripheral clocks independently of the SCN [196]. Regarding feeding, it has been recently demonstrated that not only the caloric content of the nutrients affect wellbeing, but also the timing of feeding has a key role in healthspan [223,224]. When mice are fed exclusively during their inactive time (during the light phase), they suffer from metabolic disorders. This may be due to peripheral clocks' alignment to the new feeding paradigm, which is not in phase with the SCN clock. This desynchrony between central and peripheral clocks affects negatively to peripheral tissues. For example, in skin daytime feeding reverses the sensitivity of radiation from night (the moment during the major part of progenitors undergo the S phase) to the day, which may contribute to skin pathologies involving sun damage; in liver, daytime feeding alters glycogen metabolism, which could affect global glucose homeostasis [225,226]. However, restricting feeding to their active time has a beneficial effect, even without reducing the caloric intake, as it protects animals fed with a high-fat diet from developing steatosis, obesity, and hyperinsulinemia [133,227].

In our study, both KO and muscle-RE recovered rhythmic locomotor activity, energy expenditure rates, and glucose and lipid oxidation were also oscillating as observed previously in another clockless model lacking *Cry1* and *Cry2* [134]. This means that these feeding/fasting rhythms (which in WT mice are generated by the brain clock) are sufficient to drive daily oscillations in fuel utilization. The beneficial effect of TRF specifically on peripheral clocks has been reported in liver, in which night-feeding together with liver clock drives temporal carbohydrate homeostasis when the central clock is not functioning [173]. Here we provide evidence that muscle physiology and homeostasis in KO and muscle-RE mice are improved after TRF, revealing a key impact of SCN-derived signals such as the feeding-fasting cycle on muscle physiology. Nonetheless, KO/TRF mice still have some aging traits, such as increased fibrosis and the accumulation of unhealthy mitochondria. In muscle-RE/TRF mice, these features were largely recovered. This indicates that both muscle clock and TRF have a synergistic effect on muscle health by preventing premature aging. However, the reduction in CSA of myofibers and the decrease in muscle force were not rescued in muscle-RE/TRF mice. As a possible explanation, the advanced phase of core clock genes and the reduced amplitude of circadian transcriptome of muscle-RE/TRF mice (features that were

completely restored in the RE/RE group) could be limiting the beneficial effect of TRF in muscle physiology. It is also possible that the increase in food anticipatory activity (FAA) observed in muscle-RE/TRF mice is directly affecting muscle core clock machinery. FAA has been described as the increase of activity levels in mice before food availability, and it is controlled by a food-entrainable oscillator that is independent of SCN, as SCN-ablated animals still exhibit normal FAA [228,229]. Therefore, it is possible that the increased activity observed in muscle-RE/TRF but not in animals with an intact SCN clock (RE/RE and WT) advances the phase of core clock genes in muscle having as a consequence a detrimental effect on muscle physiology (i.e., reduced CSA and muscle force compared to WT animals).

Imposed feeding/fasting rhythms prevent sarcopenia

The brain imposes feeding/fasting cycles, which can act as a synchronizing signal for peripheral tissues [173,196]. Indeed, we found that *de novo* introduction of a feeding/fasting cycle to muscle-RE animals led to restoration of clock gene rhythmicity. During physiological aging, the neuronal activity of the SCN declines. This directly affects the peripheral clocks, resulting in a loss in the integration of physiological rhythms [230]. We provide evidence that muscle clock function in old mice can be rejuvenated through the imposition of time-restricted feeding rhythms, and that these feeding/fasting cycles are a key component of brain clock-dependent communication with the muscle also in aged mice.

Contrary to muscle-RE animals, the muscles of old mice did not present an altered expression of the core clock genes, in line with previous findings in liver, skin stem cells, and satellite cells [204,205] However, there is a big reprogramming of the circadian transcriptome in old muscles, as well as a reduction in the total number of circadian genes compared to young mice. These observations have been also made in epidermal stem cells and liver [204,205]. This circadian transcriptome reprogramming in old muscles was accompanied by a decreased amplitude. It has been observed in liver from young mice that there is a circadian pattern of global protein acetylation, which is lost upon aging even in the context of largely unaltered core clock gene expression [204]. Then, it could be possible that the loss of post-transcriptional rhythmic modifications (without altering core clock genes expression) is causing this circadian transcriptome reprogramming in muscle.

The number of rhythmic genes shared between WT/ALF and old/TRF was higher than between WT/ALF and old/ALF (35% and 23% respectively) and the decreased amplitude of rhythmic gene expression in old muscles was restored upon TRF, indicating that TRF has a direct effect on muscle circadian transcriptome. The positive effect of these feeding rhythms on the muscle clock has an impact on tissue physiology. All measured signs of sarcopenia were rescued upon TRF in old animals. Similar to our results, it has been reported in both flies and mice that the effects of dietary restriction on healthspan require clock genes [139,231]. Moreover, it has been shown that longevity in mice under a caloric restriction regime is even improved when food availability is aligned with the active time due to its entrainment effect on the circadian machinery [232]. Our results, together with the aforementioned studies point to TRF as a beneficial feeding regime that acts directly on circadian rhythms.

All aging traits were rescued in old WT muscles upon TRF. As these sarcopenia features were also restored in RE/RE animals, we hypothesize that feeding rhythms are also reinforcing the output of the SCN in physiologically aged mice, thereby having a positive effect on skeletal muscle. We propose a model in which the feeding schedule directly affects metabolism, which impacts peripheral tissues. It could also be possible that peripheral tissues send signals to the central clock, improving its neuronal activity rhythms, which in turn have a beneficial effect on peripheral clocks.

Overall, our results reinforce the notion that the aging intrinsic clock machinery can be physiologically manipulated towards a more youthful functioning. A major challenge to the scientific community is to understand the mechanisms of the progressive metabolic deregulation that occurs during aging. There is increasing evidence that there is an interaction between circadian clocks and aging-related pathologies. In this work we have defined the link between muscle aging and the dampening of the circadian clock. From our results, we reasoned that both brain and muscle clocks are necessary and sufficient to mitigate muscle aging. After these observations, we have been able to propose TRF as a possible substitute (or restorative) of the brain clock. Our results are relevant for envisioning ways of preventing these circadian disruptions and for treating age-associated diseases as well as the effects of aging itself. We are now starting to understand how important is that our physiological functions are aligned to the circadian time. In near future, a circadian perspective in medicine would help to fight against diseases and aging.

CONCLUSIONS

1. The restoration of *Bmal1* expression only in skeletal muscle is necessary but not sufficient to prevent muscle aging caused by *Bmal1* constitutive deficiency.

2. *Bmal1* restoration specifically in brain causes a unique set of *de novo* muscle transcripts to be rhythmic that are independent of the autonomous clock. However, they have altered phases and amplitudes. The skeletal muscle clock has a gatekeeping role over signals from the central clock.

3. Simultaneous clock restoration in brain and skeletal muscle is necessary and sufficient to align important muscle homeostatic functions and to prevent premature aging. Nonetheless, peripheral clocks are needed for the complete circadian gene program.

4. The adrenal gland is a key node in the communication between the central and the muscle clocks.

5. Aligning the feeding schedule to the activity time of clockless mice has a beneficial impact on muscle physiology, which acts synergistically with muscle clock.

6. Time-restricted feeding can be used to delay physiological muscle aging.

In sum: brain and muscle clock communication through the adrenal gland is required to maintain the daily alignment of muscle functions. Time-restricted feeding acts as a powerful trainer to maintain muscle homeostasis, which has a beneficial effect in preventing muscle aging.

ABBREVIATIONS

ABBREVIATION	DEFINITION
ACTA1	Actin Alpha 1
ADR	Adrenaline
ADX	Adrenalectomized
AKT	AKT Serine/Threonine Kinase
ARNTL	Aryl Hydrocarbon Receptor Nuclear Translocator Like
AUC	Area Under the Curve
AVP	Arginine Vasopressin Peptide
BMAL1	Brain and Muscle ARNT-Like 1
Brain-RE	*Bmal1* reconstituted in the brain
BRE	*Bmal1* reconstituted in the brain
BSA	Bovine Serum Albumin
CCG	Clock-Controlled Gene
CK1δ	Casein Kinase 1 Delta
CLOCK	Circadian Locomotor Output Cycles Kaput
CNF	Central nucleated fiber
CRY	Cryptochrome
CSA	Cross Sectional Area
DBP	albumin D-element-Binding Protein
DEX	Dexamethasone
DPX	Dibutyl Phthalate in Xylene
EDL	Extensor Digitorum Longus
EE	Energy Expenditure
EGF	Epidermal Growth Factor
eMHC	embryonic Myosin Heavy Chain
FAP	Fibro/Adipogenic Progenitor
FoxO	Forkhead Box O
FW	Forward primer
GC	Glucocorticoid
GO	Gene Ontology Biological Processes
GR	Glucocorticoid Receptor
HPA	Hypothalamic-Pituitary-Adrenal
HPT	Hypothalamic-Pituitary-Thyroid
HSA	Human α-Skeletal Actin

imKO	inducible muscle *Bmal1*-KO
IP	Intraperitoneal
ipRGCs	intrinsically photoreceptive Retinal Ganglion Cells
JTK	Jonckheere-Terpstra-Kendall
KEGG	Kyoto Encyclopedia of Genes and Genomes
KO	Knockout
LD	12h Light/12h Dark
MAPK	Mitogen-Activated Protein Kinase
MHC	Myosin Heavy Chain
MSigDB	Molecular Signatures Database
MTOR	Mammalian Target of Rapamycin
Mu-RE	*Bmal1* reconstituted in the muscle
Muscle-RE	*Bmal1* reconstituted in the muscle
NADR	Noradrenaline
NBT	Nitro Blue Tetrazolium
NR1D1/2	Nuclear Receptor Subfamily 1 Group D Member 1/2
O/N	Overnight
OGTT	Oral Glucose Tolerance Test
PBS	Phosphate-Buffered Saline
PCA	Principal Component Analysis
PCR	Polymerase Chain Reaction
PDH	Pyruvate Dehydrogenase
PDK4	Pyruvate Dehydrogenase Kinase 4
PDP1	Pyruvate Dehydrogenase Phosphatase catalytic subunit 1
PER	Period
PSEA	Phase Set Enrichment Analysis
PVN/DMH	Paraventricular Nucleus/Dorsomedial Hypothalamus
RE/RE	*Bmal1* Reconstituted in muscle and brain
RER	Respiration Exchange Ratio
REV-ERB	Reverse-Erythroblastosis
RHT	Retino-Hypothalamic
ROR	RAR-related Orphan Receptor
RORE	Retinoid Orphan Receptor Element
RT	Room Temperature

RV	Reverse primer
SCN	Suprachiasmatic Nucleus
SD	Standard Deviation
SDH	Succinate Dehydrogenase
SEM	Standard Error of the Mean
SYT10	Synaptotagmin10
TA	Tibialis Anterior
TBS-T	Tris-Buffered Saline with 0.1% Tween
TCA	Tricarboxylic Acid
TNF	Tumor Necrosis Factor
TRF	Time-Restricted Feeding
TTFL	Transcriptional-Translational Feedback Loop
VCO_2	Carbon Dioxide production
VEGF	Vascular Endothelial Growth Factor
VIP	Vasoactive Intestinal Polypeptide
VO_2	Oxygen consumption
WT	Wild-type
ZT	*Zeitgeber* Time

REFERENCES

1. Kim, K. M., Jang, H. C. & Lim, S. Differences among skeletal muscle mass indices derived from height-, weight-, and body mass index-adjusted models in assessing sarcopenia. *Korean Journal of Internal Medicine* vol. 31 643–650 (2016).

2. Dave, H. D., Shook, M. & Varacallo, M. Anatomy, Skeletal Muscle. *StatPearls* (2021).

3. Ferrannini, E. *et al.* The disposal of an oral glucose load in patients with non-insulin-dependent diabetes. *Metabolism* **37**, 79–85 (1988).

4. Cornier, M. A. *et al.* The Metabolic Syndrome. *Endocr. Rev.* **29**, 777–822 (2008).

5. Kim, G. & Kim, J. H. Impact of Skeletal Muscle Mass on Metabolic Health. *Endocrinol. Metab.* **35**, 1–6 (2020).

6. Rubio-Ruiz, M. E., Guarner-Lans, V., Pérez-Torres, I. & Soto, M. E. Mechanisms Underlying Metabolic Syndrome-Related Sarcopenia and Possible Therapeutic Measures. *Int. J. Mol. Sci. 2019, Vol. 20, Page 647* **20**, 647 (2019).

7. Daily, J. W. & Park, S. Sarcopenia Is a Cause and Consequence of Metabolic Dysregulation in Aging Humans: Effects of Gut Dysbiosis, Glucose Dysregulation, Diet and Lifestyle. *Cells* **11**, (2022).

8. Frontera, W. R. & Ochala, J. Skeletal Muscle: A Brief Review of Structure and Function. *Behavior Genetics* vol. 45 183–195 (2015).

9. Gabriel, B. M. *et al.* Disrupted circadian oscillations in type 2 diabetes are linked to altered rhythmic mitochondrial metabolism in skeletal muscle. *Sci. Adv.* **7**, (2021).

10. Dahl, R. *et al.* Three-dimensional reconstruction of the human skeletal muscle mitochondrial network as a tool to assess mitochondrial content and structural organization. *Acta Physiol. (Oxf).* **213**, 145–155 (2015).

11. Jayasinghe, I. D. & Launikonis, B. S. Three-dimensional reconstruction and analysis of the tubular system of vertebrate skeletal muscle. *J. Cell Sci.* **126**, 4048–4058 (2013).

12. Pavelka, M. & Roth, J. Sarcoplasmic Reticulum, Triad, Satellite Cell. *Funct. Ultrastruct.* 302–303 (2010) doi:10.1007/978-3-211-99390-3_155.

13. Pham, S. & Puckett, Y. Physiology, Skeletal Muscle Contraction. *StatPearls* (2021).

14. Murgia, M. *et al.* Protein profile of fiber types in human skeletal muscle: a single-fiber proteomics study. *Skelet. Muscle* **11**, 1–19 (2021).

15. Rubenstein, A. B. *et al.* Single-cell transcriptional profiles in human skeletal muscle. *Sci. Rep.* **10**, 1–15 (2020).

16. Bentzinger, C. F., Wang, Y. X., Dumont, N. A. & Rudnicki, M. A. Cellular dynamics in the muscle satellite cell niche. *EMBO Rep.* **14**, 1062–1072 (2013).

17. Sousa-Victor, P., García-Prat, L. & Muñoz-Cánoves, P. Control of satellite cell function in muscle regeneration and its disruption in ageing. *Nat. Rev. Mol. Cell Biol. 2021 233* **23**, 204–226 (2021).

18. Joe, A. W. B. *et al.* Muscle injury activates resident fibro/adipogenic progenitors that facilitate myogenesis. *Nat. Cell Biol. 2010 122* **12**, 153–163 (2010).

19. Abou-Khalil, R., Mounier, R. & Chazaud, B. Regulation of myogenic stem cell behavior by

vessel cells: the ‘ménage à trois’ of satellite cells, periendothelial cells and endothelial cells. *Cell Cycle* **9**, 892–896 (2010).

20. Proietti, D. *et al.* Activation of skeletal muscle–resident glial cells upon nerve injury. *JCI Insight* **6**, (2021).

21. Giordani, L. *et al.* High-Dimensional Single-Cell Cartography Reveals Novel Skeletal Muscle-Resident Cell Populations. *Mol. Cell* **74**, 609-621.e6 (2019).

22. Siparsky, P. N., Kirkendall, D. T. & Garrett, W. E. Muscle Changes in Aging: Understanding Sarcopenia. *Sports Health* **6**, 36 (2014).

23. Larsson, L., Grimby, G. & Karlsson, J. Muscle strength and speed of movement in relation to age and muscle morphology. *J. Appl. Physiol.* **46**, 451–456 (1979).

24. Mosole, S. *et al.* Long-term high-level exercise promotes muscle reinnervation with age. *J. Neuropathol. Exp. Neurol.* **73**, 284–294 (2014).

25. Chakkalakal, J. V., Jones, K. M., Basson, M. A. & Brack, A. S. The aged niche disrupts muscle stem cell quiescence. *Nature* **490**, 355–360 (2012).

26. Sousa-Victor, P. *et al.* Geriatric muscle stem cells switch reversible quiescence into senescence. *Nat. 2014 5067488* **506**, 316–321 (2014).

27. Brack, A. S. *et al.* Increased Wnt signaling during aging alters muscle stem cell fate and increases fibrosis. *Science (80-.).* **317**, 807–810 (2007).

28. Vettor, R. *et al.* The origin of intermuscular adipose tissue and its pathophysiological implications. *Am. J. Physiol. - Endocrinol. Metab.* **297**, 987–998 (2009).

29. Serrano, A. L. & Muñoz-Cánoves, P. Regulation and dysregulation of fibrosis in skeletal muscle. *Exp. Cell Res.* **316**, 3050–3058 (2010).

30. Kwon, H. & Pessin, J. E. Adipokines Mediate Inflammation and Insulin Resistance. *Front. Endocrinol. (Lausanne).* **4**, (2013).

31. Plomgaard, P. *et al.* Tumor Necrosis Factor-α Induces Skeletal Muscle Insulin Resistance in Healthy Human Subjects via Inhibition of Akt Substrate 160 Phosphorylation. *Diabetes* **54**, 2939–2945 (2005).

32. Demontis, F. & Perrimon, N. FOXO/4E-BP Signaling in Drosophila Muscles Regulates Organism-wide Proteostasis During Aging. *Cell* **143**, 813 (2010).

33. García-Prat, L. *et al.* Autophagy maintains stemness by preventing senescence. *Nature* **529**, 37–42 (2016).

34. Miquel, J., Economos, A. C., Fleming, J. & Johnson, J. E. Mitochondrial role in cell aging. *Exp. Gerontol.* **15**, 575–591 (1980).

35. Leduc-Gaudet, J. P. *et al.* Mitochondrial morphology is altered in atrophied skeletal muscle of aged mice. *Oncotarget* **6**, 17923–17937 (2015).

36. Short, K. R. *et al.* Decline in skeletal muscle mitochondrial function with aging in humans. *Proc. Natl. Acad. Sci. U. S. A.* **102**, 5618–5623 (2005).

37. Gouspillou, G. *et al.* Mitochondrial energetics is impaired in vivo in aged skeletal muscle. *Aging Cell* **13**, 39–48 (2014).

38. Sebastián, D., Palacín, M. & Zorzano, A. Mitochondrial Dynamics: Coupling

Mitochondrial Fitness with Healthy Aging. *Trends Mol. Med.* **23**, 201–215 (2017).

39. Pinti, M. *et al.* Circulating mitochondrial DNA increases with age and is a familiar trait: Implications for 'inflamm-aging'. *Eur. J. Immunol.* **44**, 1552–1562 (2014).

40. Mitchell, W. K. *et al.* Sarcopenia, dynapenia, and the impact of advancing age on human skeletal muscle size and strength; a quantitative review. *Front. Physiol.* **3**, (2012).

41. Englund, D. A., Zhang, X., Aversa, Z. & LeBrasseur, N. K. Skeletal muscle aging, cellular senescence, and senotherapeutics: Current knowledge and future directions. *Mech. Ageing Dev.* **200**, 111595 (2021).

42. Meyer, C., Dostou, J. M., Welle, S. L. & Gerich, J. E. Role of human liver, kidney, and skeletal muscle in postprandial glucose homeostasis. *Am. J. Physiol. Endocrinol. Metab.* **282**, (2002).

43. Argilés, J. M., Campos, N., Lopez-Pedrosa, J. M., Rueda, R. & Rodriguez-Mañas, L. Skeletal Muscle Regulates Metabolism via Interorgan Crosstalk: Roles in Health and Disease. *J. Am. Med. Dir. Assoc.* **17**, 789–796 (2016).

44. Matsui, T. *et al.* Astrocytic glycogen-derived lactate fuels the brain during exhaustive exercise to maintain endurance capacity. *Proc. Natl. Acad. Sci. U. S. A.* **114**, 6358–6363 (2017).

45. Hui, S. *et al.* Glucose feeds the TCA cycle via circulating lactate. *Nat. 2017 5517678* **551**, 115–118 (2017).

46. Jang, C., Hui, S., Gorman, J. H., Gorman, R. C. & Rabinowitz, J. D. Metabolite Exchange between Mammalian Organs Quantified in Pigs 739 cases of organ-specific metabolite production or consumption LC-MS. *Cell Metab.* **30**, 594–606 (2019).

47. Felig, P. The glucose-alanine cycle. *Metabolism* **22**, 179–207 (1973).

48. Katz, J. & Tayek, J. A. Gluconeogenesis and the Cori cycle in 12-, 20-, and 40-h-fasted humans. *Am. J. Physiol.* **275**, (1998).

49. Birsoy, K., Festuccia, W. T. & Laplante, M. A comparative perspective on lipid storage in animals. *J. Cell Sci.* **126**, 1541–1552 (2013).

50. Challet, E. The circadian regulation of food intake. *Nature Reviews Endocrinology* vol. 15 393–405 (2019).

51. Gabriel, B. M. & Zierath, J. R. Circadian rhythms and exercise — re-setting the clock in metabolic disease. *Nat. Rev. Endocrinol.* **15**, 197–206 (2019).

52. Baron, K. G. & Reid, K. J. Circadian Misalignment and Health. *Int. Rev. Psychiatry* **26**, 139 (2014).

53. Rijo-Ferreira, F. & Takahashi, J. S. Genomics of circadian rhythms in health and disease. *Genome Med. 2019 111* **11**, 1–16 (2019).

54. Moore, R. Y. & Eichler, V. B. Loss of a circadian adrenal corticosterone rhythm following suprachiasmatic lesions in the rat. *Brain Res.* **42**, 201–206 (1972).

55. Panda, S. *et al.* Melanopsin is required for non-image-forming photic responses in blind mice. *Science* **301**, 525–527 (2003).

56. Hattar, S. *et al.* Melanopsin and rod–cone photoreceptive systems account for all major accessory visual functions in mice. *Nat. 2003 4246944* **424**, 75–81 (2003).

57. Berson, D. M., Dunn, F. A. & Takao, M. Phototransduction by retinal ganglion cells that set the circadian clock. *Science* **295**, 1070–1073 (2002).

58. Hastings, M. H., Maywood, E. S. & Brancaccio, M. Generation of circadian rhythms in the suprachiasmatic nucleus. *Nat. Rev. Neurosci. 2018 198* **19**, 453–469 (2018).

59. Crosio, C., Cermakian, N., Allis, C. D. & Sassone-Corsi, P. Light induces chromatin modification in cells of the mammalian circadian clock. *Nat. Neurosci. 2000 312* **3**, 1241–1247 (2000).

60. Mohawk, J. A. & Takahashi, J. S. Cell autonomy and synchrony of suprachiasmatic nucleus circadian oscillators. *Trends Neurosci.* **34**, 349–358 (2011).

61. Astiz, M., Heyde, I. & Oster, H. Mechanisms of communication in the Mammalian Circadian timing system. *Int. J. Mol. Sci.* **20**, (2019).

62. Buijs, R. M. *et al.* Chapter 20: Organization of circadian functions: interaction with the body. *Progress in Brain Research* vol. 153 341–360 (2006).

63. Balsalobre, A. *et al.* Resetting of circadian time in peripheral tissues by glucocorticoid signaling. *Science (80-.).* **289**, 2344–2347 (2000).

64. Lightman, S. L. & Conway-Campbell, B. L. The crucial role of pulsatile activity of the HPA axis for continuous dynamic equilibration. *Nat. Rev. Neurosci. 2010 1110* **11**, 710–718 (2010).

65. Moore, R. Y. & Eichler, V. B. Loss of a circadian adrenal corticosterone rhythm following suprachiasmatic lesions in the rat. *Brain Res.* **42**, 201–206 (1972).

66. Jones, J. R., Chaturvedi, S., Granados-Fuentes, D. & Herzog, E. D. Circadian neurons in the paraventricular nucleus entrain and sustain daily rhythms in glucocorticoids. *Nat. Commun. 2021 121* **12**, 1–15 (2021).

67. Weeke, J. & Gundersen, H. J. G. Circadian and 30 minutes variations in serum TSH and thyroid hormones in normal subjects. *Acta Endocrinol. (Copenh).* **89**, 659–672 (1978).

68. Kalsbeek, A., Fliers, E., Franke, A. N., Wortel, J. & Buijs, R. M. Functional connections between the suprachiasmatic nucleus and the thyroid gland as revealed by lesioning and viral tracing techniques in the rat. *Endocrinology* **141**, 3832–3841 (2000).

69. Shekhar, S., Hall, J. E. & Klubo-Gwiezdzinska, J. The Hypothalamic Pituitary Thyroid Axis and Sleep. *Curr. Opin. Endocr. Metab. Res.* **17**, 8 (2021).

70. Nicolaides, N. C., Charmandari, E., Chrousos, G. P. & Kino, T. Circadian endocrine rhythms: the hypothalamic-pituitary-adrenal axis and its actions. *Ann N Y Acad Sci* **1318**, 71–80 (2014).

71. Welsh, D. K., Takahashi, J. S. & Kay, S. A. Suprachiasmatic Nucleus: Cell Autonomy and Network Properties. *Annu. Rev. Physiol.* **72**, 551 (2010).

72. Su, Y., Foppen, E., Zhang, Z., Fliers, E. & Kalsbeek, A. Effects of 6-meals-a-day feeding and 6-meals-a-day feeding combined with adrenalectomy on daily gene expression rhythms in rat epididymal white adipose tissue. *Genes Cells* **21**, 6–24 (2016).

73. Lehman, M. N. *et al.* Circadian rhythmicity restored by neural transplant. Immunocytochemical characterization of the graft and its integration with the host brain. *J. Neurosci.* **7**, 1626–1638 (1987).

74. Takahashi, N., Hirata, Y., Aihara, K. & Mas, P. A Hierarchical Multi-oscillator Network

Orchestrates the Arabidopsis Circadian System. *Cell* **163**, 148–159 (2015).

75. Hall, J. C. & Rosbash, M. Genetic and Molecular Analysis of Biological Rhythms. *J. Biol. Rhythms* **2**, 153–178 (1987).

76. Siwicki, K. K., Eastman, C., Petersen, G., Rosbash, M. & Hall, J. C. Antibodies to the period gene product of drosophila reveal diverse tissue distribution and rhythmic changes in the visual system. *Neuron* **1**, 141–150 (1988).

77. Rutila, J. E. *et al.* Cycle is a second bHLH-PAS clock protein essential for circadian rhythmicity and transcription of Drosophila period and timeless. *Cell* **93**, 805–814 (1998).

78. Bargiello, T. A., Jackson, F. R. & Young, M. W. Restoration of circadian behavioural rhythms by gene transfer in Drosophila. *Nature* **312**, 752–754 (1984).

79. Yamazaki, S. *et al.* Resetting central and peripheral circadian oscillators in transgenic rats. *Science* **288**, 682–685 (2000).

80. Balsalobre, A., Damiola, F. & Schibler, U. A Serum Shock Induces Circadian Gene Expression in Mammalian Tissue Culture Cells. *Cell* **93**, 929–937 (1998).

81. Welz, P. S. *et al.* BMAL1-Driven Tissue Clocks Respond Independently to Light to Maintain Homeostasis. *Cell* (2019) doi:10.1016/j.cell.2019.05.009.

82. Koronowski, K. B. *et al.* Defining the Independence of the Liver Circadian Clock. *Cell* (2019) doi:10.1016/j.cell.2019.04.025.

83. Finger, A.-M. & Kramer, A. Peripheral clocks tick independently of their master. (2021) doi:10.1101/gad.348305.

84. Bunger, M. K. *et al.* Mop3 is an essential component of the master circadian pacemaker in mammals. *Cell* **103**, 1009–1017 (2000).

85. Gekakis, N. *et al.* Role of the CLOCK protein in the mammalian circadian mechanism. *Science (80-.).* **280**, 1564–1569 (1998).

86. Vielhaber, E., Eide, E., Rivers, A., Gao, Z.-H. & Virshup, D. M. Nuclear Entry of the Circadian Regulator mPER1 Is Controlled by Mammalian Casein Kinase I ε. *Mol. Cell. Biol.* **20**, 4888–4899 (2000).

87. Eide, E. J., Vielhaber, E. L., Hinz, W. A. & Virshup, D. M. The circadian regulatory proteins BMAL1 and cryptochromes are substrates of casein kinase Iε. *J. Biol. Chem.* **277**, 17248–17254 (2002).

88. Sanada, K., Okano, T. & Fukada, Y. Mitogen-activated protein kinase phosphorylates and negatively regulates basic helix-loop-helix-PAS transcription factor BMAL1. *J. Biol. Chem.* **277**, 267–271 (2002).

89. Sahar, S., Zocchi, L., Kinoshita, C., Borrelli, E. & Sassone-Corsi, P. Regulation of BMAL1 protein stability and circadian function by GSK3β-mediated phosphorylation. *PLoS One* **5**, (2010).

90. Harada, Y., Sakai, M., Kurabayashi, N., Hirota, T. & Fukada, Y. Ser-557-phosphorylated mCRY2 is degraded upon synergistic phosphorylation by glycogen synthase kinase-3β. *J. Biol. Chem.* **280**, 31714–31721 (2005).

91. Mohawk, J. A., Green, C. B. & Takahashi, J. S. Central and Peripheral Circadian Clocks in Mammals. *Annu. Rev. Neurosci.* **35**, 445–462 (2012).

92. Hosoda, H. *et al.* CBP/p300 is a cell type-specific modulator of CLOCK/BMAL1-mediated transcription. *Mol. Brain* **2**, (2009).

93. Etchegaray, J. P., Lee, C., Wade, P. A. & Reppert, S. M. Rhythmic histone acetylation underlies transcription in the mammalian circadian clock. *Nat. 2003 4216919* **421**, 177–182 (2002).

94. Lee, J. *et al.* Dual Modification of BMAL1 by SUMO2/3 and Ubiquitin Promotes Circadian Activation of the CLOCK/BMAL1 Complex. *Mol. Cell. Biol.* **28**, 6056–6065 (2008).

95. Asher, G. *et al.* SIRT1 Regulates Circadian Clock Gene Expression through PER2 Deacetylation. *Cell* **134**, 317–328 (2008).

96. Nakahata, Y. *et al.* The NAD+-dependent deacetylase SIRT1 modulates CLOCK-mediated chromatin remodeling and circadian control. *Cell* **134**, 329–340 (2008).

97. Ramsey, K. M. *et al.* Circadian clock feedback cycle through NAMPT-mediated NAD+ biosynthesis. *Science* **324**, 651–654 (2009).

98. Vaca-Dempere, M., Kumar, A., Sica, V. & Muñoz-Cánoves, P. Running skeletal muscle clocks on time— the determining factors. *Exp. Cell Res.* **413**, 112989 (2022).

99. Okabe, T. *et al.* REV-ERBα influences the stability and nuclear localization of the glucocorticoid receptor. *J. Cell Sci.* **129**, 4143 (2016).

100. Lamia, K. A. *et al.* Cryptochromes mediate rhythmic repression of the glucocorticoid receptor. *Nature* **480**, 552–556 (2011).

101. Zhang, E. E. *et al.* Cryptochrome mediates circadian regulation of cAMP signaling and hepatic gluconeogenesis. *Nat. Med.* **16**, 1152–1156 (2010).

102. Zhang, R., Lahens, N. F., Ballance, H. I., Hughes, M. E. & Hogenesch, J. B. A circadian gene expression atlas in mammals: Implications for biology and medicine. *Proc. Natl. Acad. Sci. U. S. A.* **111**, 16219–16224 (2014).

103. McCarthy, J. J. *et al.* Identification of the circadian transcriptome in adult mouse skeletal muscle. *Physiol. Genomics* **31**, 86–95 (2007).

104. Kondratov, R. V., Kondratova, A. A., Gorbacheva, V. Y., Vykhovanets, O. V. & Antoch, M. P. Early aging and age-related pathologies in mice deficient in BMAL1, the core component of the circadian clock. *Genes Dev.* **20**, 1868–1873 (2006).

105. JL, A. *et al.* CLOCK and BMAL1 regulate MyoD and are necessary for maintenance of skeletal muscle phenotype and function. *Proc. Natl. Acad. Sci. U. S. A.* **107**, 19090–19095 (2010).

106. Schroder, E. A. *et al.* Intrinsic muscle clock is necessary for musculoskeletal health. *J. Physiol.* **593**, 5387–5404 (2015).

107. Andrews, J. L. *et al.* CLOCK and BMAL1 regulate MyoD and are necessary for maintenance of skeletal muscle phenotype and function. *Proc. Natl. Acad. Sci. U. S. A.* **107**, 19090–19095 (2010).

108. Alibhai, F. J. *et al.* Female ClockΔ19/Δ19 mice are protected from the development of age-dependent cardiomyopathy. *Cardiovasc. Res.* **114**, 259–271 (2018).

109. Woldt, E. *et al.* Rev-erb-α modulates skeletal muscle oxidative capacity by regulating mitochondrial biogenesis and autophagy. *Nat. Med.* **19**, 1039–1046 (2013).

110. Zheng, B. *et al.* The mPer2 gene encodes a functional component of the mammalian circadian clock. *Nature* **400**, 169–173 (1999).

111. Bae, K. *et al.* Differential Effects of Two Period Genes on the Physiology and Proteomic Profiles of Mouse Anterior Tibialis Muscles. *Mol. Cells* **22**, 275–284.

112. Dyar, K. A. *et al.* Muscle insulin sensitivity and glucose metabolism are controlled by the intrinsic muscle clock. *Mol. Metab.* **3**, 29–41 (2014).

113. Zhang, X. *et al.* A non-canonical E-box within the MyoD core enhancer is necessary for circadian expression in skeletal muscle. *Nucleic Acids Res.* **40**, 3419–3430 (2012).

114. Hodge, B. A. *et al.* MYOD1 functions as a clock amplifier as well as a critical co-factor for downstream circadian gene expression in muscle. *Elife* **8**, 1–26 (2019).

115. Dyar, K. A., Schiaffino, S. & Blaauw, B. Inactivation of the intrinsic muscle clock does not cause sarcopenia. *J. Physiol.* **594**, 3161–3162 (2016).

116. Chatterjee, S. *et al.* Brain and muscle Arnt-like 1 is a key regulator of myogenesis. *J. Cell Sci.* **126**, 2213–2224 (2013).

117. Chatterjee, S., Yin, H., Nam, D., Li, Y. & Ma, K. Brain and muscle Arnt-like 1 promotes skeletal muscle regeneration through satellite cell expansion. *Exp. Cell Res.* **331**, 200–210 (2015).

118. Lipton, J. O. *et al.* The Circadian Protein BMAL1 Regulates Translation in Response to S6K1-Mediated Phosphorylation. *Cell* **161**, 1138 (2015).

119. Conlee, R. K., Rennie, M. J. & Winder, W. W. Skeletal muscle glycogen content: diurnal variation and effects of fasting. *Am. J. Physiol.* **231**, 614–618 (1976).

120. Clark, J. H. & Conlee, R. K. Muscle and liver glycogen content: Diurnal variation and endurance. *J. Appl. Physiol. Respir. Environ. Exerc. Physiol.* **47**, 425–428 (1979).

121. Dyar, K. A. *et al.* The calcineurin-NFAT pathway controls activity-dependent circadian gene expression in slow skeletal muscle. *Mol. Metab.* **4**, 823–833 (2015).

122. Glancy, B. & Balaban, R. S. Role of Mitochondrial Ca2+ in the Regulation of Cellular Energetics. *Biochemistry* **51**, 2959 (2012).

123. Hodge, B. A. *et al.* The endogenous molecular clock orchestrates the temporal separation of substrate metabolism in skeletal muscle. *Skelet. Muscle* **5**, 1–16 (2015).

124. Dyar, K. A. *et al. Transcriptional programming of lipid and amino acid metabolism by the skeletal muscle circadian clock*. *PLoS Biology* vol. 16 (2018).

125. Rennie, M. J. & Tipton, K. D. Protein and amino acid metabolism during and after exercise and the effects of nutrition. *Annu. Rev. Nutr.* **20**, 457–483 (2000).

126. Neufeld-Cohen, A. *et al.* Circadian control of oscillations in mitochondrial rate-limiting enzymes and nutrient utilization by PERIOD proteins. *Proc. Natl. Acad. Sci. U. S. A.* **113**, E1673–E1682 (2016).

127. Schmitt, K. *et al.* Circadian Control of DRP1 Activity Regulates Mitochondrial Dynamics and Bioenergetics. *Cell Metab.* **27**, 657-666.e5 (2018).

128. van Moorsel, D. *et al.* Demonstration of a day-night rhythm in human skeletal muscle oxidative capacity. *Mol. Metab.* **5**, 635–645 (2016).

129. Mieda, M., Williams, S. C., Richardson, J. A., Tanaka, K. & Yanagisawa, M. The dorsomedial hypothalamic nucleus as a putative food-entrainable circadian pacemaker. *Proc. Natl. Acad. Sci. U. S. A.* **103**, 12150–12155 (2006).

130. Challet, E. The circadian regulation of food intake. *Nat. Rev. Endocrinol. 2019 157* **15**, 393–405 (2019).

131. Damiola, F. *et al.* Restricted feeding uncouples circadian oscillators in peripheral tissues from the central pacemaker in the suprachiasmatic nucleus. *Genes Dev.* **14**, 2950–2961 (2000).

132. Le Minh, N., Damiola, F., Tronche, F., Schütz, G. & Schibler, U. Glucocorticoid hormones inhibit food-induced phase-shifting of peripheral circadian oscillators. *EMBO J.* **20**, 7128–7136 (2001).

133. Hatori, M. *et al.* Time-restricted feeding without reducing caloric intake prevents metabolic diseases in mice fed a high-fat diet. *Cell Metab.* **15**, 848–860 (2012).

134. Chaix, A., Lin, T., Le, H. D., Chang, M. W. & Panda, S. Time-Restricted Feeding Prevents Obesity and Metabolic Syndrome in Mice Lacking a Circadian Clock. *Cell Metab.* **29**, 303-319.e4 (2019).

135. Vollmers, C. *et al.* Time of feeding and the intrinsic circadian clock drive rhythms in hepatic gene expression. *Proc. Natl. Acad. Sci. U. S. A.* **106**, 21453–21458 (2009).

136. Adamovich, Y. *et al.* Circadian clocks and feeding time regulate the oscillations and levels of hepatic triglycerides. *Cell Metab.* **19**, 319–330 (2014).

137. Guan, D. *et al.* The hepatocyte clock and feeding control chronophysiology of multiple liver cell types. *Science (80-.).* **369**, 1388–1395 (2020).

138. Gill, S., Le, H. D., Melkani, G. C. & Panda, S. Time-restricted feeding attenuates age-related cardiac decline in Drosophila. *Science (80-.).* **347**, 1265–1269 (2015).

139. Ulgherait, M. *et al.* Circadian autophagy drives iTRF-mediated longevity. *Nature* **598**, 353–358 (2021).

140. Villanueva, J. E. *et al.* Time-restricted feeding restores muscle function in Drosophila models of obesity and circadian-rhythm disruption. *Nat. Commun.* **10**, 1–17 (2019).

141. de Goede, P. *et al.* Time-restricted feeding during the inactive phase abolishes the daily rhythm in mitochondrial respiration in rat skeletal muscle. *FASEB J.* **36**, (2022).

142. Jones, R. *et al.* Two weeks of early time-restricted feeding (eTRF) improves skeletal muscle insulin and anabolic sensitivity in healthy men. *Am. J. Clin. Nutr.* **112**, 1015–1028 (2020).

143. Lundell, L. S. *et al.* Time-restricted feeding alters lipid and amino acid metabolite rhythmicity without perturbing clock gene expression. *Nat. Commun. 2020 111* **11**, 1–11 (2020).

144. Lees, M. J., Hodson, N. & Moore, D. R. A muscle-centric view of time-restricted feeding for older adults. *Curr. Opin. Clin. Nutr. Metab. Care* **24**, 521–527 (2021).

145. Magnus-Levy, A. Ueber die Grösse des respiratorischen Gaswechsels unter dem Einfluss der Nahrungsaufnahme. *Arch. für die gesamte Physiol. des Menschen und der Tiere 1894 551* **55**, 1–126 (1893).

146. Zuntz, N. *Studien zu einer Physiologie des Marsches, von Zuntz und Schumburg.*

(Hirschwald, 1901).

147. Smith, F. Remarks on the Chemistry of Respiration in the Horse during rest and work. *J. Physiol.* **11**, 496–496 (1890).

148. Del Prete, Z., Musarò, A. & Rizzuto, E. Measuring mechanical properties, including isotonic fatigue, of fast and slow MLC/mIgf-1 transgenic skeletal muscle. *Ann. Biomed. Eng.* **36**, 1281–1290 (2008).

149. Segalés, J. *et al.* Sestrin prevents atrophy of disused and aging muscles by integrating anabolic and catabolic signals. *Nat. Commun. 2020 111* **11**, 1–13 (2020).

150. Lee, J. S., Jeon, Y. J., Park, S. Y. & Son, C. G. An Adrenalectomy Mouse Model Reflecting Clinical Features for Chronic Fatigue Syndrome. *Biomolecules* **10**, (2020).

151. Stanton, B. *et al.* Effects of adrenalectomy and chronic adrenal corticosteroid replacement on potassium transport in rat kidney. Effects of Adrenalectomy and Chronic Adrenal Corticosteroid Replacement on Potassium Transport in Rat Kidney. *J Clin Invest* **75**, 1317 (1985).

152. Cederroth, C. R. *et al.* Circadian Regulation of Cochlear Sensitivity to Noise by Circulating Glucocorticoids. *Curr. Biol.* **29**, 2477-2487.e6 (2019).

153. Gaspar Elsas, M. I. C. *et al.* Upregulation by glucocorticoids of responses to eosinopoietic cytokines in bone-marrow from normal and allergic mice. *Br. J. Pharmacol.* **129**, 1543–1552 (2000).

154. Terazono, H. *et al.* Adrenergic regulation of clock gene expression in mouse liver. *Proc. Natl. Acad. Sci. U. S. A.* **100**, 6795–6800 (2003).

155. Pedersen, L. *et al.* Voluntary Running Suppresses Tumor Growth through Epinephrine- and IL-6-Dependent NK Cell Mobilization and Redistribution. *Cell Metab.* **23**, 554–562 (2016).

156. Ewels, P. A. *et al.* The nf-core framework for community-curated bioinformatics pipelines. *Nat. Biotechnol. 2020 383* **38**, 276–278 (2020).

157. Kim, D., Paggi, J. M., Park, C., Bennett, C. & Salzberg, S. L. Graph-based genome alignment and genotyping with HISAT2 and HISAT-genotype. *Nat. Biotechnol. 2019 378* **37**, 907–915 (2019).

158. Liao, Y., Smyth, G. K. & Shi, W. featureCounts: an efficient general purpose program for assigning sequence reads to genomic features. *Bioinformatics* **30**, 923–930 (2014).

159. Love, M. I., Huber, W. & Anders, S. Moderated estimation of fold change and dispersion for RNA-seq data with DESeq2. *Genome Biol.* **15**, 1–21 (2014).

160. Robinson, M. D., McCarthy, D. J. & Smyth, G. K. edgeR: a Bioconductor package for differential expression analysis of digital gene expression data. *Bioinformatics* **26**, 139–140 (2010).

161. Ritchie, M. E. *et al.* limma powers differential expression analyses for RNA-sequencing and microarray studies. *Nucleic Acids Res.* **43**, e47–e47 (2015).

162. Hughes, M. E., Hogenesch, J. B. & Kornacker, K. JTK-CYCLE: An efficient nonparametric algorithm for detecting rhythmic components in genome-scale data sets. *J. Biol. Rhythms* **25**, 372–380 (2010).

163. Gu, Z., Gu, L., Eils, R., Schlesner, M. & Brors, B. circlize Implements and enhances

circular visualization in R. *Bioinformatics* **30**, 2811–2812 (2014).

164. Hulsen, T., de Vlieg, J. & Alkema, W. BioVenn - A web application for the comparison and visualization of biological lists using area-proportional Venn diagrams. *BMC Genomics* **9**, 1–6 (2008).

165. Conway, J. R., Lex, A. & Gehlenborg, N. UpSetR: an R package for the visualization of intersecting sets and their properties. *Bioinformatics* **33**, 2938–2940 (2017).

166. Liberzon, A. *et al.* The Molecular Signatures Database (MSigDB) hallmark gene set collection. *Cell Syst.* **1**, 417–425 (2015).

167. Jassal, B. *et al.* The reactome pathway knowledgebase. *Nucleic Acids Res.* **48**, D498–D503 (2020).

168. Rath, S. *et al.* MitoCarta3.0: an updated mitochondrial proteome now with sub-organelle localization and pathway annotations. *Nucleic Acids Res.* **49**, D1541–D1547 (2021).

169. Raudvere, U. *et al.* g:Profiler: a web server for functional enrichment analysis and conversions of gene lists (2019 update). *Nucleic Acids Res.* **47**, W191–W198 (2019).

170. Carbon, S. *et al.* The Gene Ontology resource: enriching a GOld mine. *Nucleic Acids Res.* **49**, D325–D334 (2021).

171. Kanehisa, M. & Goto, S. KEGG: Kyoto Encyclopedia of Genes and Genomes. *Nucleic Acids Res.* **28**, 27 (2000).

172. Petrus, P. *et al.* The central clock suffices to drive the majority of circulatory metabolic rhythms. *bioRxiv* 2022.01.24.477514 (2022) doi:10.1101/2022.01.24.477514.

173. Greco, C. M. *et al.* Integration of feeding behavior by the liver circadian clock reveals network dependency of metabolic rhythms. *Sci. Adv.* **7**, (2021).

174. Sartori, R., Romanello, V. & Sandri, M. Mechanisms of muscle atrophy and hypertrophy: implications in health and disease. *Nat. Commun.* **12**, (2021).

175. Buckingham, M. Skeletal muscle formation in vertebrates. *Curr. Opin. Genet. Dev.* **11**, 440–448 (2001).

176. Kitada, M. & Koya, D. Autophagy in metabolic disease and ageing. *Nat. Rev. Endocrinol. 2021 1711* **17**, 647–661 (2021).

177. Nelke, C., Dziewas, R., Minnerup, J., Meuth, S. G. & Ruck, T. Skeletal muscle as potential central link between sarcopenia and immune senescence. *EBioMedicine* vol. 49 381–388 (2019).

178. Tidball, J. G., Flores, I., Welc, S. S., Wehling-Henricks, M. & Ochi, E. Aging of the immune system and impaired muscle regeneration: A failure of immunomodulation of adult myogenesis. *Exp. Gerontol.* **145**, (2021).

179. Bloise, F. F., Cordeiro, A. & Ortiga-Carvalho, T. M. Role of thyroid hormone in skeletal muscle physiology. *J. Endocrinol.* **236**, R57–R68 (2018).

180. Lee, J. *et al.* Loss of Bmal1 leads to uncoupling and impaired glucose-stimulated insulin secretion in β-cells. *Islets* **3**, 381 (2011).

181. Turek, F. W. *et al.* Obesity and metabolic syndrome in circadian Clock mutant mice. *Science* **308**, 1043–1045 (2005).

182. Hood, D. A., Memme, J. M., Oliveira, A. N. & Triolo, M. Maintenance of Skeletal Muscle Mitochondria in Health, Exercise, and Aging. *Annu. Rev. Physiol.* **81**, 19–41 (2019).

183. Hernandez, G. *et al.* MitoTimer: A novel tool for monitoring mitochondrial turnover. *Autophagy* **9**, 1852–1861 (2013).

184. Laker, R. C. *et al.* A novel mitotimer reporter gene for mitochondrial content, structure, stress, and damage in vivo. *J. Biol. Chem.* **289**, 12005–12015 (2014).

185. Ferri, E. *et al.* Role of Age-Related Mitochondrial Dysfunction in Sarcopenia. *Int. J. Mol. Sci.* **21**, 5236 (2020).

186. Migliavacca, E. *et al.* Mitochondrial oxidative capacity and NAD + biosynthesis are reduced in human sarcopenia across ethnicities. *Nat. Commun.* **10**, (2019).

187. Braun, T. P. & Marks, D. L. The regulation of muscle mass by endogenous glucocorticoids. *Front. Physiol.* **6**, 12 (2015).

188. Steiner, J. L. *et al.* Adrenal stress hormone action in skeletal muscle during exercise training: An old dog with new tricks? *Acta Physiol. (Oxf).* **231**, (2021).

189. Dumbell, R., Matveeva, O. & Oster, H. Circadian clocks, stress, and immunity. *Front. Endocrinol. (Lausanne).* **7**, 37 (2016).

190. Soták, M. *et al.* Peripheral circadian clocks are diversely affected by adrenalectomy. *Chronobiol. Int.* **33**, 520–529 (2016).

191. Su, Y. *et al.* Effects of adrenalectomy on daily gene expression rhythms in the rat suprachiasmatic and paraventricular hypothalamic nuclei and in white adipose tissue. *Chronobiol. Int.* **32**, 211–224 (2015).

192. Chourpiliadis, C. & Aeddula, N. R. Physiology, Glucocorticoids. *StatPearls* (2021).

193. Scott, J. H., Menouar, M. A. & Dunn, R. J. Physiology, Aldosterone. *StatPearls* (2022).

194. Paravati, S., Rosani, A. & Warrington, S. J. Physiology, Catecholamines. *StatPearls* (2021).

195. Curtis, A. M. *et al.* Circadian variation of blood pressure and the vascular response to asynchronous stress. *Proc. Natl. Acad. Sci. U. S. A.* **104**, 3450–3455 (2007).

196. Damiola, F. *et al.* Restricted feeding uncouples circadian oscillators in peripheral tissues from the central pacemaker in the suprachiasmatic nucleus. *Genes Dev.* **14**, 2950–2961 (2000).

197. Harder, L. & Oster, H. The Tissue Clock Network: Driver and Gatekeeper of Circadian Physiology: Circadian rhythms are integrated outputs of central and peripheral tissue clocks interacting in a complex manner - from drivers to gatekeepers. *Bioessays* **42**, (2020).

198. Stokkan, K. A., Yamazaki, S., Tei, H., Sakaki, Y. & Menaker, M. Entrainment of the Circadian Clock in the Liver by Feeding. *Science (80-.).* **291**, 490–493 (2001).

199. Greenwell, B. J. *et al.* Rhythmic Food Intake Drives Rhythmic Gene Expression More Potently than the Hepatic Circadian Clock in Mice. *Cell Rep.* **27**, 649-657.e5 (2019).

200. Farajnia, S. *et al.* Evidence for neuronal desynchrony in the aged suprachiasmatic nucleus clock. *J. Neurosci.* **32**, 5891–5899 (2012).

201. Chang, H. C. & Guarente, L. XSIRT1 mediates central circadian control in the SCN by a mechanism that decays with aging. *Cell* **153**, 1448 (2013).

202. Nakamura, T. J., Takasu, N. N. & Nakamura, W. The suprachiasmatic nucleus: age-related decline in biological rhythms. *J. Physiol. Sci. 2016 665* **66**, 367–374 (2016).

203. Nygård, M., Hill, R. H., Wikström, M. A. & Kristensson, K. Age-related changes in electrophysiological properties of the mouse suprachiasmatic nucleus in vitro. *Brain Res. Bull.* **65**, 149–154 (2005).

204. Sato, S. *et al.* Circadian Reprogramming in the Liver Identifies Metabolic Pathways of Aging. *Cell* **170**, 664-677.e11 (2017).

205. Solanas, G. *et al.* Aged Stem Cells Reprogram Their Daily Rhythmic Functions to Adapt to Stress. *Cell* **170**, 678-692.e20 (2017).

206. López-Otín, C., Blasco, M. A., Partridge, L., Serrano, M. & Kroemer, G. The Hallmarks of Aging. *Cell* **153**, 1194–1217 (2013).

207. Imai, S. I. The NAD World 2.0: the importance of the inter-tissue communication mediated by NAMPT/NAD+/SIRT1 in mammalian aging and longevity control. *npj Syst. Biol. Appl. 2016 21* **2**, 1–9 (2016).

208. Mohawk, J. A., Green, C. B. & Takahashi, J. S. Central and peripheral circadian clocks in mammals. *Annual Review of Neuroscience* vol. 35 445–462 (2012).

209. Smith, J. G. *et al.* Interrogating Metabolic Interactions Between Skeletal Muscle and Liver Circadian Clocks In Vivo. *bioRxiv* 2022.02.27.482160 (2022) doi:10.1101/2022.02.27.482160.

210. Welz, P. S. *et al.* BMAL1-Driven Tissue Clocks Respond Independently to Light to Maintain Homeostasis. *Cell* **177**, 1436-1447.e12 (2019).

211. Ehlen, J. C. *et al.* Bmal1 function in skeletal muscle regulates sleep. *Elife* **6**, 1–14 (2017).

212. McDearmon, E. L. *et al.* Dissecting the functions of the mammalian clock protein BMAL1 by tissue-specific rescue in mice. *Science (80-.).* **314**, 1304–1308 (2006).

213. Yang, G. *et al.* Timing of expression of the core clock gene Bmal1 influences its effects on aging and survival. *Sci. Transl. Med.* **8**, (2016).

214. Ferri, E. *et al.* Role of age-related mitochondrial dysfunction in sarcopenia. *International Journal of Molecular Sciences* vol. 21 1–12 (2020).

215. Johnson, M. L., Robinson, M. M. & Nair, S. K. Skeletal muscle aging and the mitochondrion. *Trends Endocrinol. Metab.* **24**, 247–256 (2013).

216. Mortimer, T. *et al.* Brain-keratinocyte communication suffices for epidermal daily homeostasis. doi:10.1101/2022.01.26.477844.

217. Mortimer, T. *et al.* Brain–keratinocyte communication suffices for epidermal daily homeostasis. *bioRxiv* 2022.01.26.477844 (2022) doi:10.1101/2022.01.26.477844.

218. Nakamura, T. J., Takasu, N. N. & Nakamura, W. The suprachiasmatic nucleus: age-related decline in biological rhythms. *Journal of Physiological Sciences* vol. 66 367–374 (2016).

219. Charloux, A., Gronfier, C., Lonsdorfer-Wolf, E., Piquard, F. & Brandenberger, G. Aldosterone release during the sleep-wake cycle in humans. *Am. J. Physiol. - Endocrinol.*

Metab. **276**, (1999).

220. Pincus, G. A Diurnal Rhythm in the Excretion of Urinary Ketosteroids by Young Men. *J. Clin. Endocrinol. Metab.* **3**, 195–199 (1943).

221. Cairns, S. P. & Borrani, F. β-Adrenergic modulation of skeletal muscle contraction: key role of excitation–contraction coupling. *J. Physiol.* **593**, 4713–4727 (2015).

222. Andersson, D. C. *et al.* Stress-induced increase in skeletal muscle force requires protein kinase A phosphorylation of the ryanodine receptor. *J. Physiol.* **590**, 6381–6387 (2012).

223. Longo, V. D. & Panda, S. Fasting, Circadian Rhythms, and Time-Restricted Feeding in Healthy Lifespan. *Cell Metab.* **23**, 1048–1059 (2016).

224. Di Francesco, A., Di Germanio, C., Bernier, M. & De Cabo, R. A time to fast. *Science* **362**, 770–775 (2018).

225. Wang, H. *et al.* Time-Restricted Feeding Shifts the Skin Circadian Clock and Alters UVB-Induced DNA Damage. *Cell Rep.* **20**, 1061–1072 (2017).

226. Reznick, J. *et al.* Altered feeding differentially regulates circadian rhythms and energy metabolism in liver and muscle of rats. *Biochim. Biophys. Acta - Mol. Basis Dis.* **1832**, 228–238 (2013).

227. Chaix, A., Zarrinpar, A., Miu, P. & Panda, S. Time-restricted feeding is a preventative and therapeutic intervention against diverse nutritional challenges. *Cell Metab.* **20**, 991–1005 (2014).

228. Mistlberger, R. E. Circadian food-anticipatory activity: Formal models and physiological mechanisms. *Neurosci. Biobehav. Rev.* **18**, 171–195 (1994).

229. Stephan, F. K. The 'other' circadian system: food as a Zeitgeber. *J. Biol. Rhythms* **17**, 284–292 (2002).

230. Nakamura, T. J. *et al.* Age-related decline in circadian output. *J. Neurosci.* **31**, 10201–10205 (2011).

231. Patel, S. A., Chaudhari, A., Gupta, R., Velingkaar, N. & Kondratov, R. V. Circadian clocks govern calorie restriction-mediated life span extension through BMAL1- and IGF-1-dependent mechanisms. *FASEB J.* **30**, 1634–1642 (2016).

232. Acosta-Rodríguez, V. *et al.* Circadian alignment of early onset caloric restriction promotes longevity in male C57BL/6J mice. *Science* e (2022) doi:10.1126/SCIENCE.ABK0297.

Pels badalls del son
s'escolen els somnis
que no ansieges.
Si se t'afermen,
et revelaran vigílies
de goig inacabable.

Enric Dobón Gómez